2010-01-01

# Acoustic Reflectometry Using Gaussian-Modulated Sinusoidal Waves And The Ware-Aki Algorithm

Ernesto Rodrigo Vazquez Ceron
*University of Texas at El Paso*, ervc@correo.azc.uam.mx

# ACOUSTIC REFLECTOMETRY USING GAUSSIAN-MODULATED SINUSOIDAL WAVES AND THE WARE-AKI ALGORITHM

ERNESTO RODRIGO VAZQUEZ CERON

Department of Electrical and Computer Engineering

APPROVED:

Joseph H. Pierluissi, Ph. D., Co-Chair

Ricardo F. von Borries, Ph. D., Co-Chair

Patricia Nava, Ph. D.

Thompson Sarkodie-Gyan, Ph. D.

Harold S. Slusher, Ph. D.

Patricia D. Witherspoon, Ph.D.
Dean of the Graduate School

To my family,
my friends,
and every Mexican who believes in our beauty and lovely country

# ACOUSTIC REFLECTOMETRY USING GAUSSIAN-MODULATED SINUSOIDAL WAVES AND THE WARE-AKI ALGORITHM

by

ERNESTO RODRIGO VAZQUEZ CERON, MASTER IN SCIENCE

DISSERTATION

Presented to the Faculty of the Graduate School of

The University of Texas at El Paso

in Partial Fulfillment

of the Requirements

for the Degree of

DOCTOR OF PHILOSOPHY

Department of Electrical and Computer Engineering

THE UNIVERSITY OF TEXAS AT EL PASO

August 2010

## Acknowledgements

First of all, I wish to express my gratitude and respect to Dr. Joseph H. Pierluissi for his continued support as my advisor and my professor. Since I came to the University of Texas at El Paso, he always believed on me. Without his knowledge, guidance and valuable friendship, I would not have earned this degree. I would like to thank his schellenger project for supporting me in the Department of Electrical and Computer Engineering.

I wish to express my gratitude and respect to Dr. Ricardo F. von Borries who professionally accepted to join in this dissertation as my advisor. His knowledge, guidance, and valuable time were fundamental for the conclusion and the validation of this dissertation. He gave me all the facilities in the Biopotentials Imaging Laboratory to perform the experiments.

I am also thankful to Dr. Patricia Nava for her willing agreement to be part of my thesis committee. Her value comments have been extremely important for the development and improvement of this work. She gave me the opportunity that every PhD student at UTEP wishes to have, working as Teaching Assistant in the Department of Electrical and Computer Engineering. It allowed me to learn not only from the faculty at the University of Texas El Paso but also from the Engineering students.

I would like to thank Dr. Thompson Sarkodie-Gyan who generously supported the acquisition of the equipment for the experimental work. He helped me to design the acoustic reflectometer in the Laboratory of Industrial Metrology and Automation. His valuable comments were important during this dissertation.

I am also thankful to Dr. Harold H. Slusher for his value comments on acoustics. I am very glad to having him as my professor, because he always encouraging me during this research to do my best.

I would like to express my most sincere respect and appreciation to Dr. Sergio Cabrera and the Texas Instrument Foundation Program. His lectures on digital signal processing, homework projects, and his value comments were fundamental to develop the simulation model in this dissertation.

I would like to thank Lab Manager Frank Medina and Keck Center Laboratory for giving me all facilities to build the acoustic reflectometer and the solid cylindrical cavities which were used to validate the solution of the inverse problem.

I am especially grateful to Sukie Quezada, Linda Romero, Ralph Loya, and Jerry West for all that excellent work in the Department of Electrical and Computer Engineering.

I would like to express my most sincere appreciation to my friends and colleagues in Mexico: Dr. Rafael Quintero, Dr. Rogelio Barrales, Dr. Ezequiel Rodriguez, Dr. Raymundo Barrales, Dr. Oscar Yanez Suarez, and Eng. Ivone Hernandez for encouraging me during my PhD.

I would like to thank my friends in the United States: Laura Sierra, Ivan Sierra, Jorge Saad, Nora Saad, Ramiro Sierra, Eduardo Morales, Diana Rodriguez, Isidro Rodriguez, Shaun Felice, Carlos Rodriguez, Eduardo Morales, Berenice Verdin, Cristian Potes, Marcela Potes, Nazila Hafezi, Damian Valles, Juan de Dios Cota, and Gabriel Bravo, for sharing all those sweet and hard moments since I started my PhD, and for giving me what I never thought to find out of my country, a sincere, honest, and unique friendship.

I wish to thank to my beautiful wife Ale, my wonderful son Axl, my mother Ines, my sister Miriam, and brothers Roberto and Brandon, without them I am nothing.

Finally, I would like to thank the Government of Mexico, the Universidad Autonoma Metropolitana, and the University of Texas at El Paso for the support provided.

## Abstract

Acoustic reflectometry, a non invasive technique, consists of solving, the inverse problem of estimating the cross sectional area as function of the distance of a cylindrical cavity by impacting an audible acoustic pulse of high amplitude and short duration, and analyzing the reflected wave. The technique has been applied in Biomedical Engineering to estimate both the area of a human upper airway and the patency of endotracheal tubes as a function of distance. Several ways have been tested to improve the quality of an acoustic pulse and different algorithms have been tested to reduce the losses. However, an acoustic pulse is difficult to generate with a broad frequency bandwidth and the reconstruction algorithms require robust mathematical procedure to compensate the losses within the system. The solution of the inverse problem in this dissertation consists of sweeping the frequency bandwidth by using Gaussian-modulated sinusoidal packets. A long source tube is used not only to propagate and identify the acoustic waves generated, but also it is used to compute the frequency impulse response by using a least mean square algorithm. The Ware-Aki algorithm is recalled to compute the reflection coefficients, which are directly related with the bore profile. A computational model was developed to evaluate the quadratic error of several acoustic parameters used on acoustic reflectometry. The results obtained by the simulation model show that axial resolution depends on the frequency step size used to sweep a broad frequency bandwidth. The present study utilized an in vitro model that replaced a human upper airway to validate this method. It is based on a calibration of the reflectometer to compensate for the losses along the source tube. This work made of acoustic reflectometry a versatile technique, because the frequency response is obtained by using only one loudspeaker, and the signal-to-noise ratio is increased at high frequencies by using match filter. Therefore, the use of Gaussian-modulated sinusoidal waves and the Ware-Aki algorithm can be used to estimate a cylindrical cavity with an appropriate axial resolution.

# Table of Contents

# List of Tables

# List of Figures

# Chapter 1

## Introduction

Biomedical engineering has improved the quality of life of the human being by far. It has contributed with many sorts of instruments and equipment in hospitals to make precise diagnoses and determine the best way that a physician must follow in a specific case of disease. In biomedical engineering, one of the most versatile ways to make a diagnosis consists of using non-invasive techniques which have become powerful biomedical tools to evaluate biophysical parameters.

This dissertation is focused on acoustic reflectometry technique, a non-invasive way to physically evaluate the cross sectional area of a cylindrical cavity as function of distance, a 3-D measurement. Thereby, it is not necessary to open the cavity or introduce an optical transducer to evaluate the bore profile. The basic idea of acoustic reflectometry consists of processing and analyzing the response generated by an incident acoustic wave when it strikes a cylindrical cavity.

One of the most interesting fields of application of acoustic reflectometry lies on biomedical engineering where the technique has been used to estimate the bore profile of a human upper airway. In consequence, it is not necessary to expose a patient to dangerous doses of radiation like X-ray or CT scan to estimate the bore profile of an upper airway through images, a 2-D measurement. Even more, the right application of acoustic reflectometry replaces a study of endoscopy which is used to evaluate, in an invasive way, the upper airway.

## 1.1 History of acoustic reflectometry

In the history of acoustic reflectometry several reconstruction algorithms have been developed. They are divided in two types. The algorithms which estimate the bore profile from the input impulse response in time domain and the algorithms which compute the bore profile from the input impedance in the frequency domain. Acoustic reflectometry was initially developed to use with an acoustic pulse. However, the technique is been applied to improve the axial resolution of a cylindrical cavity by using other types of waveforms.

The application of acoustic reflectometry started in 1967. Schoeder [1] used this technique to obtain a rough estimate of the bore profile of a human vocal tract. In order to estimate the acoustic impedance, an electromechanical system was joined to a diaphragm to generate periodic incident acoustic waves, which propagated through a 4 m source tube. At the distal end, with a quite pronunciation from a patient of certain vocals, it was possible to make the physical interaction between the sound generated by a patient and the acoustic waves propagated. The vocal tract was estimated by using a complex algorithm based on the Fourier series. The axial resolution of the vocal tract as function of the distance depends on the number of eigenfrequencies calculated. The inconvenience of using this method lies in the fact that it requires knowing of the length of the vocal tract.

In 1969, Ware and Aki [2] solved the inverse problem in seismology by determining the reflection coefficients from a reflected acoustic wave generated by the propagation of an acoustic pulse (i.e. explosion of TNT) through the layers of the earth. It must be emphasized that both acoustic waves must be identified from each other. This research was initially developed to compute and compare the reflection coefficients generated when the incident acoustic wave was propagating through different densities of layers of the earth. Under certain experimental

conditions, it was possible to identify oil and water under the surface of the earth. However, averages of hundreds impulse responses were needed to improve the signal-to-noise ratio.

In Biomedical Engineering, this algorithm has been applied to compute the reflection coefficients from a unidirectional cylindrical cavity and estimate the cross sectional area as a function of distance. The inconvenience of using the Ware-Aki algorithm lies in the fact that it does not consider losses within the cylindrical cavity.

Sondhi and Gopinath [3], in 1971, described a way of using a loudspeaker joined with a long source tube which was used to drive an acoustic pulse into the vocal tract. The main idea of using a straight forward long 6 m source tube made possible a physical separation of the incident acoustic wave before the reflected acoustic wave was generated. Then, the Ware-Aki algorithm was implemented to estimate the cross sectional area of the vocal tract. In a later research with Resnick [4], they tried to compensate the acoustical losses for improving the axial resolution of a cylindrical cavity. However, the results were not sufficiently accurate because of all the approximations made.

In 1977, Jackson et al. [5, 6] estimated the area profiles of the throat of canine animals using the Ware-Aki algorithm. The acoustic pulse was generated by an electric spark. It allowed improving the content of acoustic energy; however, it was necessary to calculate an average of 1000 or more trials to improve the signal-to noise ratio.

The first reconstruction of a human upper airway by using the Ware-Aki algorithm is reported by Fredberg et al. [7] in 1980. Two more papers [8, 9] were published about this research during the 1980's. Basically, a loudspeaker was used to generate the incident acoustic wave which propagated in an environment composed of 80% He and 20% $O_2$. The goal of using this environment lied in the fact that it increased twice the speed of sound and reduced the acoustical losses. Hence, the patient was asked for breathing during two minutes before impacting the

incident acoustic wave. A comparison of results between an environment of propagation composed by $O_2$ and He-$O_2$ showed not a significant difference in the axial resolution as a function of the distance.

In 1981, Benade and Smith [10] used acoustic reflectometry to characterize musical wind instruments by comparing the acoustic impedance with respect to an acoustic pattern. A spark source was used to generate an acoustic pulse. However, it was necessary to calculate an average of the impulse responses for improving the signal-to-noise ratio. This research continued at the end of the 1980's by Watson and Bowsher [11, 12], who reported a DC offset component in the calculated impulse response when a loudspeaker was used. The DC component causes that the bore profile estimated to be characterized by either an expansion or contraction as a function of the distance. In this research, the dc component was manually adjusted until the reconstructed radius matched with a measured radius at an arbitrary position. This approach made a rigorous method of compensating the impulse response.

In the 1990's, Marshal, Mand, and Drummond [13, 14] designed and built a reflectometer which was characterized by having a short driving source tube 40 cm length. In general, the inconvenience of using a short reflectometer lies in the fact that complex algorithms in either frequency or time domain are required to identify the acoustic impedance. Thereby, the computational cost is high. The results reported were similar to those obtained by Fredberg et al. [7] who used a long source tube of 6 m to identify the reflected acoustic wave from the incident acoustic wave.

In 1993, Louis et al. [15, 16] reported a novel reflectometer with a length of the source tube of 30 cm. A second microphone was used to identify the incident acoustic wave from the reflected acoustic wave. A high pass filter was required to eliminate breathing noises in the computed

impulse response where the cutoff frequency was a function of the properties of internal wall in the upper airway.

In 1995, Amir, Rosenhouse, and Shimony [17, 18] developed a novel mathematical procedure referred as “layer peeling algorithm” to estimate the axial resolution of a cylindrical cavity. The layer peeling algorithm considers acoustical losses within the system through a space-time scattering equation. This algorithm estimates good results when the DC offset component in the acoustic impulse response is removed or compensated. The layer peeling algorithm did not require deconvolving the acoustic signals recorded to estimate the input impulse response of a cylindrical cavity. Amir reported the reconstruction of bore profiles of brass instruments with good results, however, the algorithm has not been since then implemented in biomedical engineering to estimate the human upper airway bore profile.

In 1997, Sharp [19] reported a reflectometer characterized by having a coiled driving 6m source tube. Hence, the space for a long straight forward source tube was not longer required. Sharp proposed the insertion of a 50 cm long cylindrical tube between the reflectometer and the cylindrical cavity of study. In this way, the dc component of the input impulse response was calculated and compensated. In this research, a comparison of results between the Ware-Aki algorithm and layer peeling algorithm was reported. A horn driver was used to generate the acoustic pulse. Sharp obtained good results using a stepped solid cylindrical cavity which was composed of three short cylindrical segments with different cross sectional area joined each other. Better results were obtained using the layer peeling algorithm than with the Ware-Aki algorithm. This was due to compensation of simple acoustical losses through the scattering equation in the layer peeling algorithm.

In 1998, Mansfield et al. [20] applied the acoustic reflectometry technique to qualitatively asses the position and patency of endotracheal tubes using rabbits. He designed a novel system which

connected either a reflectometer or a mechanical ventilator to an infant endotracheal tube. The system was controlled by a solenoid, such that a mechanical ventilator was connected to the infant endotracheal tube in a normal position. When the solenoid was activated by an electrical signal, the endotracheal tube was connected for few milliseconds to the reflectometer in order to generate an acoustic pulse, and to record the reflected signal. Visualizing the reflected acoustic wave in a time-pressure chart, it was possible to predict the patency along the cavity. In other words, it was possible to identify either a reduction or an expansion along the cylindrical cavity by inspection of the reflected acoustic wave. Because some patients in the Intensive Unit Care require ventilator assistance, nowadays, it is a very interesting application of acoustic reflectometry to find the position of any variation in diameter along endotracheal tubes due to secretions. When it occurs, a technician drains the tube to avoid a problem of asphyxia.

In 2000, Huang et al. [21] reported a modified version of Ware-Aki algorithm which was used to estimate cylindrical cavities with simple and short branches. The modified Ware-Aki algorithm was used to estimate the bore profile of a human nasal cavity. This application was used to assess the size and function of the pharynx during sleep. It was the first time that acoustic reflectometry was used to measure the nasopharynx in human patients.

In 2003, Forbes et al. [22, 23] proposed a singular system method, a powerful mathematical method, to deconvolve the input impulse response from both acoustic waves recorded by a reflectometer. Because singular values were gradually attenuated, Forbes et al. used an alternative procedure that combined both truncation and attenuation to estimate the impulse response. However, in this research a compensation factor was required to estimate good results. Forbes et al. used a stepped cylindrical cavity and recalled the layer peeling algorithm. They reported good results, which depended on the right number of eigenvalues selected. In this

research the signal-to-noise ratio is increased in all out spectral components by averaging the input pulse and the reflection measurements, generally require 1000 repetitions.

In the same year, Kausel [24] reported a suitable waveguide model which could be applied to estimate the bore profile of solid cylindrical cavities. The algorithm was based on the sensitivity of the input impedance magnitude, which was related to bore variation. The advantage of using this model lied in the fact that it was not necessary to measure the phase. However, it was very demanding to obtain high measurement accuracy. On the other hand, the model was suitable for as long as the bore dimensions were smaller than the wave lengths and the discontinuities were not too significant. Kausel reported good results for estimating the bore profile of a stepped cylindrical cavity.

In 2004, Babb et al. [25] reported a study to assess otitis media with effusion. In this research the estimation of a bore profile as function of the distance was not the parameter to be measured, but the difference of phase between the incident and the reflected acoustic waves. In order to quantify the phase shift, a reflectometer was used to impact a chirp signal in an ear channel. The chirp signal was used to sweep from 1.8 to 4.4 kHz. The reflection generated due to both the tympanic membrane and fluid filled ears produced an out of phase wave which was related to otitis media with effusion. They reported that it was possible to evaluate several levels of otitis media with effusion.

In 2005, Aijun et al. [26, 27] proposed to increase the axial resolution of the bore profile of a cylindrical cavity by combining the impulse responses obtained from acoustic pulses and bursts of sinusoidal acoustic wave packets. The former and later waves were used to sweep relatively low frequencies and relatively high frequencies, respectively. The layer peeling algorithm was recalled to estimate the bore profile of a steeped cylindrical cavity, and a compensation factor was required in the procedure to avoid the singular solution due to the low signal to noise ratio.

In 2006, Gligor et al. [28] conducted a pilot study for obtaining the acoustic reflectometry images associated with endotracheal tube in children using the Ware-Aki algorithm. In this research a novel reflectometer with a very short source tube of a few centimeters and two microphones was used to make of acoustic reflectometry a practical technique to evaluate the patency of endotraqueal tubes. The acoustic wave propagated through a flexible tube which was introduced into the endotracheal tube. The reflectometer was able to measure areas up to a maximal axial distance of 35 cm from the distal end of the wave tube. Instead of using an acoustic impulse, a truncated *sinc (x)* function was used to produce a band-limited impulse of 2 ms duration. A low-pass filter was used with a cutoff frequency of 3500 Hz to correct for minor oscillations and minimize profile instability. In this research the acoustical losses were low due to the fact that the acoustic reflectometer was introduced along the endotracheal tube. In a later research 2007, David [29] conducted a real-time study with a third-generation reflectometer to evaluate the placement of an endotracheal tube: tracheal, bronchial, or esophageal.

Kinar and Pomeroy [30], in 2009, used acoustic reflectometry to determine the location of the snow water equivalent. A maximum length sequence was used to model the sound pressure wave as it passed through the snowpack. Embedded systems were designed to implement the signal processing and calculations so that snow water equivalent could be quickly determined at a field location.

## 1.2 Problem statement

Acoustic reflectometry is generally classified as being an inexpensive technique and easy to be applied with the correct instrumentation.

Despite of acoustic reflectometry being used in biomedical engineering, it is necessary to update the method and make of this technique a more versatile way to evaluate the bore profile of a cylindrical cavity because:

1) The correct application of acoustic pulse reflectometry using the Ware-Aki algorithm requires calculating and eliminating the DC offset component generated when an acoustic pulse is propagated in the source tube. The most common way to compute the DC component consists of adding a DC source tube in the acoustic reflectometer. In other cases, the DC offset component has been calculated by trial and error, but this required the knowledge of the bore profile of the cavity of study.

2) The layer peeling algorithm, used to compensate the acoustical losses, has only been implemented to estimate the bore profile of solid cylindrical cavities. Its right application requires a compensation factor in the estimation of the impulse response to avoid the high level of noise at high frequencies. It also requires the DC offset cancellation.

3) The size of instrumentation used has been reduced at present time, but the computational cost is increased due to the use of robust algorithms to identify both acoustic waves.

4) The frequency response obtained in acoustic pulse reflectometry requires an average of thousands of signals to improve the signal-to-noise ratio. So, it makes of acoustic reflectometry a rigorous technique to be applied.

5) The main problem in acoustic pulse reflectometry lies in the fact that it is limited in frequency, because it is not accurate enough in representing a true impulse. In spite of the acoustic pulse has been generated by using several loudspeakers and electric discharges.

## 1.3 Proposed solution

Initially, it is emphasized that the use of Gaussian-modulated acoustic packets has been implemented in the layer peeling algorithm by Aijun et al. [26]. In such application, the frequency impulse response was obtained by combining an acoustic pulse and Gaussian modulated acoustic packets. It allowed for the increasing of the frequency response of a stepped cylindrical cavity.

The solution of the inverse problem in this dissertation consists of:

i) Recalling the Ware-Aki algorithm to apply Gaussian modulated sinusoidal packets in the Ware-Aki algorithm. It allows focusing over certain ranges of frequency and superposing the impulse responses obtained along the frequency bandwidth. This approach is not possible when acoustic pulses are used.

ii) Developing a simulation model to evaluate the acoustic parameters in the solution of the inverse problem through the quadratic error of the bore profile and determine the minimum content of frequency required in an experimental measurement.

iii) Using a long source tube to physically identify the acoustic waves and reduce the computational cost. It may also be used to record a stable sound signal such that the amplitude, phase, and DC offset component is calculated by using a least mean square analysis. So, the frequency response of a cylindrical cavity is obtained and the DC offset component is eliminated.

iv) Evaluating the axial resolution of the bore profile as function of the frequency step size to sweep the entire frequency bandwidth. Instead of using thousands of acoustic pulses and Gaussian modulated packets, the solution of the inverse problem is evaluated by using 200 sound waves and only one loudspeaker.

v) Filtering undesired components of frequency and improving the signal-to noise ratio by using matched filter. In this way, the entire audible range of frequency is swept.

vi) Compensating the losses in the frequency impulse response experimentally measured. Thereby, a characterization of amplitude and phase as function of frequency is performed by using propagation of acoustic waves. The acoustic pressures are recorded in three different positions along the source tube to calculate their attenuation.

In summary, acoustic waves modulated in amplitude are used to compute the impulse response of a cylindrical cavity by sweeping several frequency intervals, which cover a total frequency bandwidth from 50 Hz to 10 kHz. The total impulse response of a cylindrical cavity is obtained by superposition and the bore profile of such cavity is calculated from the reflection coefficients computed by the Ware-Aki algorithm. Relatively low frequencies are used to estimate the general bore profile of a cylindrical cavity and relatively high frequencies are used to refine the result.

This dissertation includes a simulation model and experimental measurements. Thereby, the results obtained in the simulation model are validated using two solid cylindrical cavities; a cylindrical cavity with a square bore profile and a vitro model which represent the bore profile of a human upper airway. The results obtained are discussed to define a possible application in patients.

## 1.4 Outline of dissertation

This research work is presented in six chapters:

Chapter 2 describes the acoustic coefficients required to define the cross sectional area as function of reflection coefficients. It is known as the solution of the forward problem.

In Chapter 3, The Ware-Aki algorithm is described in terms of the Space-Time diagram. The link between the reflection coefficients and the input pulse response (or vice versa) is discussed.

Chapter 4 describes the design and characterization of the acoustic reflectometer used in the experimental measurements. The parameters used to generate the sound waves are discussed and the entire solution of the inverse problem is described. It is also shown the way to compensate the losses along the source tube.

In Chapter 5, the simulation model is described to evaluate the independent parameters in the solution of the inverse problem for six different cylindrical cavities. The results described are used to test the fact of estimating a bore profile.

Chapter 6 shows the validation of solving the inverse problem by using Gaussian modulated acoustic waves. A solid cylindrical cavity is coupled to the reflectometer to compare the results in both the experimental situation and the simulation model.

Chapter 7 describes the simulation model of a model in vitro which represents the bore profile of an upper airway.

The last chapter discussed the limits in the solution of the inverse problem and the future enhancement.

# Chapter 2

# Acoustic Coefficients and the Space-time Diagram

## 2.1 Introduction

The sound waves used in acoustic reflectometry must propagate along an axially unidirectional cylindrical pipe which is referred as the source tube. The theory used in acoustic reflectometry [31] assumes a plane wavefront. In consequence of the assumption, the wavelength must be larger than the diameter of the source tube.

The frequency content of such waves must lie in the audible range (20 Hz-20 kHz). When the acoustic waves lie in the ultrasound range (> 20 kHz), the sound wave does not propagate along an axially unidirectional direction and starts to bounce in a zig-zag pattern [20]. So, a distortion of the acoustic waves occurs during the propagation.

In order to understand the theory considered in acoustic reflectometry, this chapter starts with the general solution of one-dimensional wave equation to define the acoustic coefficients which are used to estimate the cross sectional area as function of the distance.

The Space-Time diagram [19] is discussed to compute the input pulse response from the acoustic coefficients, which are directly related to the bore profile of a cylindrical cavity. This is known as the forward problem.

## 2.2 Acoustic propagation in a simple cylindrical cavity

The nature of an acoustic wave requires a medium of propagation to travel from one point to another. To represent the propagation of an acoustic wave along the *x*-axis as a function of the time *t*, it is necessary to recall the wave equation in terms of the acoustic pressure ***P***, given by

$$\frac{\partial^2 \boldsymbol{P}}{\partial x^2} = \frac{1}{c^2}\frac{\partial^2 \boldsymbol{P}}{\partial t^2} \tag{2.1}$$

This equation is named the linear equation because it assumes that the medium of propagation is lossless, homogeneous and isotropic. Where *c* denotes the speed of sound given in m/s , which in turn depends on the temperature $\tau$ ºC of the medium of propagation by

$$c = 331.6\sqrt{1+\frac{\tau}{273}} \tag{2.2}$$

The general solution of (2.1) is given by

$$\boldsymbol{P}(x,t) = \boldsymbol{P}^{+}(x,t) + \boldsymbol{P}^{-}(x,t) \tag{2.3}$$

Where $\boldsymbol{P}^{+}(x,t)$ represents an acoustic wave propagating along the positive x-direction and $\boldsymbol{P}^{-}(x,t)$ denotes an acoustic wave propagating along the negative x-direction. Mathematically, each acoustic wave is defined as

$$\boldsymbol{P}^{+}(x,t) = \boldsymbol{P}^{+} e^{j(\omega t - k x)} \tag{2.4}$$

and

$$\boldsymbol{P}^{-}(x,t) = \boldsymbol{P}^{-} e^{j(\omega t + k x)} \tag{2.5}$$

Where $\boldsymbol{P}^{+}$ and $\boldsymbol{P}^{-}$ are the acoustic pressures at time $t$ for a given position $x$, ω is the angular frequency given by

$$\omega = 2\,\pi\, f \tag{2.6}$$

The frequency $f$ is given in Hz, and the wave number $k$ in $m^{-1}$, which in turn is given by

$$k = \frac{\omega}{c} \tag{2.7}$$

The wave number is a parameter that characterizes the phase progress of the sound wave.

## 2.3 Continuity equations between two cylindrical segments

In the rest of this document, the notation used to represent the dependence of time and distance in the propagation of an acoustic wave is simplified, in order to specify the cylindrical segment where the acoustic wave is propagating. It will make it easier to explain all the theory used in later chapters.

In the next sections, an upper positive sign denotes propagation along the positive *x*-direction; a upper negative sign denotes propagation along the negative *x*-direction and the lower sub-index denotes propagation through a given cylindrical segment.

To relate the propagation of an acoustic wave to the acoustic coefficients (reflection and transmission coefficients), assume two cylindrical cavities with different cross sectional areas given by $S_0$ and $S_1$, joined at $X=0$.

When an incident acoustic wave $P_0^+$ propagates along the first cylindrical cavity $S_0$, a reflected acoustic wave $P_0^-$ is generated, after the former acoustic wave finds a change in acoustic impedance which, in turns is related to a change in the cross sectional area in the second cylindrical segment $S_1$. At the same time, a transmitted acoustic wave $P_1^+$ is propagated along the second cylindrical segment $S_1$. Figure 1 shows the respective acoustic waves generated and propagated along its respective cylindrical segment.

This pattern is repeated in both directions as soon as each acoustic wave generated finds a discontinuity along its way of propagation. The number of sample of acoustic pressure recorded becomes an important parameter to increase the resolution and represent both forward and backward space-time propagations which are directly related with a change in diameter along a cylindrical cavity.

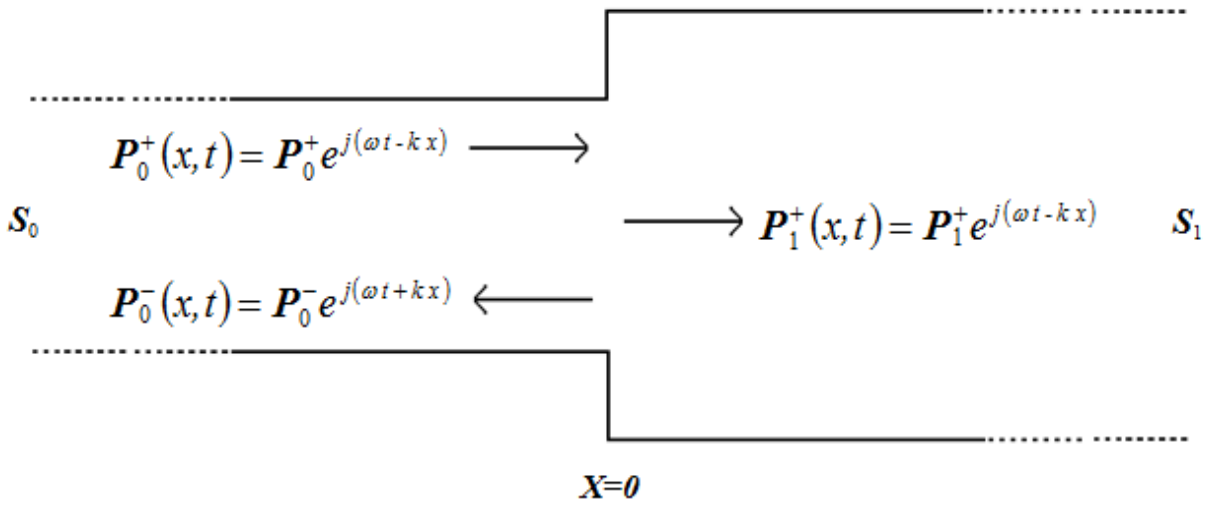


Figure 1. Change in acoustic impedance in a cylindrical cavity.

The boundary conditions at X require continuity of the acoustic pressure $\boldsymbol{P}$ and volume velocity $\boldsymbol{U}$, that is

$$\boldsymbol{P}_0^+ + \boldsymbol{P}_0^- = \boldsymbol{P}_1^+ \tag{2.8}$$

and

$$\boldsymbol{U}_0^+ + \boldsymbol{U}_0^- = \boldsymbol{U}_1^+ \tag{2.9}$$

Those continuity equations are used in acoustic reflectometry when the wavefront of the wave is assumed to be planar and normal to the direction of propagation.

## 2.4 Acoustic coefficients in terms of specific acoustic impedance

The specific acoustic impedance $\boldsymbol{Z}$ of a fluid at a cross sectional area $\boldsymbol{S}$ is defined as the complex ratio of acoustic pressure $\boldsymbol{P}$ and the volume velocity $\boldsymbol{U}$. Mathematically, it means that

$$\boldsymbol{Z} = \frac{\boldsymbol{P}}{\boldsymbol{U}} \tag{2.10}$$

Hence, it is possible to define the specific acoustic impedance for each cylindrical segment denoted by $\boldsymbol{Z}_0$ and $\boldsymbol{Z}_1$. Dividing (2.9) by (2.8) gives

$$\frac{\boldsymbol{P}_0^+ + \boldsymbol{P}_0^-}{\boldsymbol{U}_0^+ + \boldsymbol{U}_0^-} = \frac{\boldsymbol{P}_1^+}{\boldsymbol{U}_1^+} \tag{2.11}$$

After some algebraic manipulations, and using (2.10), it is possible to define the reflection coefficient $r_{01}$ in terms of either specific acoustic pressure or specific acoustic impedance as

$$r_{01} = \frac{\boldsymbol{P}_0^-}{\boldsymbol{P}_0^+} = \frac{\boldsymbol{Z}_1 - \boldsymbol{Z}_0}{\boldsymbol{Z}_1 + \boldsymbol{Z}_0} \tag{2.12}$$

Physically, the reflection coefficient $r_{01}$ is the ratio of the pressure amplitude of the reflected acoustic wave and the pressure amplitude of the incident acoustic wave between cylindrical segments $\boldsymbol{S}_0$ and $\boldsymbol{S}_1$.

When (2.8) is divided by $\boldsymbol{P}_0^+$, the transmission coefficient $t_{01}$ may be defined as

$$t_{01} = \frac{\boldsymbol{P}_1^+}{\boldsymbol{P}_0^+} = 1 + r_{01} \tag{2.13}$$

The transmission coefficient $t_{01}$ is thus defined as the ratio of the pressure amplitude of the transmitted acoustic wave to the pressure amplitude of the reflected acoustic wave, between both cylindrical segments $\boldsymbol{S}_0$ and $\boldsymbol{S}_1$, respectively. In terms of the specific acoustic impedance, the reflection coefficient may also be given as

$$t_{01} = \frac{2\boldsymbol{Z}_1}{\boldsymbol{Z}_1 + \boldsymbol{Z}_0} \tag{2.14}$$

Note that both acoustic coefficients are defined by a change in acoustic impedance.

## 2.5 Acoustic coefficients in terms of cross sectional area

When an acoustic wave propagates through a cylindrical cavity with a cross sectional area $\boldsymbol{S}$, the specific acoustic impedance $\boldsymbol{Z}$ is related with the characteristic impedance $\mathbf{Z}_c$ by

$$\boldsymbol{Z} = \frac{\mathbf{Z}_c}{\boldsymbol{S}} \tag{2.15}$$

The characteristic impedance $\mathbf{Z}_c$ is a material property of the medium where the acoustic wave propagates and it is the given by

$$\mathbf{Z}_c = c\rho \tag{2.16}$$

Where $\rho$ is the density of the medium given in kg $m^{-3}$. Substituting (2.16) into (2.15), it defines the specific acoustic impedance for each cylindrical segment described in Figure1 as

$$\boldsymbol{Z}_0 = \frac{c\rho}{\boldsymbol{S_0}} \tag{2.17a}$$

$$\boldsymbol{Z}_1 = \frac{c\rho}{\boldsymbol{S_1}} \tag{2.17b}$$

Assuming that the acoustic wave is propagated through the same medium in both cylindrical segments, (2.12) and (2.14) may be recalled to define the acoustic coefficients as functions of specific acoustic impedance $\boldsymbol{Z}_0$ and $\boldsymbol{Z}_1$, given by equation (2.17). Thereby, the reflection

coefficient and the transmission coefficient are defined in terms of the cross sectional area $\boldsymbol{S}_0$ and given by

$$r_{01} = \frac{\boldsymbol{S}_0 - \boldsymbol{S}_1}{\boldsymbol{S}_0 + \boldsymbol{S}_1} \tag{2.18}$$

and

$$t_{01} = \frac{2\boldsymbol{S}_0}{\boldsymbol{S}_0 + \boldsymbol{S}_1} \tag{2.19}$$

The previous equations were deduced by Kinsler [18], and it is noted that each acoustic coefficient depends on a change in the cross sectional area. These equations are used when the incident acoustic wave propagates in a positive x-direction. A similar analysis is performed to obtain the acoustic coefficients when the acoustic wave propagates in the negative x-direction, that is

$$r_{10} = \frac{\boldsymbol{S}_1 - \boldsymbol{S}_0}{\boldsymbol{S}_0 + \boldsymbol{S}_1} = -r_{01} \tag{2.20}$$

and

$$t_{01} = \frac{2\boldsymbol{S}_1}{\boldsymbol{S}_0 + \boldsymbol{S}_1} = 1 + r_{01} = 1 - r_{01} \tag{2.21}$$

Because the acoustic wave is bouncing on each cylindrical segment until the acoustic pressure decay as function of the time, it is necessary to define the transmission loss equation as

$$t_{01}\, t_{10} = (1 + r_{01})(1 - r_{01}) = 1 - r_{01}^2 \tag{2.22}$$

Because the transmission coefficient is represented as a function of the reflection coefficient between two consecutive cylindrical segments, the transmission loss equation is defined as a function of the reflection coefficient.

## 2.6 Space-Time diagram

It is possible to extend this theory and consider a long cylindrical cavity composed by different cylindrical segments joined each other. A better representation of the history of propagation of an acoustic pulse through a long cylindrical cavity is described by a Space-Time diagram. Mathematically, the incident acoustic wave is represented by a discrete delta function represented as

$$\boldsymbol{P}^{+}[n] = \delta[n] = \begin{cases} 1 & \rightarrow \quad n = 0 \\ 0 & \rightarrow \quad n \neq 0 \end{cases} \tag{2.23}$$

and the reflected acoustic wave is referred as the input impulse response $iiir$ given by

$$\boldsymbol{P}^{-}[n] = iiir[n] \tag{2.24}$$

When the acoustic pulse δ[n] is propagated through the cylindrical cavity, all forward and reflected acoustic waves are represented as a Space-Time function, see Figure 2.

Several forward and backward propagations are generated as function of time (along the vertical time axis) when each acoustic propagation passes through a variation in the cross sectional area (along the horizontal distance axis).

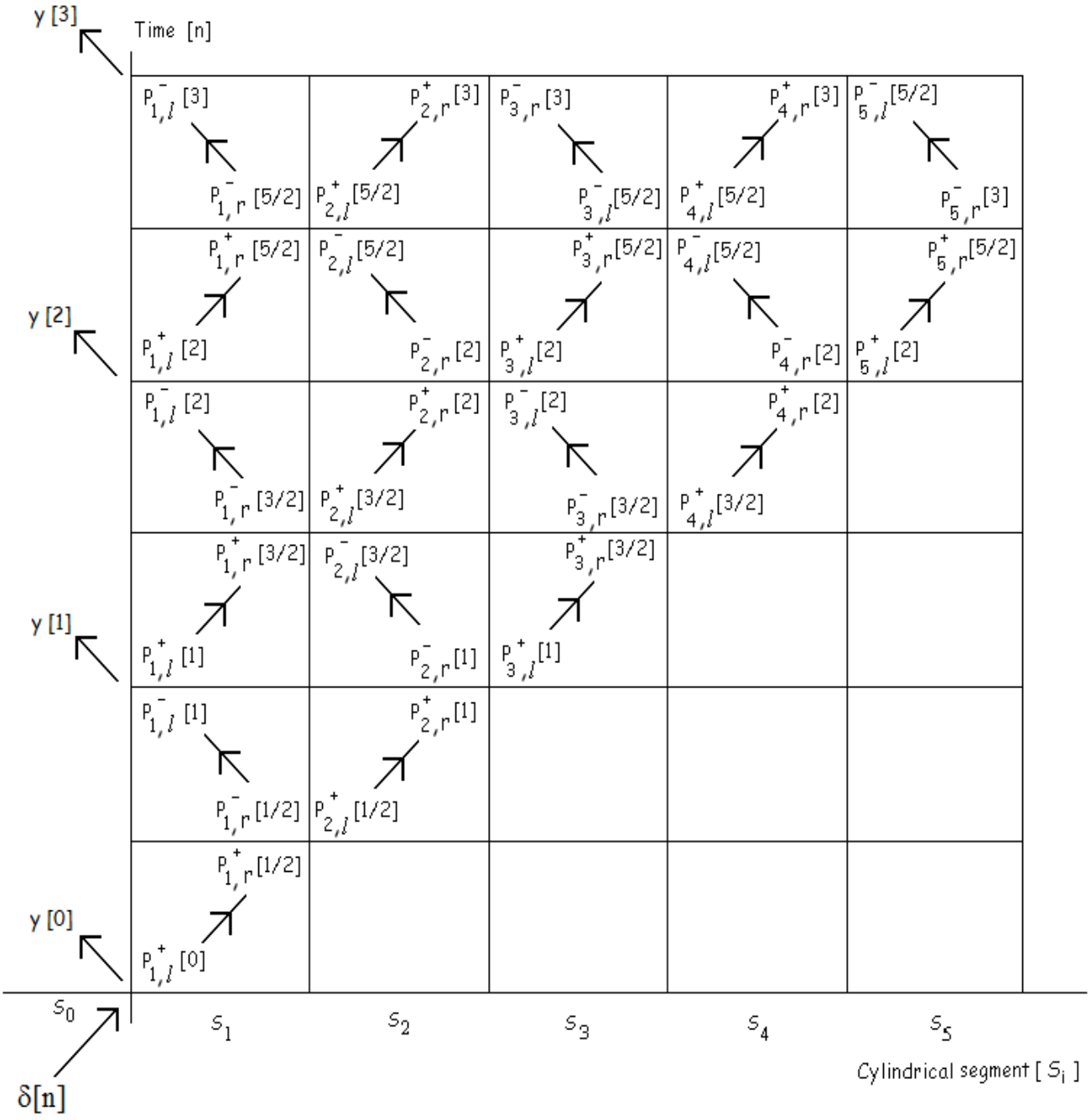


Figure 2. Space-Time diagram.

Each acoustic pressure in the Space-Time diagram is denoted by both upper and lower indices, which define the acoustic pressure for a given Space-Time relationship. The direction of propagation of the acoustic wave is denoted by a sign and the time of propagation is denoted by square brackets. The lower sub-indexes denote, by a number, the cylindrical segment in which the acoustic wave propagates and the letters *l* and ***r*** denote the position of the front wave at either proximal end or distal end of each cylindrical segment. The sub-index *l* is used to indicate that the front wave of the acoustic wave is located to the left side or the proximal end. The sub-index ***r*** denotes that the front wave of the acoustic wave is located to the right side or the distal end for each cylindrical segment.

It is evident that the axial resolution increases with the number of pressure waves recorded. The Space-Time diagram is characterized to be a causal system because a reflected wave is only generated when an incident wave finds a discontinuity in the cross sectional area along the cylindrical cavity. Thereby, the Space-Time diagram is characterized to indicate zero acoustic pressure below the main diagonal.

### 2.6.1 Impulse response in terms of acoustic coefficients

In terms of acoustic signals recorded (incident and reflected) by a reflectometer, the incident acoustic wave is represented in the Space-Time diagram by only a forward pressure wave, located at the origin $\delta[n]$. All backward acoustic pressures $y[n]$ displayed on the left side along the y-axis represent the entire reflected acoustic wave as function of time. Hence, the Space-Time diagram describes in sequential order the generation of the reflected acoustic wave $y[n]$ in terms of both forward and reflected acoustic waves which are directly related to both the reflection and transmission coefficients.

It is assumed that an acoustic pulse is generated and propagated through the source tube with a uniform cross sectional area $\boldsymbol{S}_0$. For n = 0, a reflected acoustic wave is generated when the incident wave δ[n] finds a change in the acoustic impedance due to the variation in the cross sectional area between both cylindrical segments $\boldsymbol{S}_0$ and $\boldsymbol{S}_1$. The first value of the reflected acoustic wave $y[0]$ is given by the ratio of both acoustic amplitude pressures, which defines the first reflection coefficient, that is

$$y[0] = \frac{\boldsymbol{P}_{0,r}^{-}}{\boldsymbol{P}_{0,r}^{+}} = r_{0,1} \tag{2.25}$$

The Space-Time diagram shows that the path to compute the next value of the reflected acoustic wave, for n = 1, is composed of a forward transmitted acoustic wave between segments $\boldsymbol{S}_0$ and $\boldsymbol{S}_1$, a backward reflected acoustic wave between segments $\boldsymbol{S}_1$ and $\boldsymbol{S}_2$, and a backward transmitted acoustic wave between segments $\boldsymbol{S}_0$ and $\boldsymbol{S}_1$. Using the transmission loss (2.22), it is possible to represent the value for $y[1]$by

$$y[1] = \overrightarrow{t}_{0,1}\,\overleftarrow{r}_{1,2}\,\overleftarrow{t}_{1,0} = r_{1,2}(1 - r_{0,1}^2) \tag{2.26}$$

For n = 2, the value of the reflected acoustic wave is composed of two acoustic trajectories denoted as a primary reflection and a high order reflection.

$$y[2] = \vec{t}_{0,1}\,\vec{t}_{1,2}\,\vec{r}_{2,3}\,\vec{t}_{2,1}\,\vec{t}_{1,0} - \vec{t}_{0,1}\,\vec{r}_{1,2}\,\vec{r}_{0,1}\,\vec{r}_{1,2}\,\vec{t}_{1,0}$$

$$y[2] = r_{2,3}\left(1 - r_{1,2}^2\right)\left(1 - r_{0,1}^2\right) - r_{1,2}^2 r_{0,1}\left(1 - r_{0,1}^2\right) \tag{2.27}$$

A primary reflection refers that the reflected acoustic wave is composed of one simple reflection, while a high reflection is composed by more than one simple reflection. This is noted in the Space-Time diagram.

The path to obtain the values of the reflected acoustic wave for n = 3 is composed of 5 high acoustic trajectories. The reader should be able to determine the possible paths to define the value of the reflected acoustic wave. The computational process becomes more and more complex for n=4, 5, 6,….n-1.

The simulation model developed in this dissertation uses the sequential structure of the Space-Time diagram in both forward and inverse problems to estimate the reflected acoustic wave and compute the impulse response of a cylindrical cavity, respectively. The mathematical procedure to decompose the impulse response and obtain the reflection coefficients is referred as Ware-Aki algorithm [2] which is described in a later section.

## 2.7 Forward problem in acoustic reflectometry

In order to represent the bore profile of a cylindrical cavity as a tridimensional relationship, it is necessary to quantify the *l* axial length. This parameter represents the length of each cylindrical segment used along the *x*-axis in the Space-Time diagram. When the temperature in the medium of propagation is assumed to be isotropic, the sampling frequency is the only parameter involved to define the *l* axial length as

$$l = \frac{c}{2F_s} \tag{2.28}$$

$F_s$ represents the sampling frequency used to record the acoustic waves. Physically, it means that a cylindrical cavity is composed of short cylindrical segments, joined each other, with a cross sectional area $\boldsymbol{S}_n$ and a constant axial length $l$. Hence, the higher the sampling frequency, the more the cylindrical segments required to represent an entire cylindrical cavity.

Mathematically, the cross sectional area of an entire cylindrical cavity is represented as a function of the $l$ axial length by a row vector. In other words, each value represents the cross sectional area of each cylindrical segment with an axial length $l$.

$$\textit{cross}\ \text{sectional area} = \begin{bmatrix} \boldsymbol{S}_0 & \boldsymbol{S}_1 & \dots & \boldsymbol{S}_n \end{bmatrix}$$

Graphically, the longitudinal axial resolution is shown in Figure 3. Note the bore profile is assumed to have an infinite length.

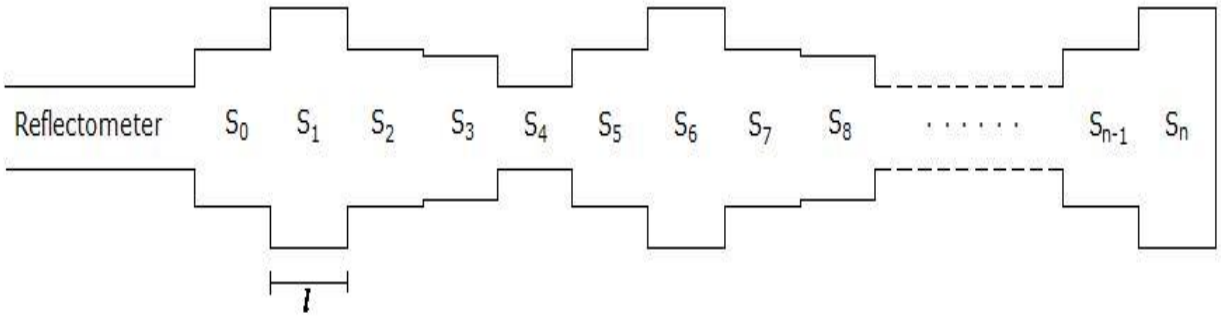


Figure 3. A cylindrical cavity describe in terms of the axial length $l$.

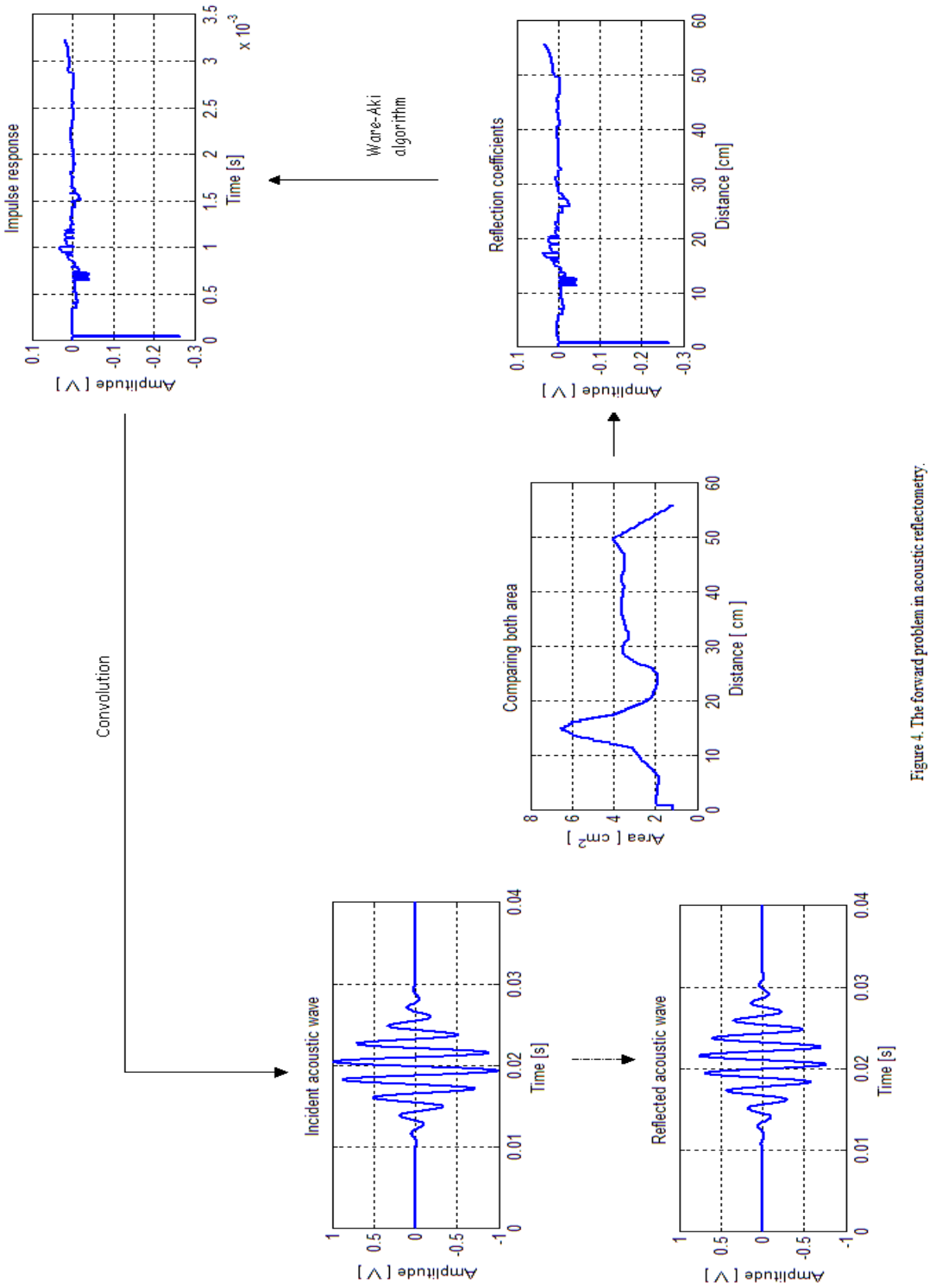


Figure 4. The forward problem in acoustic reflectometry.

In this dissertation, the forward problem consists of computing the reflection coefficients from a known cylindrical cavity by using (from 2.18 to 2.22) obtained by Kinsler [31]. Then, the impulse response is obtained from the reflection coefficients using the Ware-Aki algorithm, to be described in Chapter 3.

The forward problem is then used in acoustic reflectometry to perform the convolution between the input impulse response and an incident acoustic wave. In this way, the reflected acoustic wave is predicted. A block diagram is shown in Figure 4. This simple solution, to estimate the acoustic waves, does not consider the acoustical losses that there exist in the cavity.

The forward problem is implemented to test several mathematical procedures and deconvolve the impulse response from the acoustic signals which are recorded by a reflectometer. Thereby, it is possible to evaluate the solution of the inverse problem and estimate the appropriate experimental conditions.

The forward problem is used in the simulation model to cover a frequency bandwidth. Theoretically, there is no limit in the frequency generated. However, because there are constraints mentioned in the introduction, the allowed frequency bandwidth is the audible range.

## 2.7 Concluding remarks

The relationship between the cross sectional area and the reflection coefficients has been discussed using the Space-Time diagram. The analysis shows that not only a reflected and a transmitted acoustic wave are generated when they strike an object, but also they are generated when the incident acoustic wave finds a change in the acoustic impedance due to a change in the bore profile of a cylindrical cavity.

# Chapter 3

# Reconstruction Algorithm

## 3.1 Introduction

The efficiency of the reconstruction algorithms [2, 17, 18, 24] developed in acoustic reflectometry has been evaluated in different experimental conditions. For instance, they have been tested in solid stepped cylindrical cavities, musical wind instruments, model in vitro of the respiratory system, and real upper airways.

No matter what algorithm may be used, the acoustic signals must require of having a high signal-to-noise ratio along a wide frequency bandwidth and a low DC offset component generated in the propagation of an acoustic wave within the source tube. Under ill-conditions, the algorithms estimate a cross sectional area of either long expansions or small reductions as function of the distance. It is a consequence of the accumulative error on each iteration.

Despite of the Ware-Aki algorithm [2] does not consider losses within the cylindrical cavity, it is still been used like reference to processing the signals acquired by several biomedical devices [25, 28, 29, 32] to estimate either the bore profile of a human upper airway or the patency of an endotracheal tube. Its performance in real-time applications [33] makes of this algorithm a good biomedical tool. Hence, it is necessary to evaluate its performance using other type of acoustic pulses like Gaussian-modulated sinusoidal waves. This chapter is entirely dedicated to describe the Ware-Aki algorithm and its role in both forward and inverse problems.

## 3.2 Reflection coefficients in terms of input pulse response

In the solution of the forward problem, the Ware-Aki algorithm is recalled to compute the input impulse response of a cylindrical cavity. Thereby, this algorithm is the link between the impulse response of a cylindrical cavity and its reflection coefficients.

In terms of the acoustic waves displayed in the Space-Time diagram, the Ware-Aki algorithm is a powerful mathematical method to relate such acoustic waves recorded by an acoustic reflectometer, y[n] and δ[n], with the information of the bore profile of a cylindrical cavity. This part in the solution of the inverse problem and, the entire solution is described in Chapter 4.

The discussion of the Ware-Aki algorithm starts recalling (2.25).

$$r_{0,1} = y[0] \tag{3.1}$$

Because the incident acoustic wave is a delta function δ[n], the first reflection coefficient between cylindrical segments $\boldsymbol{S}_0$ and $\boldsymbol{S}_1$ is defined by the first amplitude value in the reflected acoustic wave $y[0]$.

Recalling (2.26), it is possible to define the second reflection coefficient between cylindrical segments $\boldsymbol{S}_1$ and $\boldsymbol{S}_2$ to have that

$$r_{1,2} = \frac{y[1]}{\left(1 - r_{0,1}^2\right)} \tag{3.2}$$

Using the first reflection coefficient $r_{01}$ and the second value of the reflected acoustic wave $y[1]$, the second reflection coefficient is calculated.

Now, recalling (2.27), the third reflection coefficient is given by

$$r_{2,3} = \frac{y[2] + r_{0,1}\ \mathrm{r}_{1,2}^2 \left(1 - r_{0,1}^2\right)}{\left(1 - r_{0,1}^2\right)\left(1 - r_{1,2}^2\right)} = \frac{y[2] + r_{0,1}\ \mathrm{r}_{1,2}\ \mathrm{y}[1]}{\left(1 - r_{1,2}^2\right)\left(1 - r_{1,2}^2\right)} \tag{3.3}$$

Note that the values obtained on (3.1), (3.2), and the third value of the reflected acoustic wave $y[2]$ must be required to compute the third reflection coefficient between segments $\boldsymbol{S}_2$ and $\boldsymbol{S}_3$. The above analysis shows the base to explain the Ware-Aki algorithm. In other words, it must be noticed that each new reflection coefficient may be computed by a recursive process which depends on the previously computed values.

It may be also deduced that the error computed is recursively increased when there is either a low signal-to-noise ratio or a significant DC offset component in the acoustic waves recorded. Those issues are discussed in Chapter 4.

## 3.3 Ware-Aki algorithm

The Ware-Aki algorithm computes the reflection coefficients by using a recursive equation, that is

$$r_{i,i+1} = \frac{\sum_{m=0}^{i-1} a_m\ y[i - m]}{\prod_{m=0}^{\mathrm{i-1}} \left(1 - r_{m,m+1}^2\right)} \tag{3.4}$$

where

$r_{i,i+1}$ denotes the new reflection coefficient between two consecutive cylindrical segments $i$ and $i$+1.

$r^2_{m,m+1}$ is the previous reflection coefficient between segments $m$ and $m$+1.

$y[i-m]$ is the value of pressure of the reflected acoustic wave at y[$n$].

and

$a_m$ is the coefficient of $z^m$ recursive polynomial denoted by $A_{i-1}(z)$.

The recursive polynomial $A_{i-1}(z)$ is defined as function of $z$ which denotes a delay for each value computed for $y[n]$. This polynomial increases its order as function of each new reflection coefficient computed. This general recursive polynomial is given by

$$A_{i-1}(z) = a_0 + a_1 z + a_2 z^2 + \ldots + a_{i-1} z^{i-1} \tag{3.5}$$

It must be emphasized that only the coefficients $a_m$ are used in (3.4), which represent the reflection coefficients previously calculated.

The mathematical procedure to compute all coefficients of $A_{i-1}(z)$ is a little bit more robust because such recursive polynomial depends, at the same time, on other recursive polynomial denoted by $B_{i-1}(z)$.

Mathematically, both polynomials are given by

$$A_{i-1}(z) = A_{i-2}(z) + z\, r_{i-1,i}\, B_{i-2}(z) \tag{3.6}$$

$$B_{i-1}(z) = r_{i-1,i} A_{i-2}(z) + z\, B_{i-2}(z) \tag{3.7}$$

The next two initial conditions must be used in the process to compute the reflection coefficients

$$A_0(z) = 1 \tag{3.8}$$

and

$$B_0(z) = r_{01} \tag{3.9}$$

The respective values for n = [0, 1, 2, 3] of $A_{i-1}(z)$ recursive polynomial are shown below.

$$A_0(z) = 1 \tag{3.10}$$

$$A_1(z) = 1 + r_{0,1}r_{1,2}z \tag{3.11}$$

$$A_2(z) = 1 + \left(r_{0,1}r_{1,2} + r_{1,2}r_{2,3}\right)z + \left(r_{0,1}r_{2,3}\right)z^2 \tag{3.12}$$

$$A_3(z) = 1 + \left(r_{0,1}r_{1,2} + r_{1,2}r_{2,3} + r_{2,3}r_{3,4}\right)z + \left(r_{1,2} + r_{0,1}r_{2,3} + r_{0,1}r_{2,3}r_{2,3}\right)z^2 + \left(r_{0,1}r_{3,4}\right)z^3 \tag{3.13}$$

On the other hand, the respective $B_{i-1}(z)$ polynomials for n = [0, 1, 2, 3] are given by

$$B_0(z) = r_{0,1} \tag{3.14}$$

$$B_1(z) = r_{1,2} + r_{0,1}z \tag{3.15}$$

$$B_2(z) = r_{2,3} + \left(r_{0,1}r_{1,2}r_{2,3}\right)z + r_{0,1}z^2 \tag{3.16}$$

$$B_3(z) = r_{3,4} + \left(r_{0,1}r_{1,2}r_{3,4} + r_{1,2}r_{2,3}r_{3,4} + r_{2,3}\right)z + \left(r_{0,1}r_{2,3}r_{3,4} + r_{0,1}r_{1,2}r_{2,3} + r_{1,2}\right)z^2 + r_{0,1}z^3 \tag{3.17}$$

The reader may be able to compute other next possible values, but the computational method strictly requires of calculating both polynomials for each iteration.

## 3.4 Computing the axial resolution of a cylindrical cavity

Once all reflection coefficients $r_{i,i+1}$ have been calculated, the axial resolution may be computed by using the next recursive equation

$$\boldsymbol{S}_{i+1} = \boldsymbol{S}_i \frac{1 - r_{i,i+1}}{1 + r_{i,i+1}} \tag{3.18}$$

The variable $\boldsymbol{S}_i$ denotes an initial condition, which represents the cross sectional area of the source tube, $\boldsymbol{S}_{i+1}$ denotes the cross sectional area for the *i*-cylindrical segment which composed the entire cylindrical cavity, see Figure 3.

Hence, the first initial condition $\boldsymbol{S}_0$, for $i = 0$, and the first reflection coefficient $r_{0,1}$ are used to estimate the area of the first cylindrical segment $\boldsymbol{S}_1$. This value is again used, in the next iteration as the new initial condition, besides the reflection coefficient $r_{1,2}$, to estimate the cross sectional area of $\boldsymbol{S}_2$.

The procedure is repeated until all reflection coefficients are used. The number of reflection coefficients required to estimate the entire bore profile is a function of the sampling frequency which, in turn is related to the *l* axial length defined in equation (2.28). When all reflection coefficients computed from the impulse response are used, it is possible to estimate the bore profile of the current cylindrical cavity of study and a further bore profile is computed from later multiple reflections. Note that the error in the estimated bore profile of each cylindrical segment may be increased due to the round off error. So, it is important to implement a good digital signal processing to filter the acoustic waves such that the noise does not be considered as a factor of increasing the round off error.

## 3.5 Concluding remarks

In general, the Ware-Aki algorithm is a recursive equation based on recursive *z*-polynomials to compute all reflection coefficients as function from a Space-Time relationship. The Ware-Aki algorithm is a robust mathematical procedure, but this algorithm becomes an easy computational procedure when it is well implemented by software. Finally, the recursive equation to compute the bore profile from the reflection coefficients previously calculated was also discussed.

# Chapter 4

# Inverse Problem in Acoustic Reflectometry

## 4.1 Introduction

In the history of acoustic pulse reflectometry several ways to improve the quality in the sound waves have been tested. In this way, the content of acoustic energy has been improved, but the frequency content is still limited. Hence, new ways to improve the frequency response of a cylindrical cavity are required in the solution of the inverse problem.

Acoustic reflectometry, not only requires a reconstruction algorithm, but also an efficient way to deconvolve the impulse response from the acoustic waves generated and recorded from the acoustic reflectometer.

In this chapter, the instrumentation required in the building of an acoustic reflectometer is described. Because Gaussian-modulated acoustic packets are used in the Ware-Aki algorithm, the procedure to compute the impulse response, the compensation of losses along the source tube, and the DC offset component generated in the propagation of sound waves are also described. At the end, all sections are recalled to define the solution of the inverse problem.

## 4.2 Acoustic reflectometer

In order to analyze the acoustic signals, it is necessary to design and build an acoustic reflectometer, which is defined as all required instrumentation to generate and record the acoustic waves produced by the propagation of an incident wave through a source tube.

A Gaussian-modulated sinusoidal wave data base is generated in Matlab software. The signals are exported into a digital acquisition card, Biopac MP150. This system has input/output channels, which allow generating and recording the signals required. Hence, the Biopac system is used to drive a digital waveform to the loudspeaker, JBL 2425.

Because the power provided by the Biopac system is too low to generate an incident acoustic wave with enough acoustic energy, it is necessary to amplify the electrical signal using a linear power amplifier. The gain in the power amplifier, NADY AUDIO XA-900, is carefully selected to avoid distortion in the acoustic waves. The approximated gain of the amplifier is 7 dB.

The incident acoustic wave propagates through a source tube with a uniform diameter of 1.1 cm and of 805.5 cm length. It has been referred in previous chapters as the source tube. The incident wave strikes a cylindrical cavity placed at the distal end of the source tube. A reflected acoustic wave is generated and propagated in opposite direction of the former wave, as it was described in Chapter 2.

A microphone, ELECTRET 33-1052, set flushing with the inside wall and placed at the middle of source tube is used to record both acoustic waves. To improve the signal-to-noise ratio, the signals recorded by the microphone are amplified by an instrumentation amplifier INA122P. Then, the signals are digitalized and stored by the Biopac system. The time to generate and record each signal is 0.12 s. A block diagram of the instrumentation required in the acoustic reflectometer is shown in Figure 5.

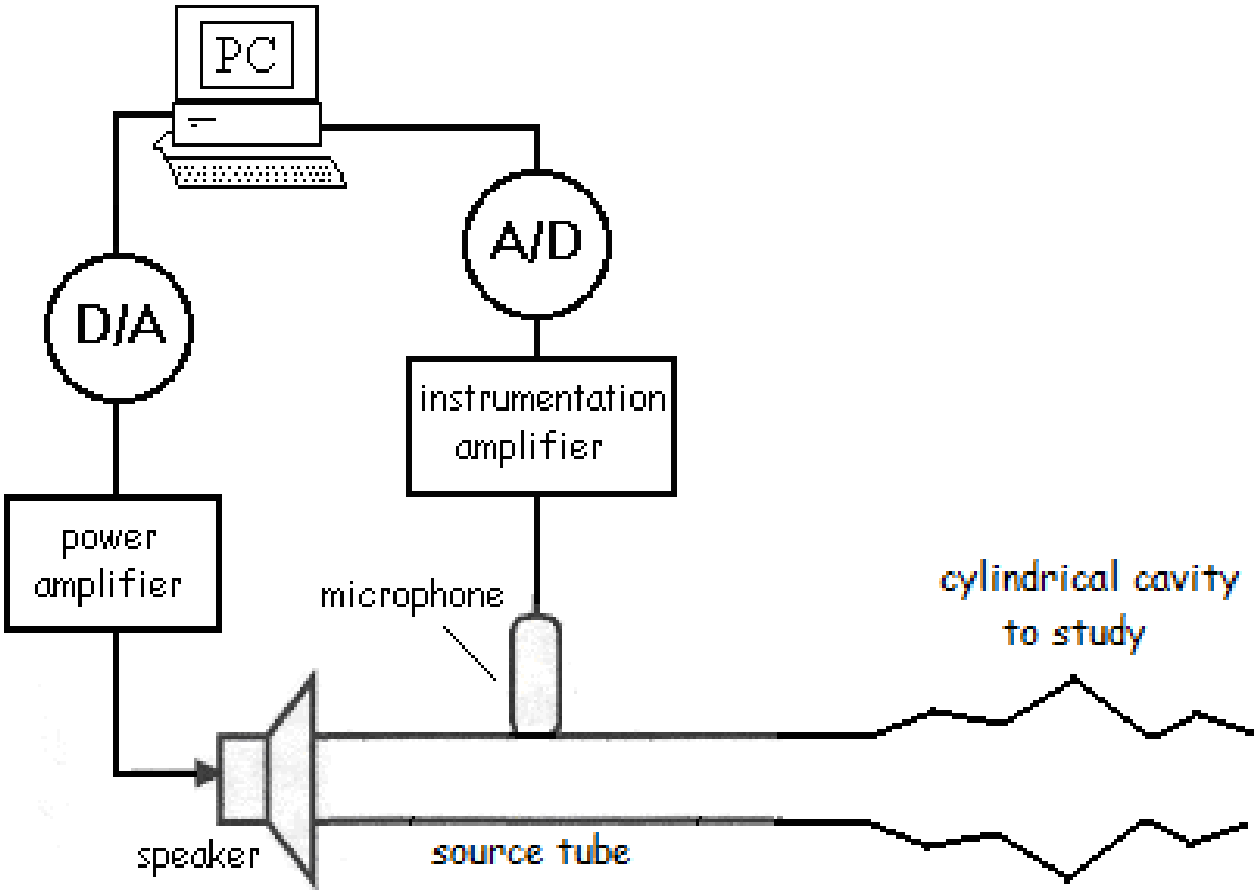


Figure 5. Schematic block diagram of an acoustic reflectometer.

It is important to emphasize that several ways to generate and record the sound waves have been used throughout the history of acoustic reflectometry. Figure 5 shows the most versatile way because a computer is used to test different acoustic waveforms to be propagated along the source tube. In this way, the sound waves generated are characterized by having a well defined waveform. Figure 6 shows the actual acoustic reflectometer located in the Biopotentials Imaging Laboratory at the University of Texas El Paso.


Figure 6. Acoustic reflectometer used in this research.

One of main reasons for using a long source tube lies in the fact that a physical identification of the incident acoustic wave is achieved before the reflected acoustic wave is generated. Thereby the computational cost is reduced. Another meaningful reason consists of recording a stable signal in the time domain, which is used to calculate amplitude, phase and DC offset component for each acoustic wave recorded and, respectively, identified.

## 4.3 Gaussian-modulated acoustic packets

Instead of using an acoustic pulse limited in frequency, acoustic sinusoidal packets were used to estimate the impulse response of a cylindrical cavity. A Gaussian-modulated sinusoidal wave is

generated when a sinusoidal wave is multiplied by a Gaussian function [26]. This type of acoustic waves are easy to generate and have a modulated narrow bandwidth.

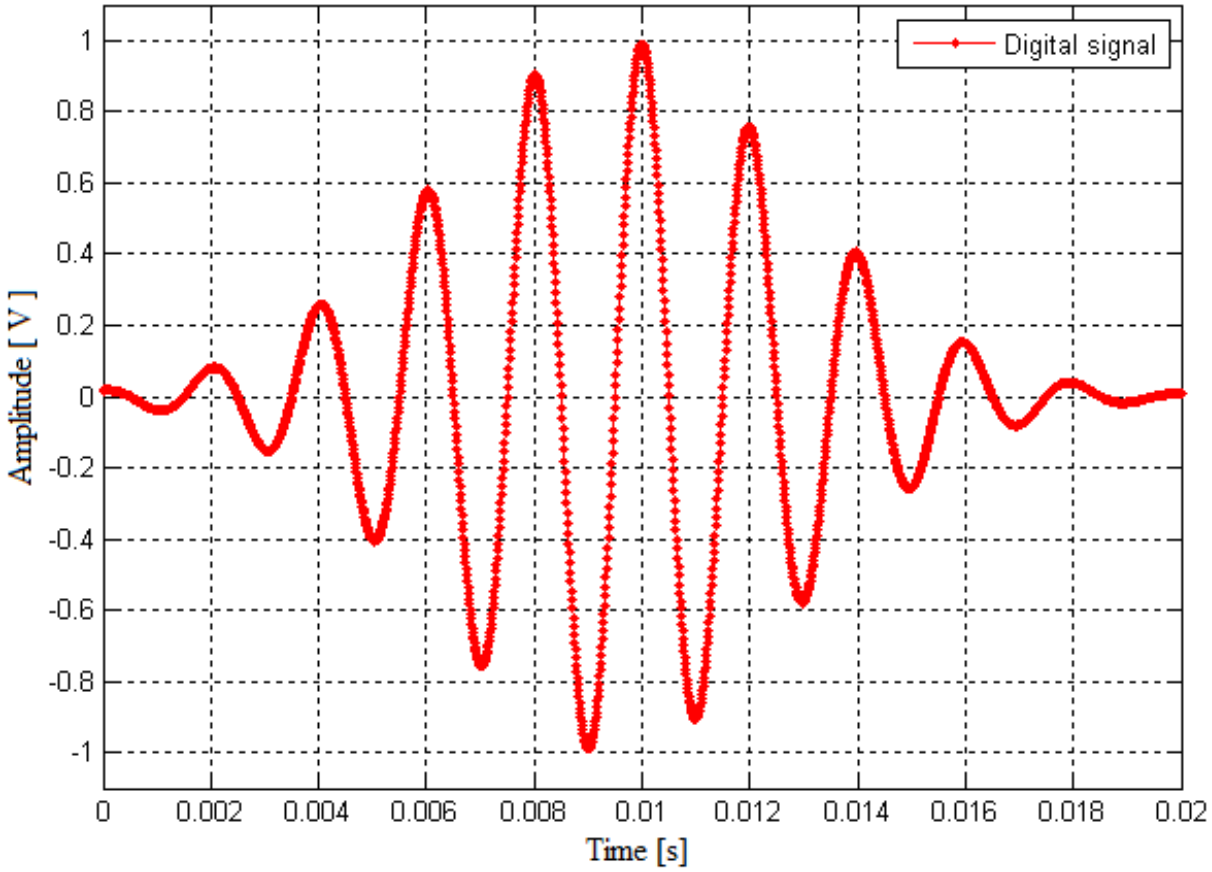


Figure 7. Gaussian-modulated sinusoidal wave at 500 Hz.

A data base of Gaussian-modulated sinusoidal packets is available in the Matlab software. Each digital signal is based on an algorithm which defines the desire frequency, the time of propagation and the number of cycles within a short period of time.

A digital Gaussian-modulated sinusoidal wave at 500 Hz is shown in Figure 7. A sampling frequency of 100 kHz is used in the respective generation and acquisition of data. The signal generated by the reflectometer is displayed in Figure 8. After the reflected acoustic wave, there are multiple reflections that are not useful to estimate the impulse response of the cylindrical

cavity. The multiple reflections are a consequence of the reflected acoustic wave, when it strikes the loudspeaker and generates other reflected waves.

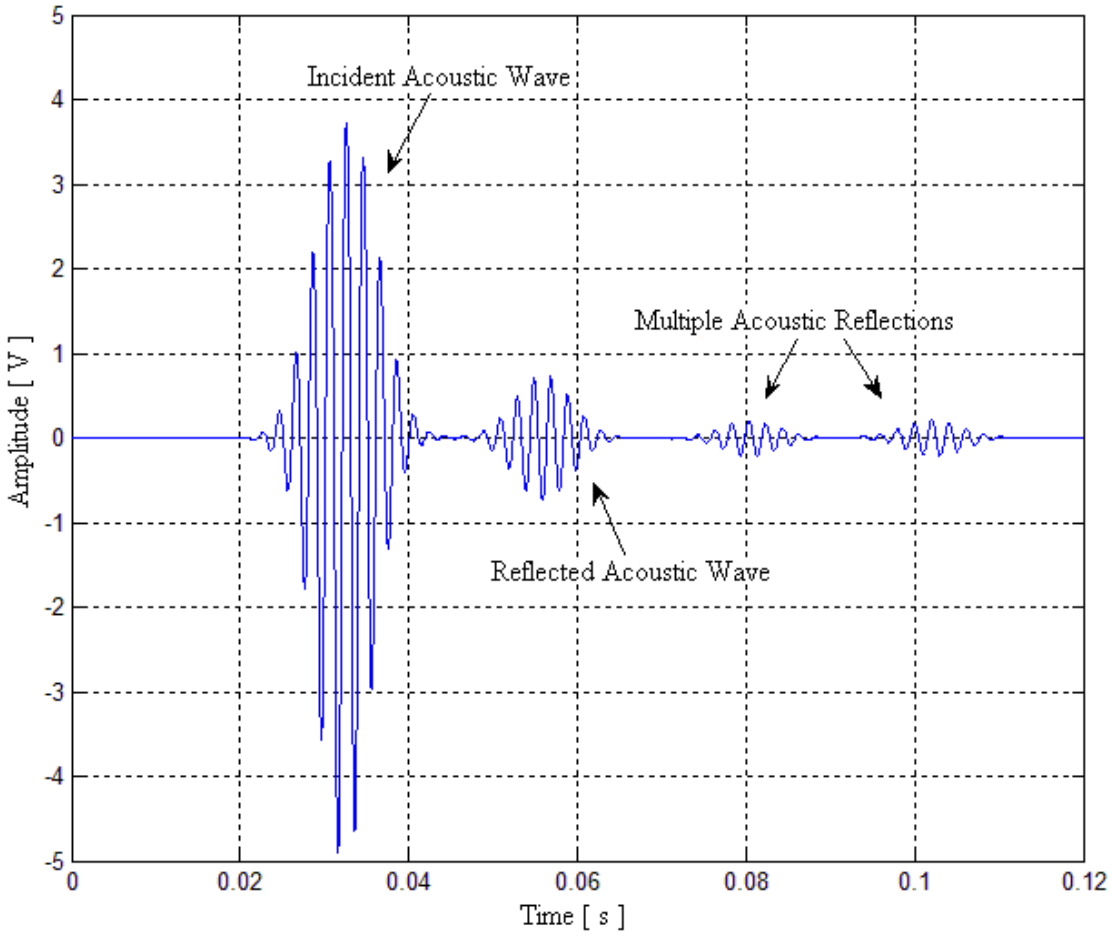


Figure 8. Acoustic wave recorded by the reflectometer at 500 Hz.

The first issue to be noticed is that the incident wave may be easily identified from the reflected wave. The second issue lies in the fact that the incident acoustic wave does not display the same peak values. In other words, the acoustic wave is not symmetric in amplitude with respect to the base time. The third issue, and probably the most important, is that it seems that the DC offset component is practically nonexistent when this type of acoustic wave is propagated in the reflectometer.

## 4.4 Filtering the acoustic waves

The experimental data base recorded by the reflectometer is denoted by decreasing the amplitude of both acoustic waves as function of the frequency. At relatively high frequencies, this fact becomes a serious problem because the signal to noise ratio is too low. On the other hand, at relatively low frequencies the peak values of the acoustic signal is not the same. Matched filter is not only used on each acoustic wave to make the amplitude of the peak values symmetric in amplitude, but also it is used to improve the signal-to-noise ratio at high frequencies, as it is shown in figure 9.

Matched filter is used in the mathematical procedure to improve the measurement of the frequency response of a cylindrical cavity at high frequencies.

It is important to emphasize that despite the fact that the signal-to-noise ratio may be improved, it is necessary to compensate the losses during the propagation of both acoustics along the source tube. Without this compensation the maximum frequency available in the analysis is about 4 kHz. A later section describes the way of determining the acoustic attenuation and the compensation in the frequency impulse response.

The first step in the mathematical procedure to compute the frequency impulse response of a cylindrical cavity consists of separating the incident from the reflected acoustic wave. Then, time intervals of both acoustic waves, around their peak value, are used to fit a sinusoidal signal given by

$$y(t) = B + A\sin(\omega t + \theta) \tag{4.1}$$

Such that a least mean square algorithm is used on each signal to compute its amplitude *A*, angular frequency $\omega$, phase $\theta$, and DC offset component *B*. These regions of time are the same

for all the frequencies used in the analysis. Because the time interval at low frequencies covered few cycles of the acoustic signals, a very small DC offset component is computed at frequencies below 300 Hz.

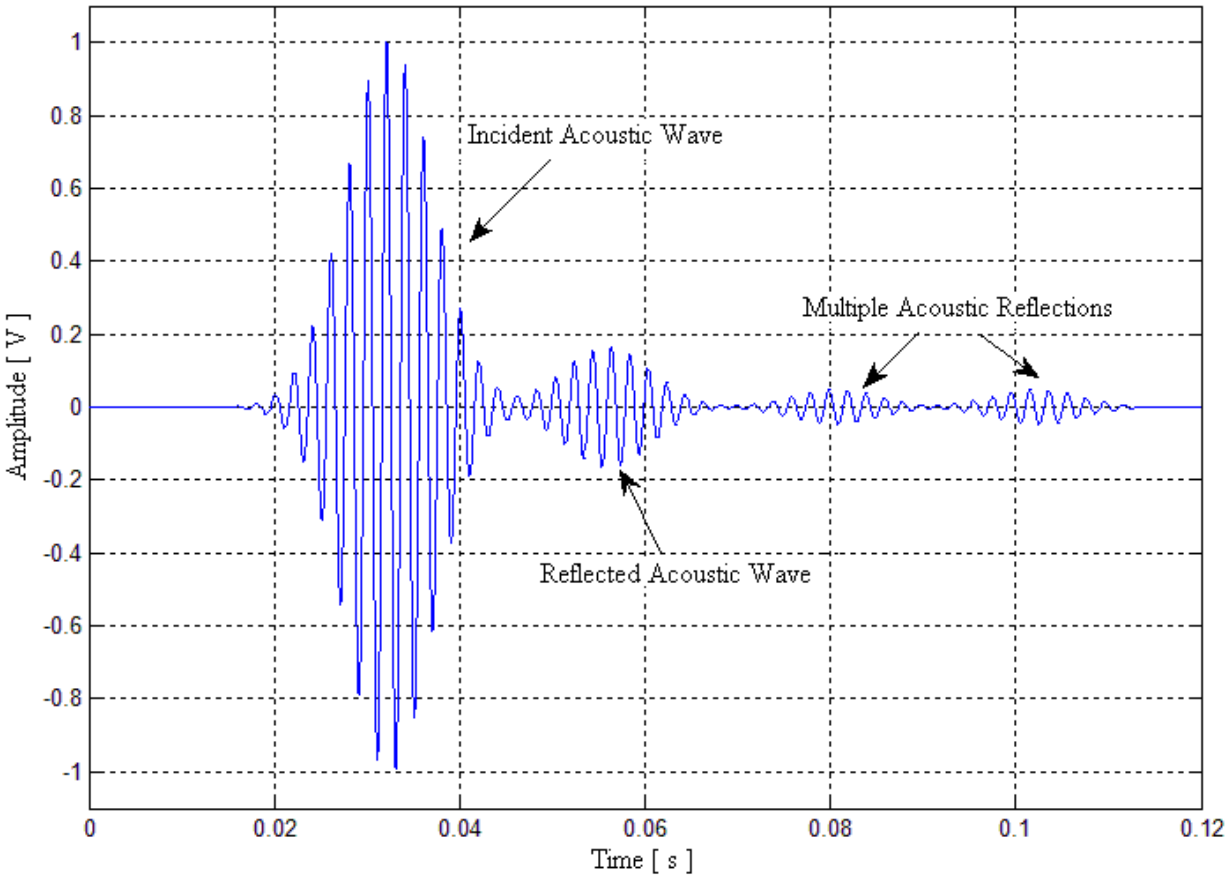


Figure 9. Filtered acoustic wave by matched filter.

## 4.5 Frequency impulse response of a cylindrical cavity

The frequency impulse response of a cylindrical cavity is obtained by deconvolving the signals generated from a reflectometer. This mathematical procedure can be done either in frequency or time domain. For instance, in acoustic pulse reflectometry, the most common procedure consists of dividing the Fourier transform of the reflected acoustic wave by the Fourier transform of the

incident acoustic wave [6, 7, 15, 16]. However, singular value decomposition [22], a powerful mathematical procedure, has been also performed to obtain the impulse response in the time domain. The good performance of these methods depends on eliminating the DC offset component and compensating the signal-to-noise ratio.

In this dissertation the frequency impulse response is computed by using the values computed in (4.1). Once the amplitude and phase of each acoustic wave for each frequency is calculated, the amplitude response of the cylindrical cavity is given by

$$A(\omega) = \frac{A_r(\omega)}{A_i(\omega)} \tag{4.2}$$

Where $A_r(\omega)$ and $A_i(\omega)$ denote the amplitude response of reflected wave and incident wave, respectively, at frequency $\omega$. On the other hand, the phase response of the cylindrical cavity is computed by the difference between their phases as given by

$$\theta(\omega) = \theta_r(\omega) - \theta_i(\omega) \tag{4.3}$$

Where $\theta_r(\omega)$ and $\theta_i(\omega)$ denote the phase response of the reflected and incident acoustic wave, respectively. It is clear that the total frequency impulse response $iir(\omega)$ of a cylindrical cavity is computed as function of each frequency used to sweep the bandwidth according to the relation.

$$iir(\omega) = A(\omega)e^{\theta(\omega)} \tag{4.4}$$

The resolution of the frequency impulse response depends on the frequency step size, which is the interval of frequency used to sweep the audible frequency range.

The Inverse Discrete Fourier Transform, IDFT, is used to represent the impulse response in time domain and it is used in the Ware-Aki algorithm to estimate the reflection coefficients $r_{i,i+1}$, which in turn represents a space-time relationship of the variation of the cross sectional area as a function of distance.

As it is noted in Figures 8 and 9, the application of Gaussian-modulated acoustic waves seems to eliminate the DC offset component along the source tube. However, the procedure used to compute the frequency impulse response detects a very small DC offset component at relatively low frequencies (< 300 Hz). The same value is computed when the signals acoustic are characterized by (4.1). Thereby, this factor is compensated by adding both components as function of their respective frequencies.

As it was mentioned, it is necessary to compensate the losses along the source tube before implementing the Ware-Aki algorithm is described in the next section.

## 4.7 Attenuation of sound waves in the acoustic reflectometer

An acoustic pressure wave $\boldsymbol{P}$ attenuates as it propagates in any lossy medium. The equation which describes an attenuated acoustic pressure wave is given by

$$P = \boldsymbol{P}\, e^{-\gamma \xi} \tag{4.5}$$

where

$$\gamma = \alpha + j\beta\,, \tag{4.6}$$

and α and β are the attenuation and the phase constant of the acoustic wave which are functions of distance and frequency. So, the general equation to describe the propagation is represented in terms of a fundamental frequency $\omega_n$ and a distance $\xi_n$ as given by

$$P(\omega_n, \xi_n) = \boldsymbol{P}\, e^{-\alpha(\omega_n)\xi_n}\, e^{-j\beta(\omega_n)\xi_n} \tag{4.7}$$

In acoustic reflectometry, it is necessary to estimate the exponential attenuation along the source tube to compensate the acoustic waves which provide the information necessary from the cylindrical cavity placed at the end of the source tube.

Figure 10 (a) shows the propagation of an incident acoustic wave along the positive *x*-direction. The signal is recorded by only one microphone placed at the middle point denoted by $\xi_m$. However, the incident acoustic wave is exponentially attenuated along its path before it strikes the cavity.

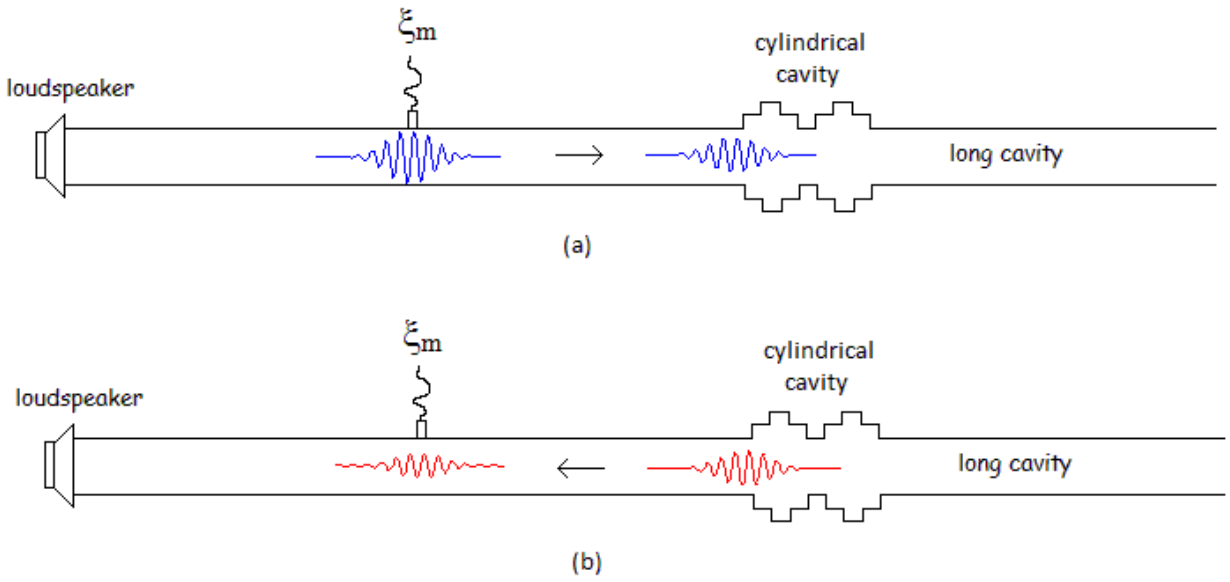


Figure 10. Propagation of an incident acoustic wave (a) and a reflected acoustic wave (b).

A change of acoustic impedance generates the reflected acoustic wave which propagates in negative *x*-direction. Figure 10 (b) shows the propagation of a reflected acoustic wave which is recorded by the same microphone. The distance between the microphone and the cavity is such that, the incident acoustic wave is recorded before the reflected wave is generated. Because the reflected acoustic wave propagates the same distance, it is assumed that the reflected acoustic wave is exponentially attenuated by the same magnitude as the former acoustic wave.

In the laboratory, both factors $\alpha$ and $\beta$ were calculated by propagating an acoustic wave through the source tube. The acoustic pressure is recorded at two different positions separated by a distance *d*. In this research, both positions are referred as the middle point and the cavity point, denoted by $\xi_m$ and $\xi_c$, respectively, as shown in Figure 11. This $\xi_c$ position is placed such that it denotes the distance where the cylindrical cavity of study is placed in the acoustic reflectometer.

The reflected acoustic wave is avoided by keeping the acoustic impedance along the source tube. In other words, a long cylindrical cavity with the same diameter as the source tube is joined to the reflectometer.

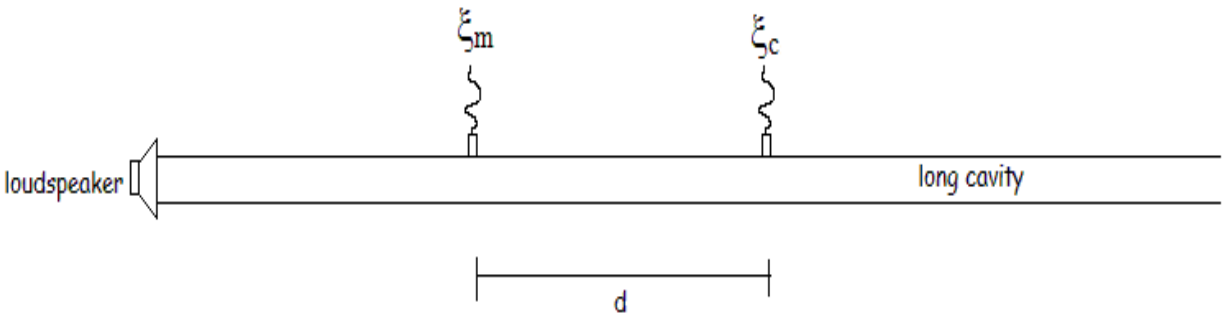


Figure 11. Two characteristic positions along the source tube.

Figure 12 shows the real acoustic waves recorded at both positions; the fundamental frequency is $\omega_1 = 500\,\text{Hz}$. The amplitude of the acoustic wave recorded at $\xi_m$ is greater than the amplitude of the acoustic wave at $\xi_c$. It is due to the attenuation when the acoustic wave propagating along the positive x-direction within the source tube. However, this attenuation is also a function of the fundamental frequency $\omega_n$ in the acoustic wave.

It is necessary to deduce the mathematical relationship which describes the dependence of the attenuation along a distance $d$ for any frequency $\omega_n$.

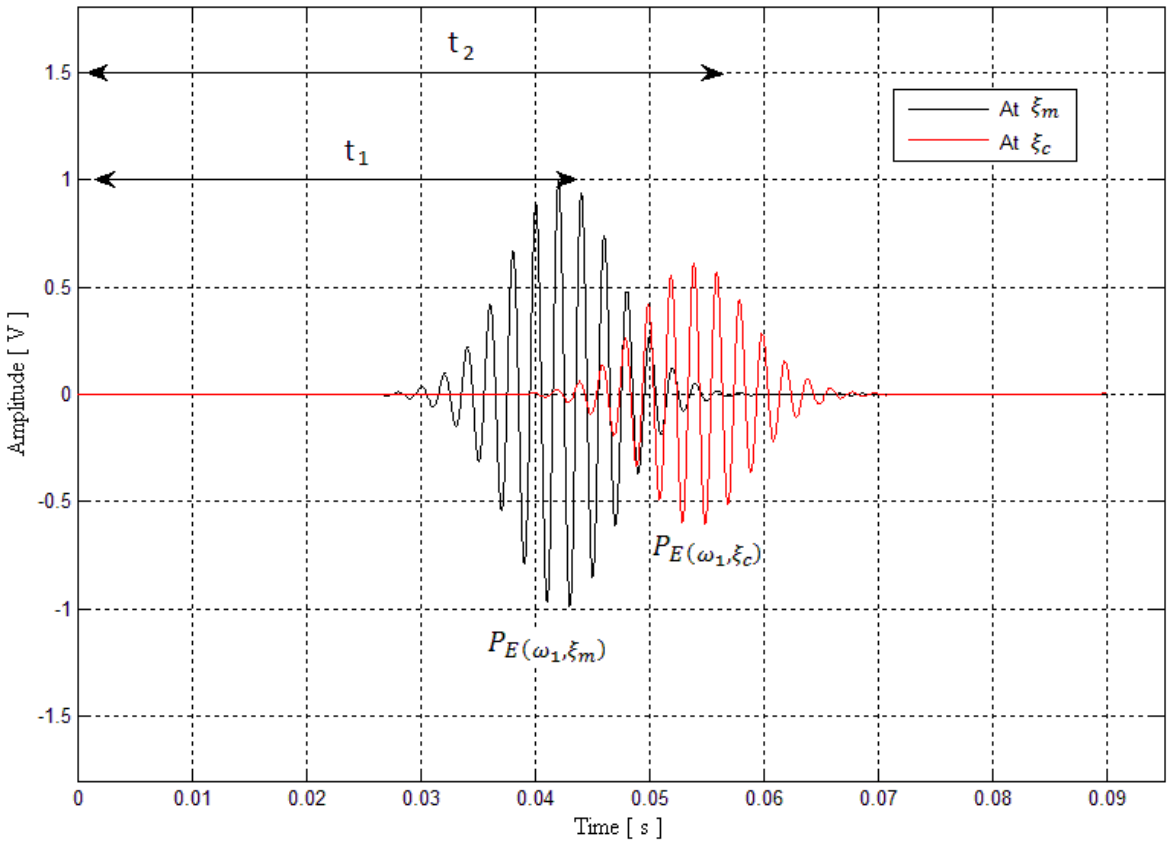


Figure 12. An incident acoustic wave attenuated along the source tube.

Despite the fact that the experimental acoustic waves are not exactly sinusoidal, they may be characterized by its peak value in phasor notation. In other words, the amplitude and phase of the experimental acoustic pressure $P_E$ recorded at $\xi_m$ may be given by

$$P_E(\omega_n, \xi_{\mathrm{m}}) = \left|P(\omega_n, \xi_{\mathrm{m}})\right| \angle \phi(\omega_n, \xi_{\mathrm{m}}) \tag{4.8}$$

The amplitude and phase of the experimental acoustic pressure $P_E$ recorded at $\xi_m$ for any frequency $\omega_n$ may be represented by

$$P_E(\omega_n, \xi_{\mathrm{c}}) = \left|P(\omega_n, \xi_{\mathrm{c}})\right| \angle \phi(\omega_n, \xi_{\mathrm{c}}) \tag{4.9}$$

On the other hand, (4.6) is used to represent the theoretical acoustic pressure $P_T$ at $\xi_m$ and at $\xi_c$, which are given by

$$P_T(\omega_n, \xi_c) = \boldsymbol{P}\, e^{-\alpha \xi_c}\, e^{-j\beta \xi_c} \tag{4.10}$$

and

$$P_T(\omega_n, \xi_m) = \boldsymbol{P}\, e^{-\alpha \xi_m}\, e^{-j\beta \xi_m} \tag{4.11}$$

Dividing equations (4.9) and (4.10) defines the attenuation ratio $\Gamma$ along the positive *x*-direction from $\xi_m$ to $\xi_c$ as

$$\Gamma = \frac{P_T(\omega_n, \xi_{\mathrm{c}})}{P_T(\omega_n, \xi_m)} \tag{4.12}$$

or

$$\Gamma = e^{-\alpha(\xi_c - \xi_m)}\, e^{-j\beta(\xi_c - \xi_m)} \tag{4.13}$$

At this point, there are two scenarios to be related each other, in order to compute the parameters α and β. The first scenario consists of using the amplitudes to describe the propagation of the acoustic waves recorded at $\xi_m$ and $\xi_c$ to derive the α coefficient. The second scenario consists of using the phases of the acoustic waves at the same positions to derive the parameter β.

The mathematical procedure to derive α consists of equating only the magnitudes of all previous expressions at their respective positions as function of frequency. In other words, for any $\omega_n$ at $\xi_m$ it gives that

$$\boldsymbol{P}\, e^{-\alpha(\omega_n)\xi_m} = \left|P\left(\omega_n, \xi_m\right)\right| \tag{4.14}$$

and for $\omega_n$ at $\xi_c$ it gives that

$$\boldsymbol{P}\, e^{-\alpha(\omega_n)\xi_c} = \left|P\left(\omega_n, \xi_c\right)\right| \tag{4.15}$$

Dividing (4.13) by (4.14), the parameter $\boldsymbol{P}$ cancels out, and assuming that α is a constant parameter at a given frequency $\omega_n$, it gives

$$\alpha(\omega_n) = -\frac{\ell \mathrm{n}\left(\dfrac{\left|P(\omega_n, \xi_c)\right|}{\left|P(\omega_n, \xi_m)\right|}\right)}{(\xi_c - \xi_m)} \tag{4.16}$$

The mathematical procedure for compute $\beta$ consists of equating the phase shift in equation (4.12) to the experimental phase shift measured in the acoustic waves, as shown in Figure 11. That is

$$\beta(\omega_n)(\xi_c - \xi_m) = \phi(\omega_n, \xi_c) - \phi(\omega_n, \xi_m) \tag{4.17}$$

The parameter β is either described by

$$\beta(\omega_n) = \frac{\Delta\phi}{(\xi_c - \xi_m)} \tag{4.18a}$$

or

$$\beta(\omega_n) = \frac{\omega_n(t_2 - t_1)}{(\xi_c - \xi_m)} \tag{4.18b}$$

Hence, the entire attenuation between $\xi_m$ and $\xi_c$ along a positive *x*-direction is then given by

$$\Gamma = \frac{|\,\mathrm{P}(\omega_\mathrm{n}, \xi_c)\,|}{|\,P(\omega_n, \xi_m)\,|} e^{-j\ \omega_n(t_2 - t_1)} \tag{4.19}$$

The attenuation of the reflected wave which propagates along negative *x*-direction must be considered. Because α and β may be assumed to be at the same value along the same distance, it means that the total attenuation in the frequency response is twice. That is

$$\Gamma = 2\frac{\left|\mathrm{P}(\omega_{\mathrm{n}},\xi_c)\right|}{\left|P(\omega_n,\xi_m)\right|}e^{-j\,2\,\omega_n(t_2-t_1)} \tag{4.20}$$

The attenuation is used in the solution of the inverse problem to compensate the losses in the frequency impulse response.

## 4.8 Compensation along the source tube

In order to compensate the attenuation in the source tube, it is necessary to experimentally calculate α and β.

In this experimental analysis, one more characteristic position $\xi$ is considered. Its purpose is being to analyze the exponential attenuation along the entire source tube. The new position, denoted by $\xi_s$, refers to the position at the loudspeaker. Figure 16 shows the distances Xn among those three characteristic positions along the setup.

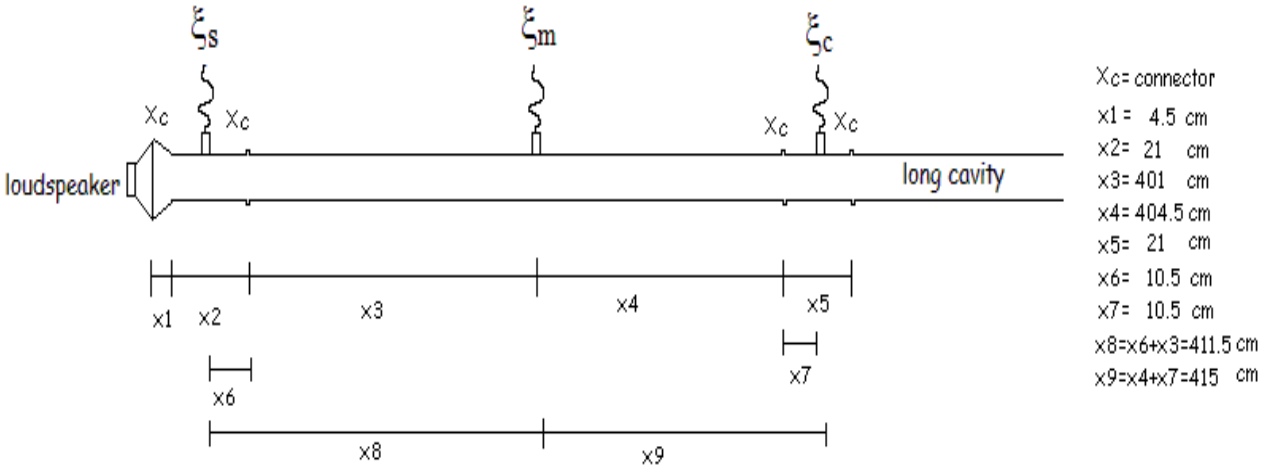


Figure 13. Three characteristic positions $\xi_n$ along the source tube.

In Figure 13, $x_c$ denotes the location of a connector which is used to join a short cylindrical segment of 10.5 cm with the source tube. This segment has the same diameter as the source tube and it is used to place the microphone at both ends of the source tube.

The acoustic impedance generated at the connector $x_c$ is very low to claim that the reflected acoustic wave does not modify the acoustic wave propagated along positive *x*-direction.

The experimental procedure consists of sweeping the frequency bandwidth using Gaussian-modulated acoustic waves to record the acoustic pressure at each position. Once the acoustic pressures are recorded, a modified version of equations (4.15) and (4.17), with the respective positions of distance, are recalled to represent the respective parameters.

Three values of each parameter, α and β, are calculated. The first value corresponds to the interval between $\xi_c$ and $\xi_m$. The second parameter represents the values between $\xi_m$ and $\xi_s$, and the last case is that given between $\xi_c$ and $\xi_s$.

The algorithm used to compute the impulse response is recalled again to compute the amplitude and phase of each acoustic wave used in this analysis. Figure 14 and 15 display the values of α and β computed at their respective positions.

The attenuation is assumed to be constant along the source tube. On the other hand, in a dispersive medium, the phase velocity varies with frequency and it is not the same at the group velocity of the wave.

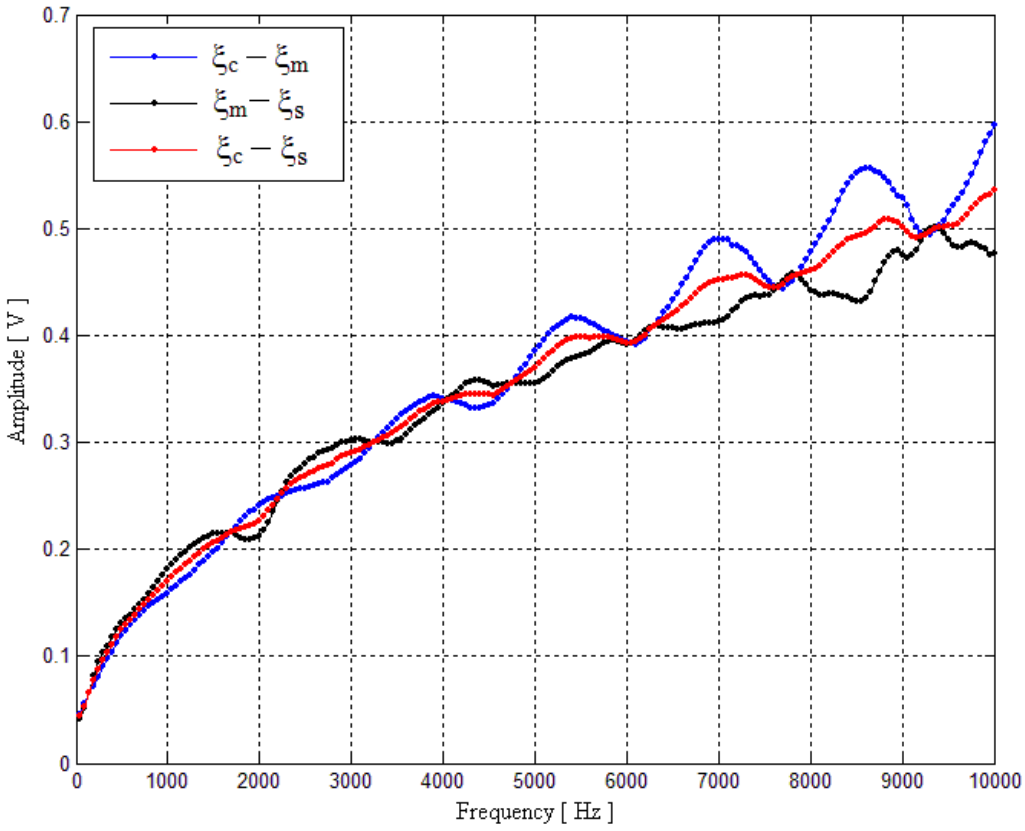


Figure 14. Parameter α as a function of frequency.

In theory, any of those three cases may be used to compensate the losses with the correct assumption in the distance along the source tube. For instance, when the parameters α and β either between $\xi_c$ and $\xi_m$ or between $\xi_m$ and $\xi_s$ are used, (4.18) is recalled to compensate the attenuation along the distance cover by both acoustic waves. On the other hand, when the parameters calculated of α and β between $\xi_c$ and $\xi_s$ are used, a modified version of (4.19) may be rewritten as

$$\Gamma = \frac{\left| \mathrm{P}\left(\omega_{\mathrm{n}}, \xi_c\right) \right|}{\left| P\left(\omega_n, \xi_s\right) \right|} e^{-j\ \omega_n (t_2 - t_1)} \tag{4.21}$$

In this way, the attenuation is assumed along the same distance covered by (4.20).

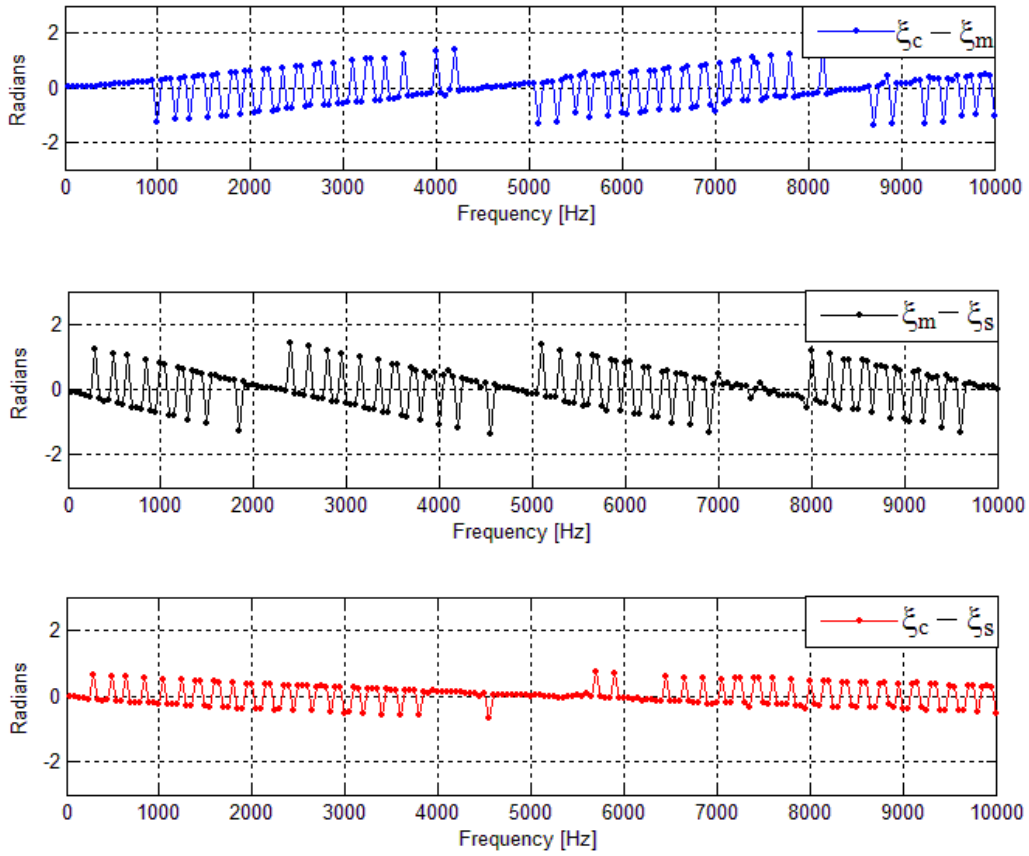


Figure 15. Parameter β as a function of frequency.

## 4.9 Solution of the inverse problem

The solution of the inverse problem consists of integrating all issues discussed in all previous sections. In summary, instead of using acoustic pulses limited in frequency, Gaussian-modulated sinusoidal waves may be used to sweep either a frequency bandwidth or specific frequency ranges within a frequency bandwidth. The resolution of the frequency impulse response depends on the frequency step size. The signal-to-noise ratio at high frequencies is improved applying a simple matched filter computation.

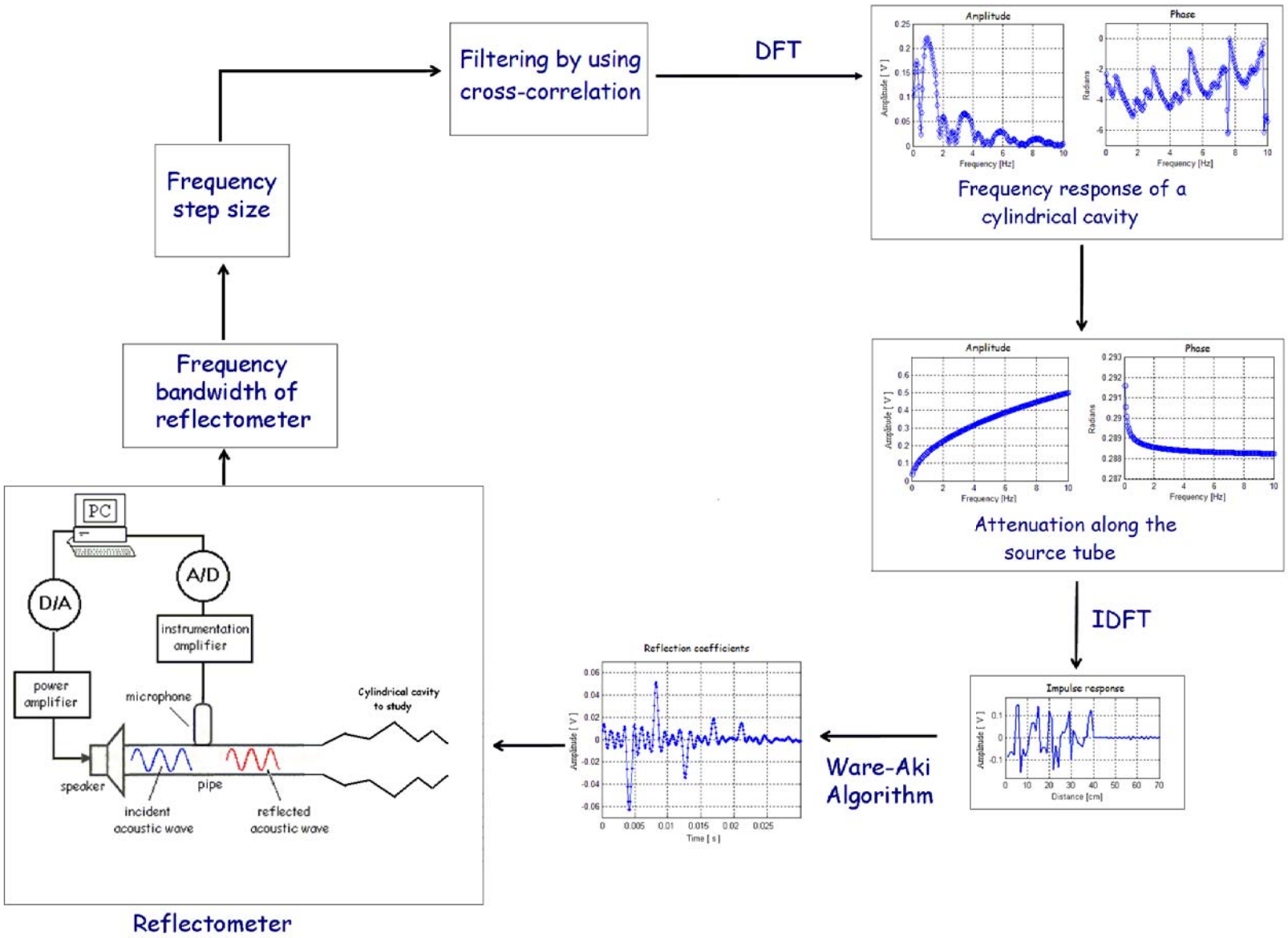


Figure 16. The solution of the inverse problem.

The compensation of the DC offset component in the amplitude response and the compensation of losses along the source tube is performed in the frequency domain.

The Inverse Discrete Fourier Transform, IDFT, is used to map the frequency impulse response into time domain and the Ware-Aki algorithm is used to calculate the reflection coefficients which provide the axial resolution of a cylindrical cavity.

A block diagram of the solution of the inverse problem is summarized in Figure 16. It is referred as the entire solution of backward problem in acoustic reflectometry. The versatility in the solution of the inverse problem allows focusing within specific ranges of frequency along the audible frequency bandwidth; such issue is not possible to perform when an acoustic pulse reflectometry is used.

The audible frequency bandwidth may be divided in sub-intervals of frequency and calculate a total frequency response by superposition. In other words, each impulse response obtained for each specific sub-interval of frequency is integrated.

Significant frequencies are identified along the audible frequency bandwidth such that relatively low frequencies are used to estimate the general shape of a cylindrical cavity and relatively high frequencies are used to refine the axial resolution of the bore profile.

This dissertation also evaluates the role of the frequency step size along the frequency response of a reflectometer. It is possible to find an optimum number of acoustic waves to sweep the frequency bandwidth and evaluate several rates of frequency step size, such as: a relatively small constant frequency step size, a relatively high frequency step size, a logarithm frequency step size, or a linear frequency step size.

Because the overall analysis is denoted by the content of frequency which is a function of frequency step size, it is possible to reduce the number of acoustic waves required to estimate the

frequency impulse response and obtain a good axial resolution. Those parameters are evaluated in a simulation model to evaluate the importance of each one.

## 4.10 Concluding remarks

The entire solution of the inverse problem has been described in terms of each parameter used in the acoustic reflectometry. Because the amplitude of the acoustic waves decreases as function of the frequency, it is necessary to improve the signal to noise ratio at high frequencies and compensate the losses along the source tube.

# Chapter 5

# Simulation Model in Acoustic Reflectometry

## 5.1 Introduction

In general, the use of computer software has contributed to several aspects in science and research. For instance, it has been used not only to reduce the computational cost of complex mathematical procedures, but also to predict and represent the nature of a physical phenomena.

In this way, expenses may be reduced, and the convenience to repeat the results in several scenarios, as many times as it is required, makes a simulation model a very attractive tool. However, the parameters involved must be well defined by mathematical equations and tables to describe the reality with an appropriate accuracy.

This chapter describes the potential of a simulation model to evaluate the performance of applying Gaussian-modulated sinusoidal waves to the Ware-Aki algorithm for six different cylindrical cavities. Ideal conditions are assumed in the sound waves, such that it is possible to identify a short time of a stable signal and estimate the frequency bandwidth of a cylindrical cavity.

The frequency step size as function of the bandwidth are quantified through the quadratic error between a proposed test cavity in the forward problem, and an estimated test cavity computed by the inverse problem. Hence, three possible scenarios are described to estimate the bore profile with an appropriate axial resolution.

## 5.2 Independent parameters in the solution of the inverse problem

The independent parameters in the solution of the inverse problem consist of sweeping a frequency bandwidth using a finite frequency step size. Because the solution of the inverse problem controls the frequency content, the bandwidth may cover either the entire audible range, or a limited spectral range. The frequency step size denotes the interval between each frequency used to sweep the frequency bandwidth.

In order to test the performance of solving the inverse problem by using a simulation model and evaluate the independent parameters, the forward problem is recalled to simulate the reflected signals that may be obtained from an acoustic reflectometer.

A sampling frequency of 100 kHz is used to represent the bore profile of cylindrical cavities using (2.28). In this way, the first proposed test cavity is characterized by having a well known bore profile as function of distance, as it is shown in Figure 17.

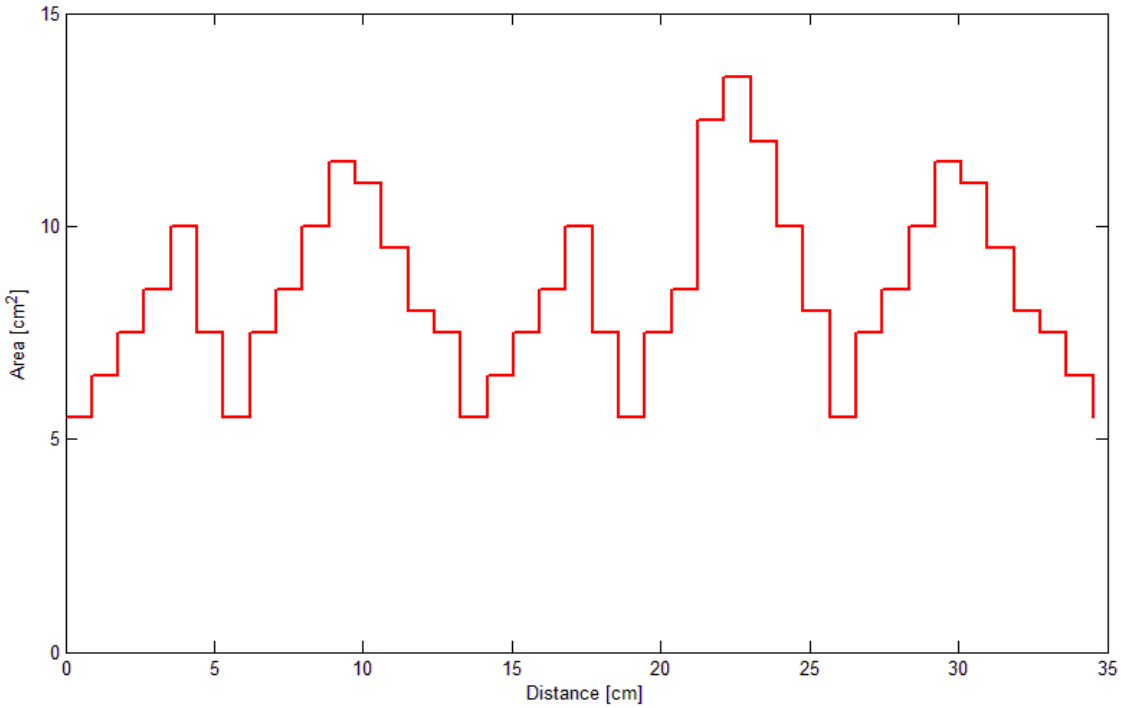


Figure 17. Proposed test cavity used in the forward problem.

### 5.2.1 Superposition of the impulse response

One of the most ideal conditions requires of sweeping the half audible frequency range with a small frequency step size of 50 Hz. This frequency bandwidth in turn was divided in 10 equally spaced frequency subintervals to qualify and quantify the axial resolution obtained for each subinterval.

The magnitude and phase response for each interval of 1 kHz are displayed in the two first columns of Figure 18, respectively, while the time impulse response is displayed in the third column. A comparison between the estimated test cavity, black line, and the proposed test cavity, red line, is displayed in the fourth column.

The frequency content in the impulse response seems to have a relationship with the axial resolution of a cylindrical cavity. It means that there are frequencies which provide relevant information of the bore profile as function of the distance.

The axial resolution as function of the distance for relatively high frequencies (> 4 kHz) is characterized to define a bore profile with a uniform cross sectional area. However, for relatively low frequencies (< 4 kHz), the estimated bore profile is characterized by having soft variations in the cross sectional area as function of the distance.

One of the main advantages of having control over the frequency content in the acoustic wave lies in the fact that all impulse responses obtained might be superposed to integrate a total impulse response which covers a wide frequency bandwidth.

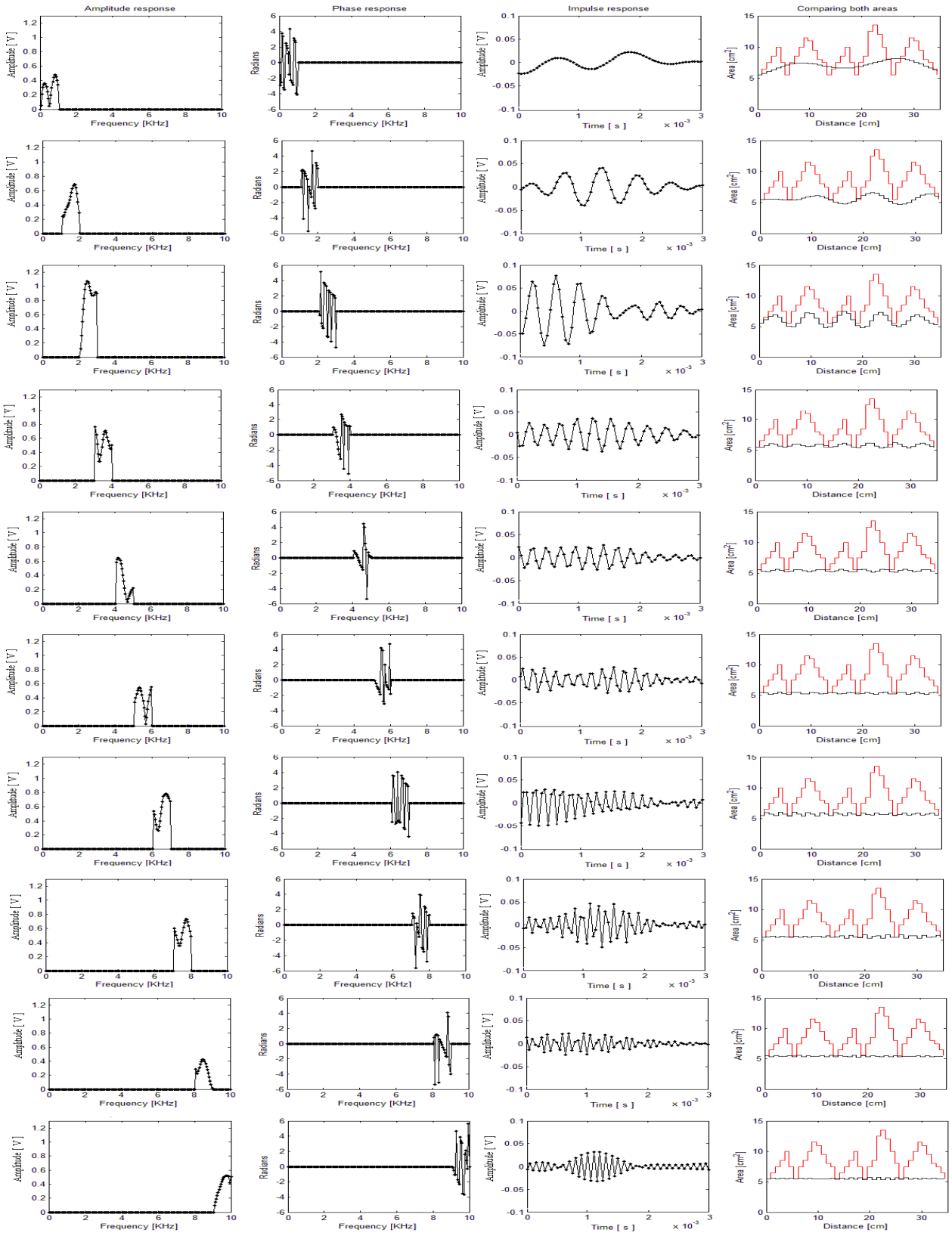


Figure 18. Frequency bandwidth divided in ten equally spaced intervals of frequency

Figure 19 shows the first scenario to compute the bore profile with high accuracy. It consists of integrating the impulse response in frequency and time domain, respectively, along the entire frequency bandwidth.

A comparison between the proposed test cavity, red line, and the estimated test cavity, black line, is shown in the fourth chart of this figure. Note that an excellent axial resolution may be obtained when all frequencies are used. The computational cost depends on the number of acoustic waves used during the computational procedure.

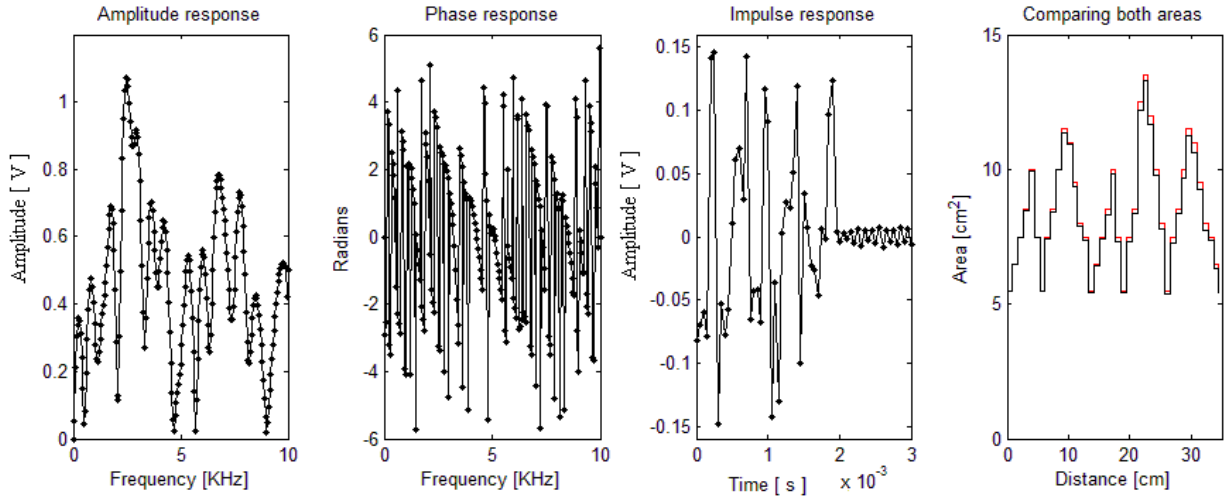


Figure 19. Solution of the inverse problem in the range of frequency from 50 Hz to 10 kHz.

### 5.2.2 Significant frequencies in acoustic reflectometry

The result obtained by considering all possible frequencies, in the linear frequency analysis, is directly related to improve the axial resolution of a cylindrical cavity by increasing the frequency response of the cylindrical cavity. In order to quantify this finding, the quadratic error between the estimated and proposed test cylindrical cavities was computed as function of an increment of 1 kHz in the frequency bandwidth, as shown in Figure 20. In other words, the impulse response of each subinterval along the frequency bandwidth is integrated.

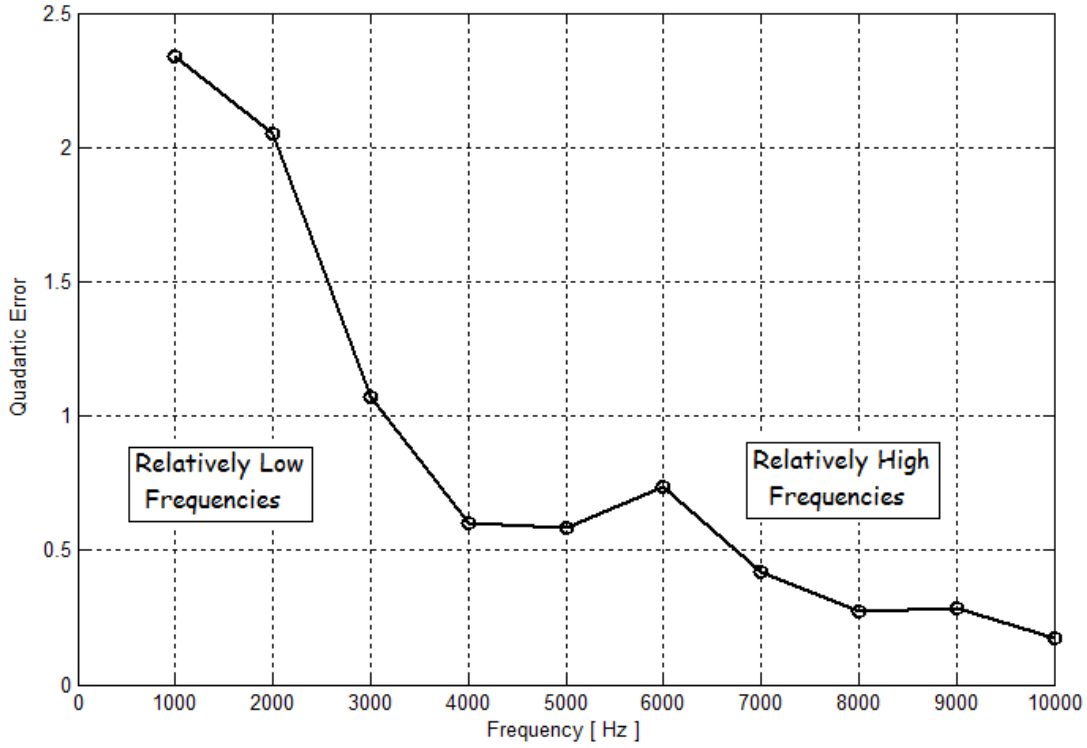


Figure 20. The quadratic error as function of an increment in the bandwidth.

The largest quadratic error is computed when the frequency response covers the lowest subinterval of frequency, 50 Hz – 1 kHz. On the other hand, the quadratic error is significantly reduced when the frequency bandwidth of 4 kHz is covered. Above 4 kHz, there is no such significant reduction in the quadratic error, but it is still reduced.

This finding assumes that relatively low frequencies provide a general shape in the cross sectional area as function of the distance and relatively high frequencies refine the result to improve its axial resolution.

Using the principle of superposition, it is possible to identify the range of frequency, which provides the main information to estimate the bore profile with an appropriate resolution; such interval may be referred to as “the significant frequencies”.

The significant frequencies for the proposed test cavity lie in a bandwidth of 4 kHz. Hence, the bore profile of this cylindrical cavity may be estimated with appropriate accuracy, as it is shown in Figure 21.

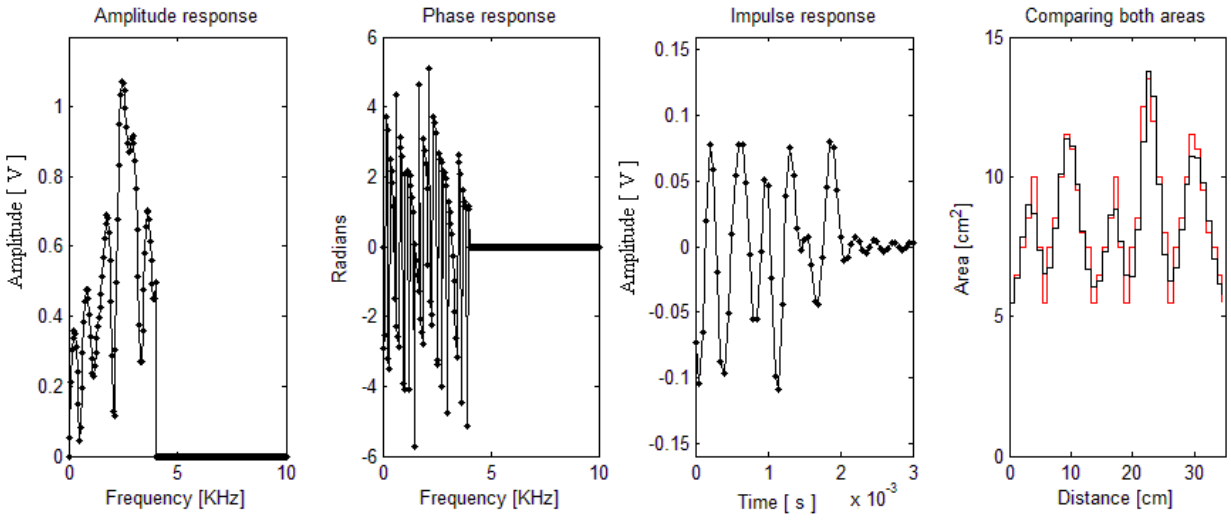


Figure 21. Significant frequencies for the proposed test cavity.

Hence, the second scenario to estimate the bore profile with an appropriate axial resolution consists of identifying the significant frequencies. It means that not only the number of acoustic signals may be reduced, but also undesired components due to the instrumentation at experimental high frequencies may be avoided. In consequence, the computational cost of processing this information may be reduced.

It is important to emphasize that the significant frequencies depend on the bore profile of the cylindrical cavity to study, as it is shown in the next section.

### 5.2.3 Constant frequency step size along a frequency bandwidth

The frequency step size denotes the resolution of the frequency impulse response within a frequency bandwidth. In consequence, the resolution of both the impulse response and the bore profile of a cylindrical cavity depend also of such parameter.

Several values of the frequency step size may be used along different frequency bandwidths to compute the bore profile of a cylindrical cavity and determine not only the optimum frequency step size in the solution of the impulse response, but also the range of frequency where the significant frequencies lie in the bandwidth.

Hence, the quadratic error between the estimated and the proposed test cavities is computed as function of the frequency step size within a covered frequency bandwidth. The bandwidth is scanned increasing its range of frequency response by 1 kHz until it covers 10 kHz. Figure 22 denotes the respective bandwidths covered.

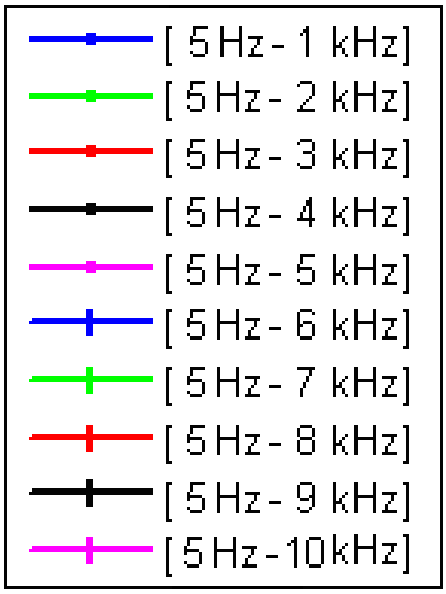


Figure 22. Ten bandwidths were covered using several frequency step sizes.

Six different cylindrical cavities, which are shown in the first column of Figure 26, are used to make the analysis using several constant frequency step sizes. The second column, in the same figure, shows the quadratic error computed as function of a constant frequency step size within the respective frequency bandwidth.

The procedure consisted in calculating the quadratic error for a frequency bandwidth of 1 kHz by using a frequency step size of 10 Hz. Then, assuming the same frequency bandwidth, the quadratic error is again evaluated, but now using a frequency step size of 20 Hz. This procedure was consecutively performed for all frequency bandwidths shown in Figure 25, once at a time, until the maximum frequency step size is 500 Hz.

The first proposed test cavity shown in Figure 23 is that initially used in this chapter to compute the quadratic error in Figure 20. Note that in both figures, a significant reduction of the quadratic error occurred when the significant frequencies were covered. It is for a frequency bandwidth of 4 kHz. On the other hand, the quadratic error seems to be constant on each frequency bandwidth, no matter what value of frequency step size may be used.

The bore profile shown in both second and third cylindrical cavities have been used in some papers [19, 26] to test the solution of the inverse problem. Their bore profiles are characterized by having an increased and a reduced stepped bore profile, respectively. Because those cavities are composed by three different cross sectional areas, it is possible to assume that they may have a simple bore profile, but the analysis of the quadratic error shows the contrary.

In both cases, there are two issues to be emphasized, the first refers to the significant frequencies contained along the entire frequency bandwidth. The second issue lies in the fact that the quadratic error is highly increased as function of the frequency step size. It means that the computational cost to estimate the bore profile of this type of cylindrical cavities is high, because

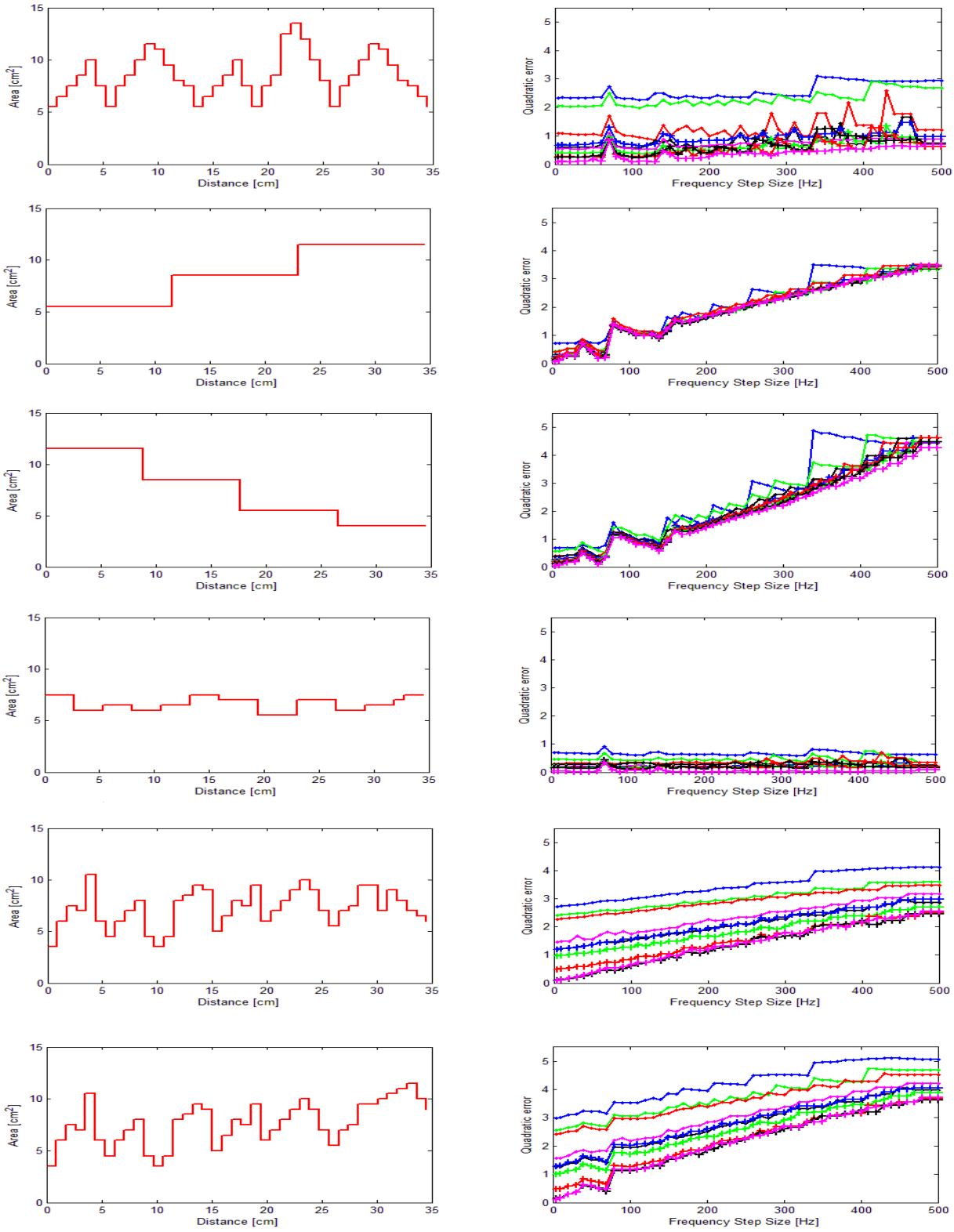


Figure 23. Quadratic error evaluated for six different cylindrical cavities.

it requires a small frequency step size and a high frequency bandwidth. This is the only way to estimate a high axial resolution. The fourth cylindrical cavity was composed of a very small variation in the cross sectional area as function of the distance. The analysis shows that significant frequencies are also grouped. However, in this particular case, the quadratic error is very low and constant, no matter what frequency step size is used to estimate the cylindrical cavity. In consequence, the computational cost is low, because it is not required both a high frequency bandwidth and a small frequency step size to estimate a good axial resolution of the cross sectional area.

The analysis for the last two cylindrical cavities shows that the significant frequencies are contained in a frequency bandwidth of 5 kHz. Note that the quadratic error increased as function of frequency step size. It means that the bore profile is again improved for a wide frequency bandwidth and a small frequency step size.

In general, the solution of the inverse problem denotes a tradeoff between an appropriate axial resolution and computational cost, but it depends on the variation of cross sectional area as function of the distance.

Because the above analysis shows that the low frequencies provide the general shape of the bore profile and the high frequencies refine the result, the simulation model may be used to evaluate the solution of the inverse problem by using different rates of frequency step size.

Either a logarithmic or linear frequency step size may be used to sweep the frequency bandwidth. In this way, the analysis is focused to obtain the general shape of the cylindrical cavity by using more frequencies in the lower frequency bandwidth and fewer high frequencies are used to refine the axial resolution.

### 5.2.4 Different rates of frequency step size along a frequency bandwidth

In order to quantify the performance of using different rates of frequency step size, the quadratic error is computed into five scenarios, given in Table 1, for each proposed test cavity shown in Figure 23.

The frequency bandwidth is dived in 10 equally spaced frequency subintervals such that either a different or a constant frequency step size is used to sweep each subinterval. Then, the total impulse response is integrated in time domain to compute the estimated test cavity and determine the quadratic error respect to the proposed test cavity.

Table 1. The quadratic error is evaluated using different frequency step sizes for each cylindrical cavity.

| Quadratic Error | Frequency Step Size (Hz) | Frequency Bandwidth (Hz) | Number of Frequencies |
|---|---|---|---|
| | Linear [50, 100, 150, 200, 250, 300, 350, 400, 450, 500] | 10 k | 56 |
| | Logarithmic [50, 64, 82, 105, 134, 171, 219, 280, 358, 457] | 10 k | 78 |
| | Small constant [50, 50, 50, 50, 50, 50, 50, 50, 50, 50] | 10 k | 200 |
| | Large constant [500, 500, 500, 500, 500, 500, 500, 500, 500, 500] | 10 k | 20 |
| | Large constant [500, 500, 500, 500, 500] | 5 k | 10 |

For instance, the first case denotes a linear rate in the frequency step size to sweep a frequency bandwidth of 10 kHz. In this way, the first subinterval, from 50 Hz to 1 kHz, is swept by using a frequency step size of 50 Hz. The second subinterval, from 1 kHz to 2 kHz, is swept by using a frequency step size of 100 Hz. The frequency step size is linearly increased on each interval until the last subinterval, from 9 kHz to 10 kHz, is swept by a frequency step size of 500 Hz. In this case, the computational cost is based on 56 acoustic waves, which were linearly distributed from 50 Hz to 10 kHz. This process is repeated for the next four cases in Table 1.

The parameters specified in the second row denote a logarithmic rate frequency step size, which required 78 frequencies distributed along a frequency bandwidth of 10 kHz.

The third and fourth rows represent two constant rates in the frequency step size, with 50 Hz and 500 Hz respectively, to sweep a frequency bandwidth of 10 kHz. The computational cost required 200 and 20 frequencies, respectively, on each case. The last row, in Table 1, is given by the worst condition using a large frequency step size and a truncated frequency bandwidth of 5 kHz.

Figure 24 quantifies the quadratic error obtained for each cylindrical cavity ruled by those conditions in Table 1.Despite the computational cost was very low when the last two parameters were used; a high quadratic error was computed in four cylindrical cavities. Thereby, it seems to be the worst case to be applied in the solution of the inverse problem. A lower quadratic error is computed when more frequencies are used to sweep the frequency bandwidth. It occurs for a linear and logarithmic frequency step sizes.

The analysis shows that no matter what cylindrical cavity may be used in the inverse problem, the lowest error computed occurs when a small, constant frequency step size is used to sweep the entire frequency bandwidth. The third row denotes the appropriate conditions to estimate a bore profile.

On the other hand, note that the difference in the error obtained in both linear and logarithmic is not so different to that obtain by using a constant frequency step size.

In order to qualify that computed quadratic error, it is necessary to make a graphical comparison between the estimated test cavity and the proposed test cavity. So, ruled by the parameters shown in Table1, the estimated test cavities are shown in Figure 25.

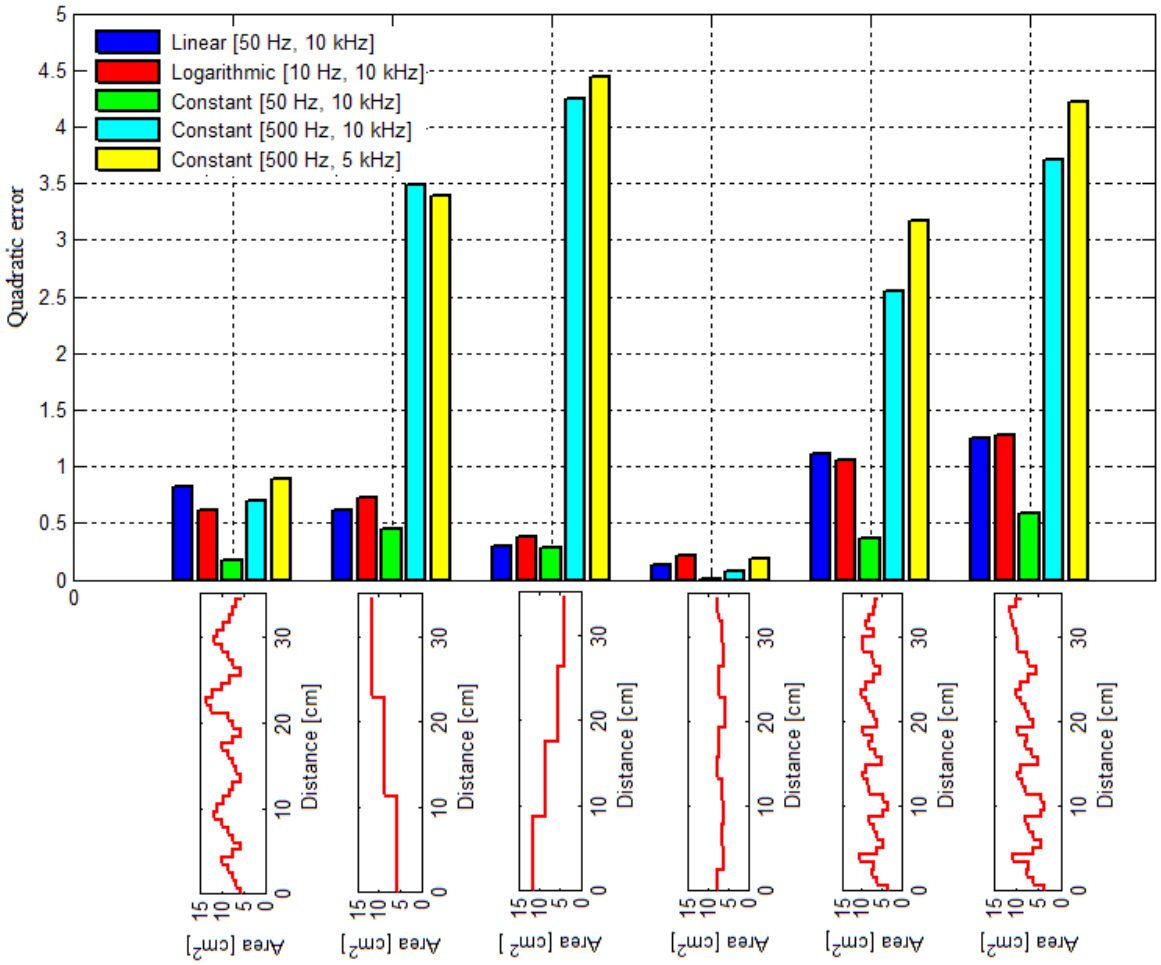


Figure 24. Quadratic error of the bore profile using different rates of frequency step sizes.

The proposed test cavity is displayed in color red and the estimated test cavity is displayed in color black. It graphically shows that a high axial resolution may be computed by using any of the first three rates in the frequency step size.

It is noted that the bore profile of certain cylindrical cavities may be obtained with an appropriate accuracy by using a large frequency step size or a truncated frequency bandwidth. However, it depends on the variation of the bore profile of a cylindrical cavity.

So, the results obtained by using several rates of frequency step size, suggest that the third scenario to compute the general bore profile of a cylindrical cavity consists of using either a

linear or logarithmic frequency step size. The axial resolution seems to be appropriated and the computational cost is lower than using a small, constant frequency step size.

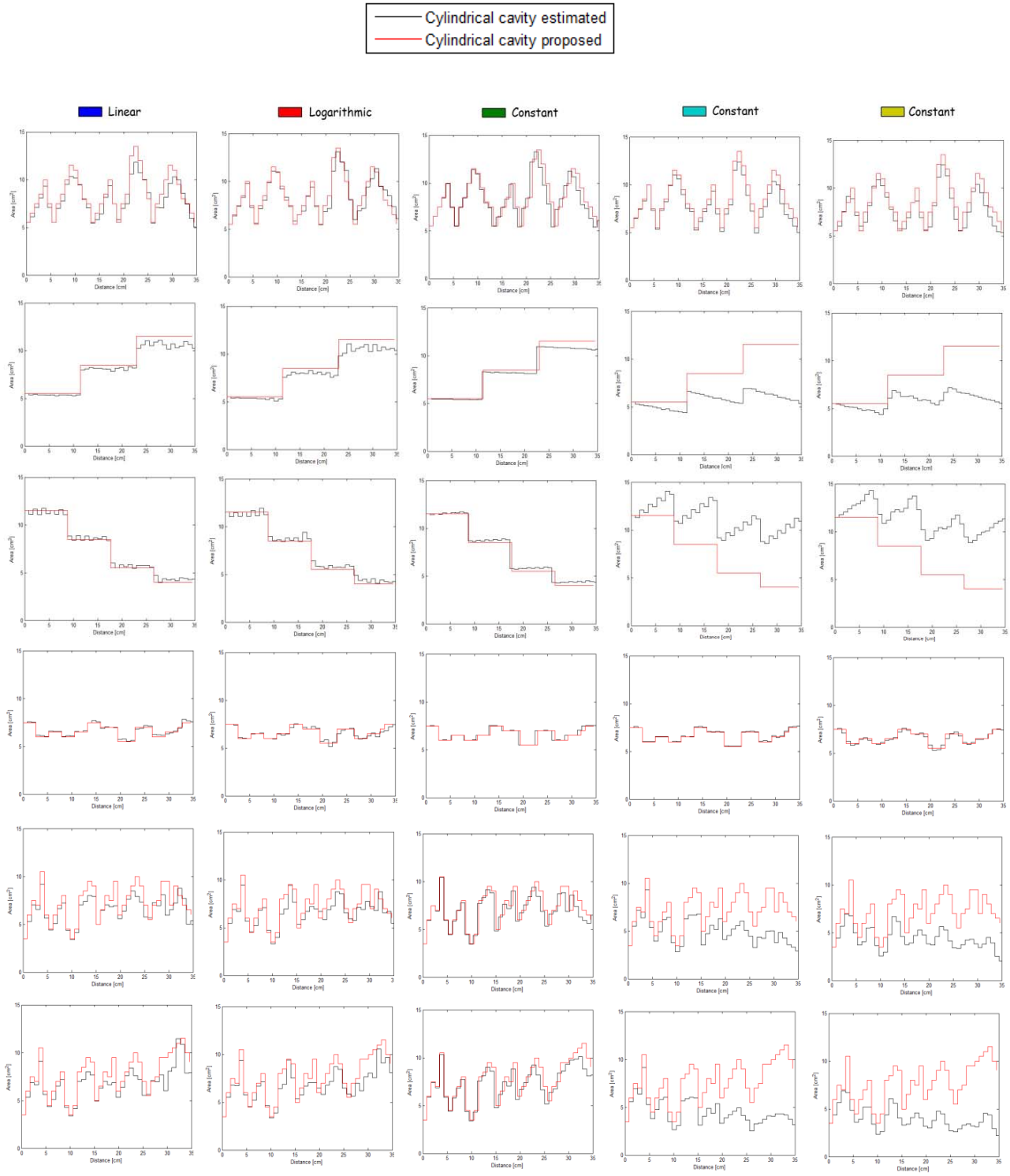


Figure 25. Qualitative comparison of the bore profiles.

### 5.2.5 Impulse response

The impulse responses of the second proposed test cavity using several rates of frequency step size are displayed in Figure 26. It is noted a few difference among the amplitudes of the impulse responses. However, a large difference between the estimated and proposed cavity is found when a large frequency step size is applied along the frequency bandwidth. Thereby, a quantitative and a qualitative analysis between third and forth cases in the Table 1 is performed in this section.

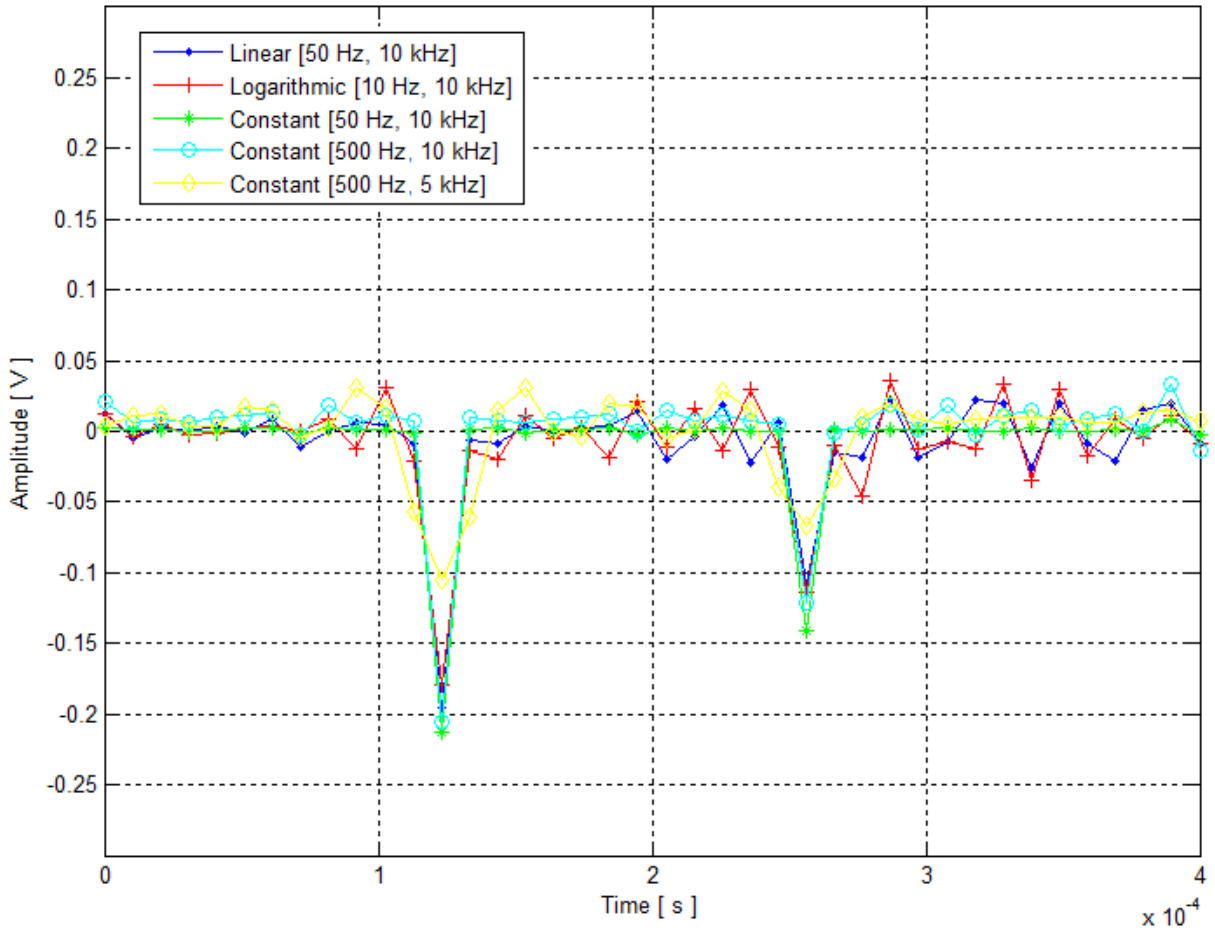


Figure 26. Impulse responses for the second cylindrical cavity.

The difference between both impulse responses obtained by using a frequency step size of 50 and 500 Hz is displayed in Figure 27. A small constant DC offset component of 0.008 V is present along the entire impulse response as function of the time.

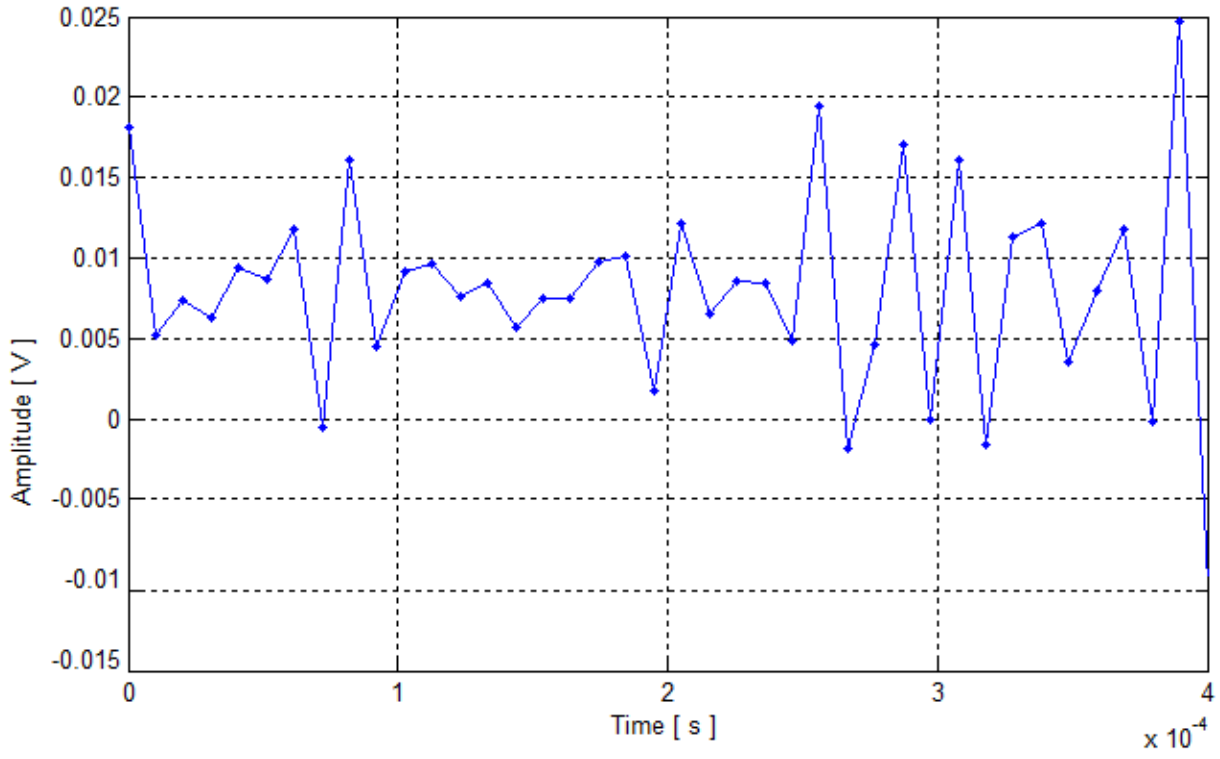


Figure 27. Difference between two impulse responses for the second cylindrical cavity.

This procedure was repeated for the proposed test cavities and their values are displayed in Table 2.

The values of this DC offset component were added to the impulse response when a large frequency step size of 500 Hz is used to sweep the frequency bandwidth of 10 kHz, and the quadratic error is computed and displayed in Figure 28.

Table 2. DC offset components along the difference between two impulse responses.

| Cylindrical cavity | DC offset computed (V) |
|---|---|
| 1 | 0.0012 |
| 2 | 0.008 |
| 3 | -0.011 |
| 4 | 0.00005 |
| 5 | 0.007 |
| 6 | 0.0106 |

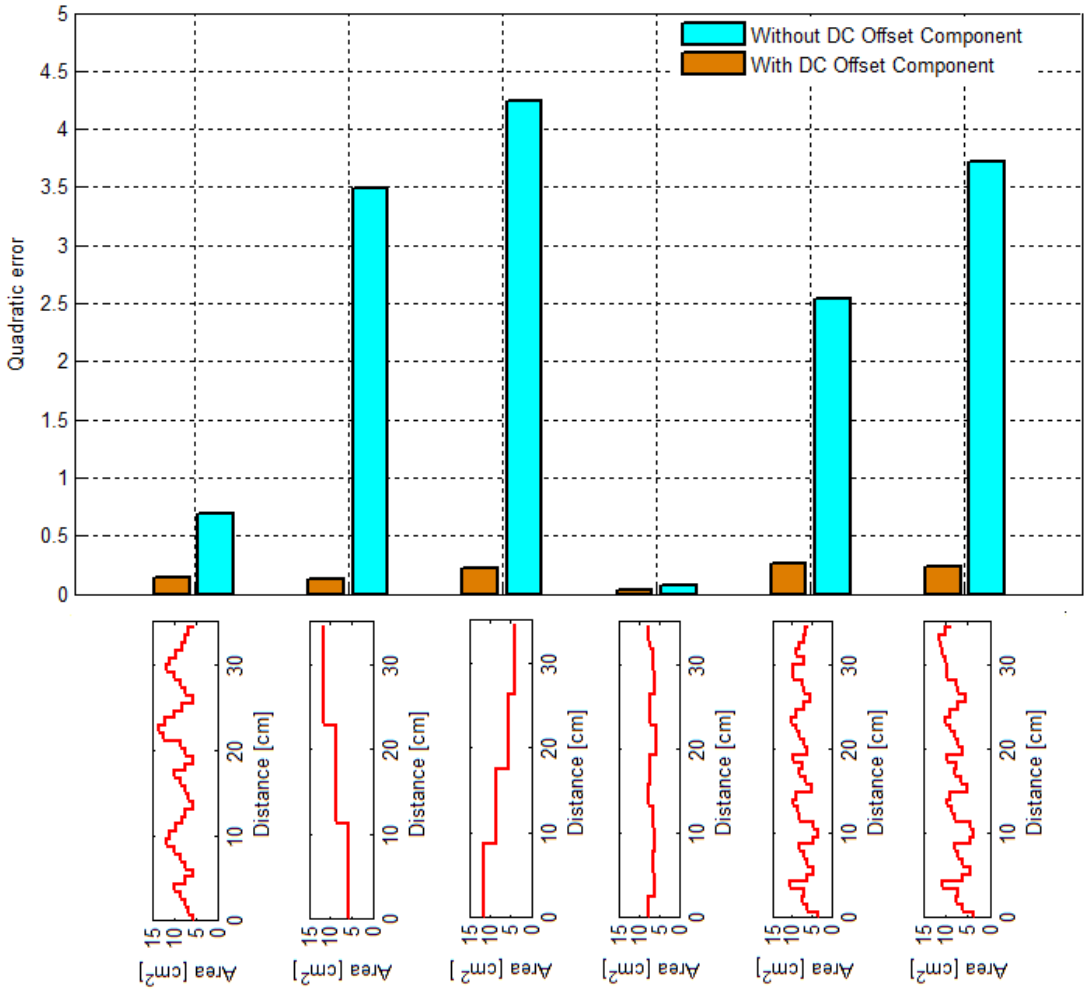


Figure 28. Quantitative comparison of quadratic error by adding a DC offset component.

A qualitative comparison between the proposed and test cylindrical cavities by adding this DC offset component is displayed in Figure 29.

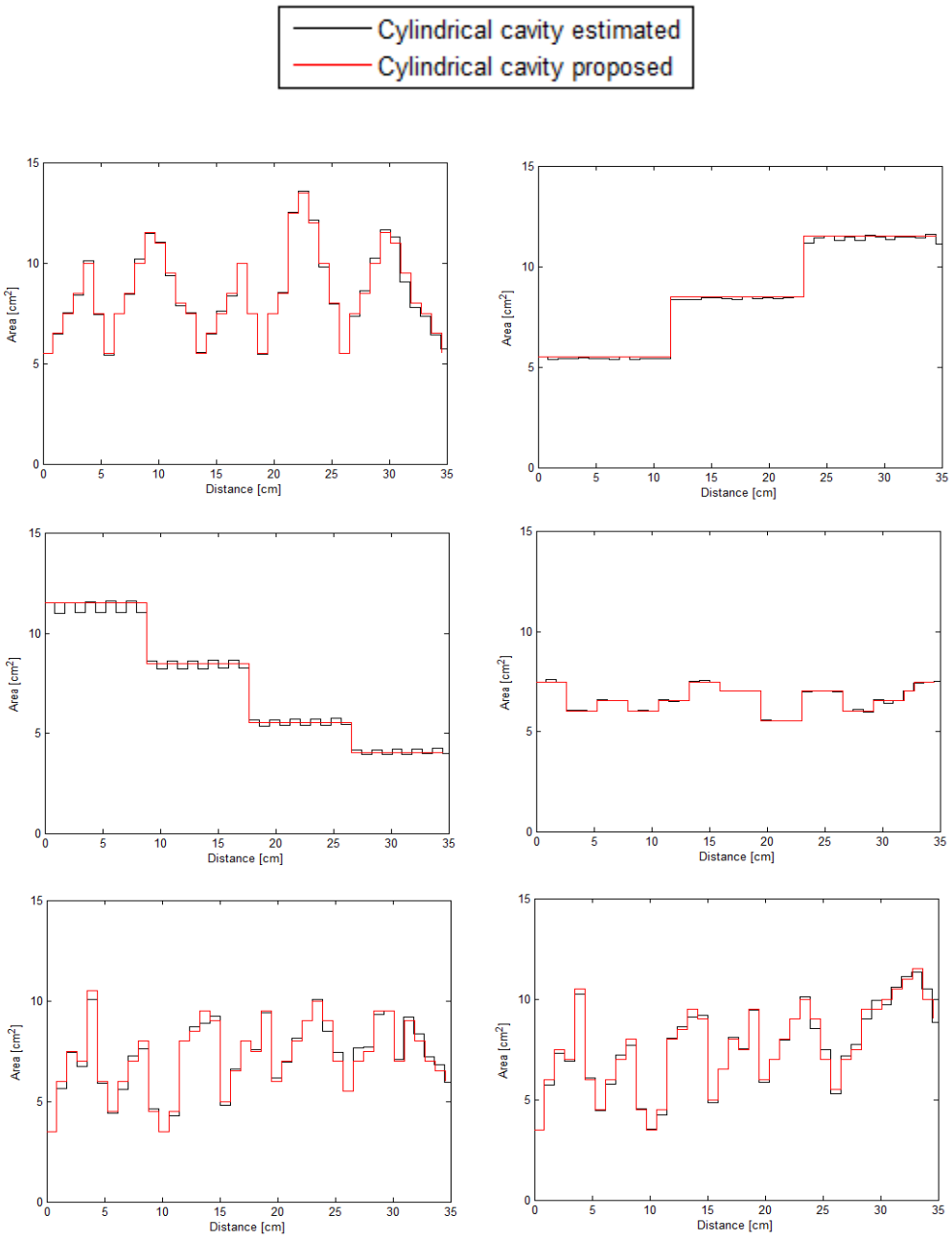


Figure 29. Qualitative comparison of quadratic error by adding a DC offset component.

A high axial resolution between the estimated and proposed test cavities is evident. However, it just mean that the solution of the inverse problem is very sensitive to the acquisition noise.

## 5.3 Concluding remarks

The use of Gaussian modulated sinusoidal waves has been evaluated through a simulation model to solve the inverse problem in acoustic reflectometry. A trade off is evident in the process to estimate the bore profile with high accuracy.

The simulation model shows that under ideal condition, the computational cost may be reduced by adding a DC offset component in the impulse response.

Chapter 5 described the potential of using a simulation model in this dissertation, which was used to evaluate the parameters involved in the solution of the inverse problem. In this way, it is possible to predict the ideal conditions to estimate a bore profile of any cylindrical cavity with an appropriate resolution.

# Chapter 6

# Part I: Results

## 6.1 Introduction

This chapter reports the experimental results using Gaussian-modulated acoustic waves and the Ware-Aki algorithm. The solution of the inverse problem is applied to a solid cylindrical cavity characterized by having a square bore profile.

Based on the results obtained by the simulation model, the lowest error is computed when a relatively small constant frequency step size of 50 Hz is used to sweep the frequency interval from 50 Hz to 10 kHz. Those parameters are used in the simulation model and the experimental results to solve the inverse problem.

This chapter provides a comparison of results obtained from the simulation model and the experimental acoustic reflectometer. The proposed test cylindrical cavity used to solve the forward problem in the simulation model is represented in the red color. On the other hand, both results obtained, in the simulation model and in the experimental situation, are represented in black and blue, respectively.

## 6.2 Simulation of a square cylindrical cavity

A cylindrical cavity composed of three cylindrical segments was used to evaluate the solution of the inverse problem. The first and third cylindrical segments were designed to have 1.1 cm diameter and the second segment of 1.6 cm diameter. Each segment was 7 cm long. The segments were consecutively joined each other by a connector and coupled at the end distal of the reflectometer.

Because the simulation model assumes an infinite cylindrical cavity, a long cylindrical cavity was coupled at the end distal of the cavity. The entire setup is shown in Figure 30.

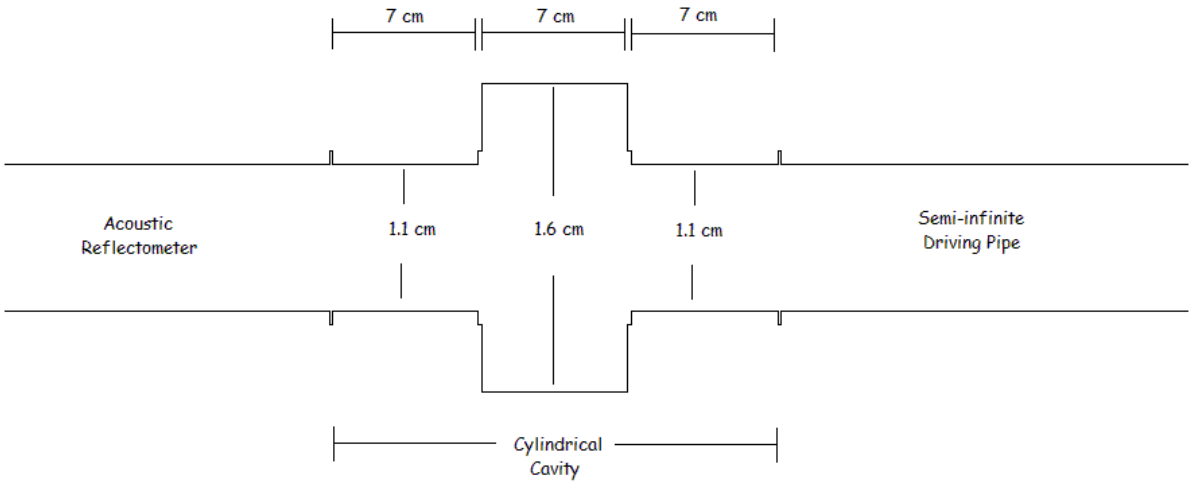


Figure 30. A square cylindrical cavity composed by three segments.

The next step consisted in representing this cylindrical cavity in the simulation model to evaluate the distribution of the quadratic error as function of the frequency step size. So, the entire bore profile as function of the distance is represented by using a certain number of short cylindrical segments, as shown in Figure 3.

A sampling frequency of 100 kHz was used and a speed of sound of 345.28 m/s was assumed in (2.28), giving an axial length of

$$\ell = 0.1726 \text{ cm.} \tag{6.1}$$

Physically, it means that 120 short cylindrical segments were required to represent the proposed test cavity. Each connector in turn was represented in the simulation model using a short cylindrical segment of diameter 1.2 cm.

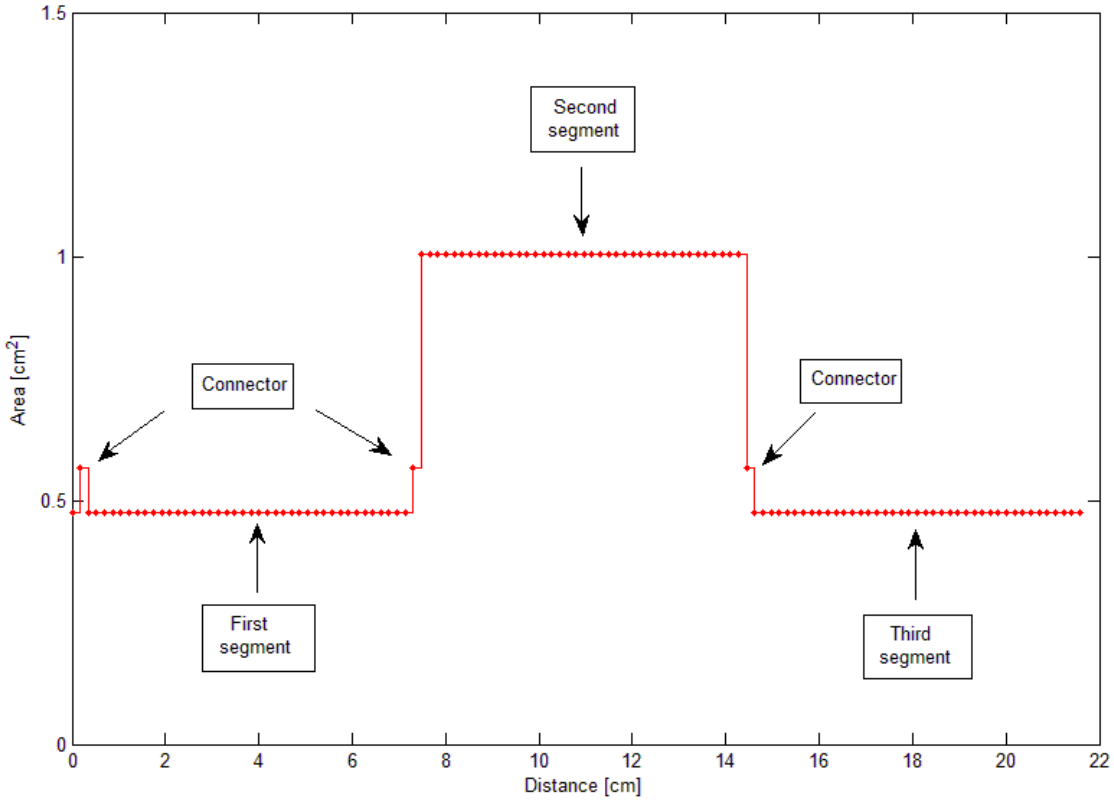


Figure 31. The square cylindrical cavity represented by short cylindrical segments.

The cross sectional area is represented in Figure 31 as function of the distance. In this particular case, it is displayed by using dots, which denote a short cylindrical segment used to represent the entire cavity.

Following the same procedure depicted in Figures 26 and 27, the simulation model was used to scan the bandwidth using several frequency step sizes. Hence, the quadratic error was quantified as function of the frequency step size, as shown in Figure 32.

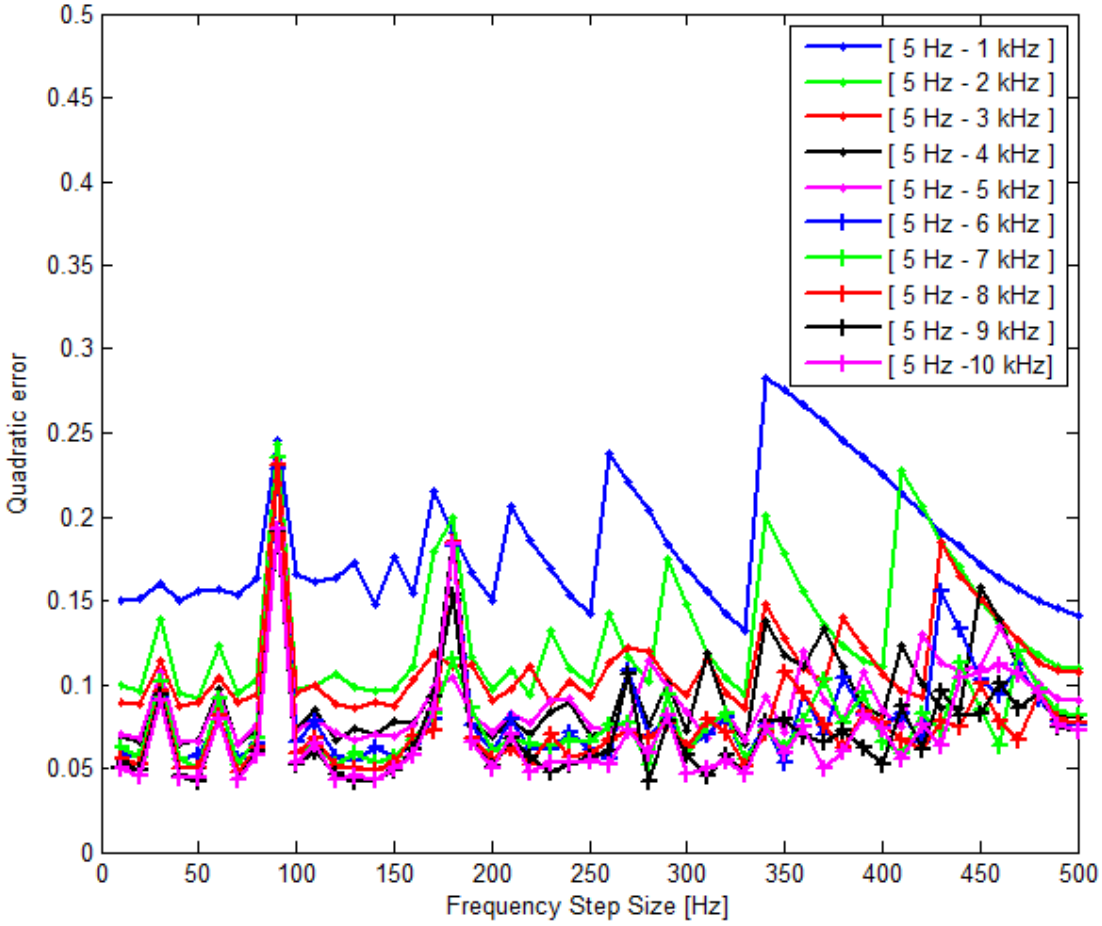


Figure 32. Quadratic error of a square cylindrical cavity as function of frequency step size.

The results obtained by the simulation model show that the predominant frequencies are located in the interval from 50 Hz to 4 kHz.

## 6.3 Experimental results in a square cylindrical cavity

To validate the application of Gaussian-modulated sinusoidal waves in acoustic reflectometry, a frequency bandwidth from 50 Hz to 10 kHz was swept using a frequency step size of 50 Hz and acoustical losses were compensated along the source tube by using (4.20).

The bandwidth was divided into ten equally spaced intervals of frequency to compare the cylindrical cavity for each interval of frequency.

The first two columns, in Figure 33, display the frequency response for each interval of frequency (amplitude and phase). The third column shows the impulse response in time domain which is used in the Ware-Aki algorithm to compute the reflection coefficients and display the bore profile. The fourth columns displays both the bore profile experimentally computed, shown in blue, versus the proposed test cavity, shown in red.

It is noted that the first two ranges of frequency, 50 Hz to 1 kHz and 1050 Hz to 2 kHz, provide a significant bore profile. The range of frequency between 2050 Hz and 3 kHz does not provide a significant contribution to the bore profile, but the range between 3050 Hz and 4 kHz contributes more significantly.

Above 4 kHz, the bore profile estimated is constant with a few variations as function of distance. It is also noted that last three frequency ranges (7050 kHz to 10 kHz) provide a constant bore profile. Hence, the contribution of those frequencies is relatively small.

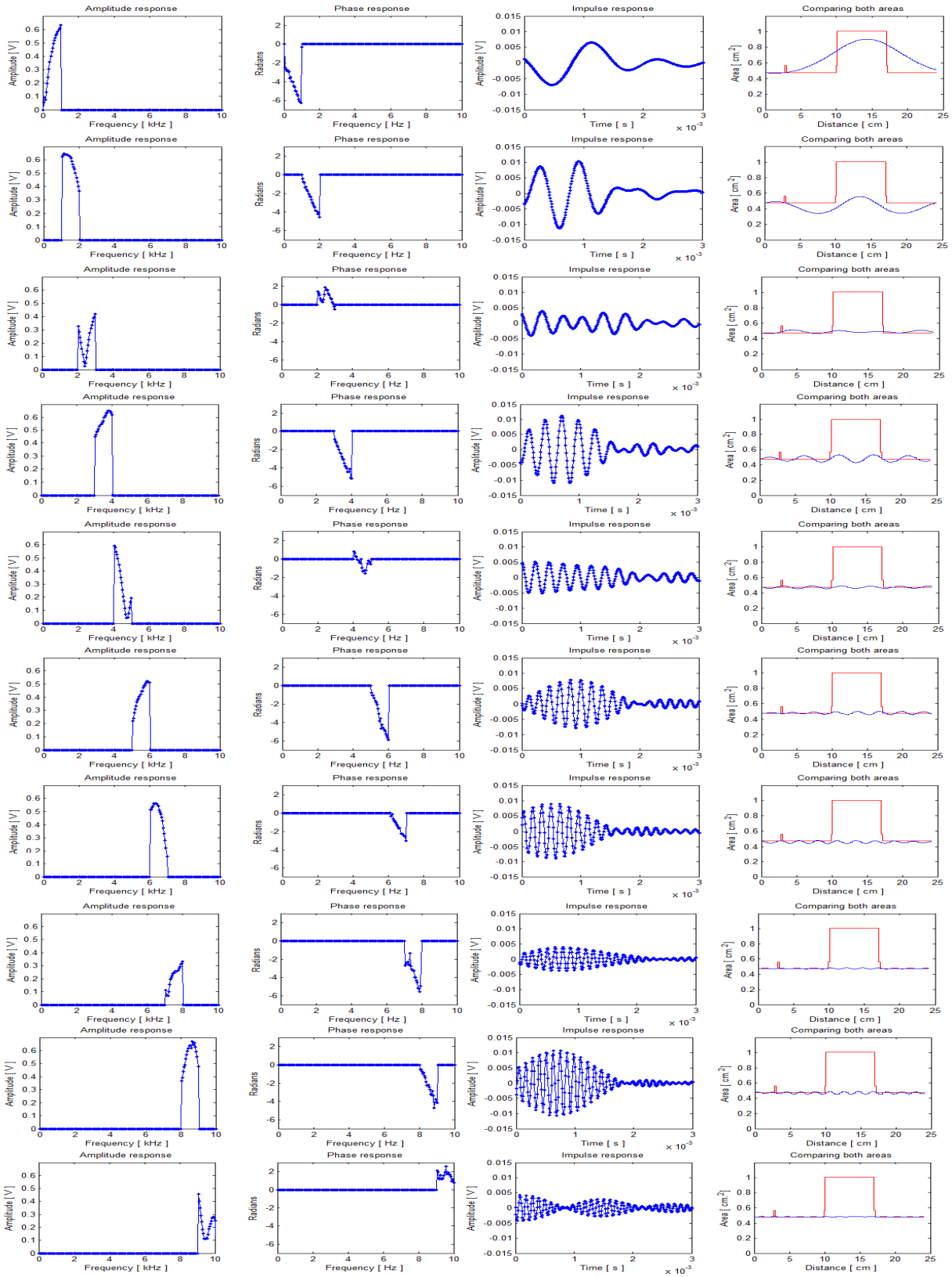


Figure 33. Ten equally spaced intervals of frequency for a square cylindrical cavity.

## 6.4 Superposition of the impulse response for a square cylindrical cavity

The influence of each interval of frequency may be integrated to evaluate the improvement of the axial resolution. This procedure of superposition may be computed either in frequency or time domain.

The first two columns in Figure 34 display the superposition of frequency intervals. In other words, the bandwidth is increased in intervals of 1 kHz to cover the interval from 50 Hz to 10 kHz. The impulse response obtained for each interval of frequency is also provided in Figure 39. The last column shows a comparison between the bore profile experimentally computed, given in blue, and the proposed test cavity, given in red.

It is noted in the plot of Figure 34 that the first two ranges of frequency define a bore profile close to the proposed test cavity. The third interval of frequency, 2050 Hz to 3 kHz, does not significantly contribute to the bore profile. However, another significant contribution is obtained when the fourth interval of frequency, 3050 Hz to 4 kHz, is superposed. Above this frequency the bore profile is refined such that the square bore profile may be better characterized. For instance, the impulse response above 7 kHz is used to refine the sharp discontinuities present along the bore profile.

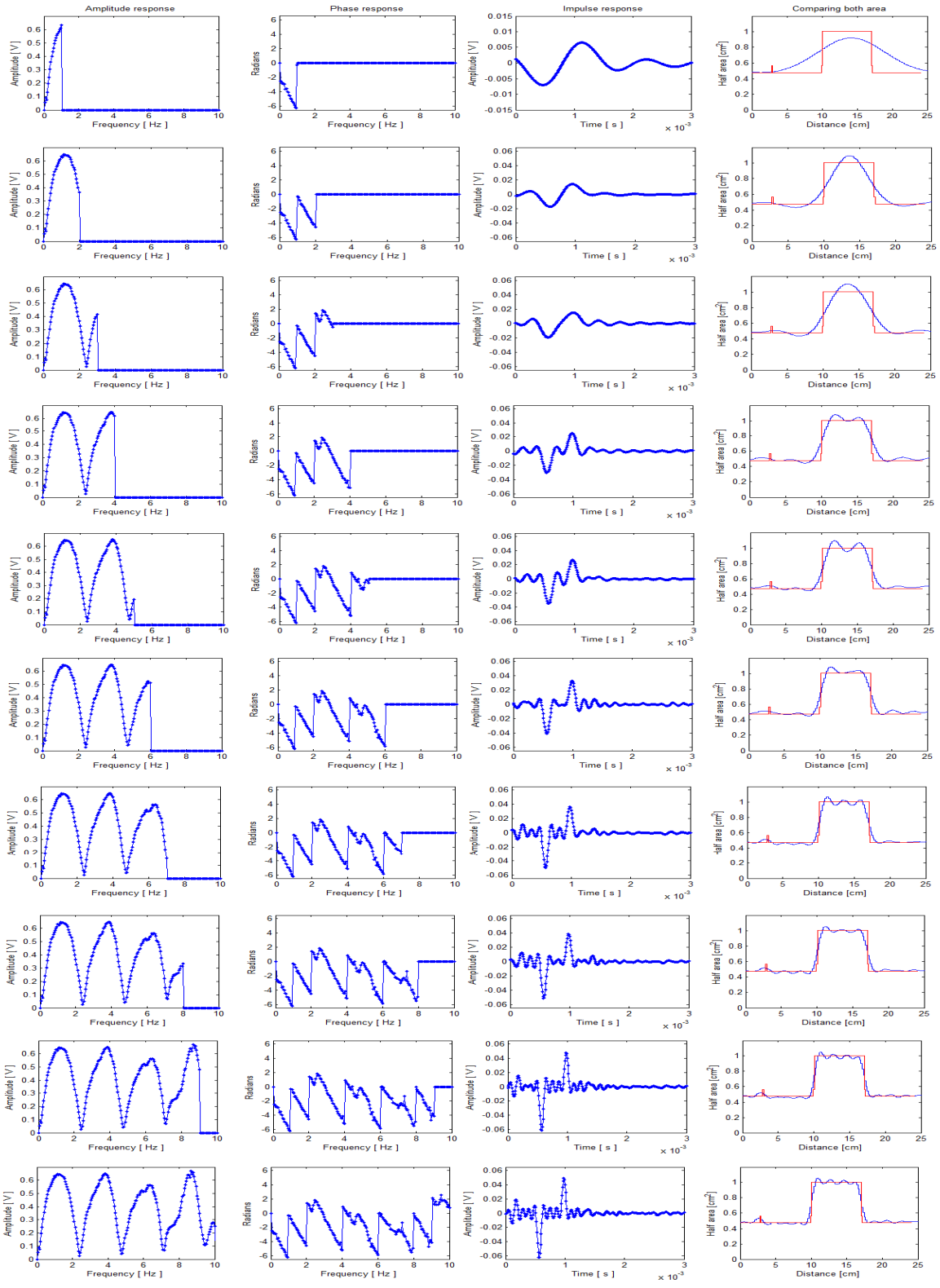


Figure 34. Superposition of impulse response of a square cylindrical cavity.

This analysis may be quantified by calculating the quadratic error between the proposed test cavity and the cavity experimentally obtained. Thereafter, the error is computed as function of an increment in the bandwidth, as shown in Figure 35.

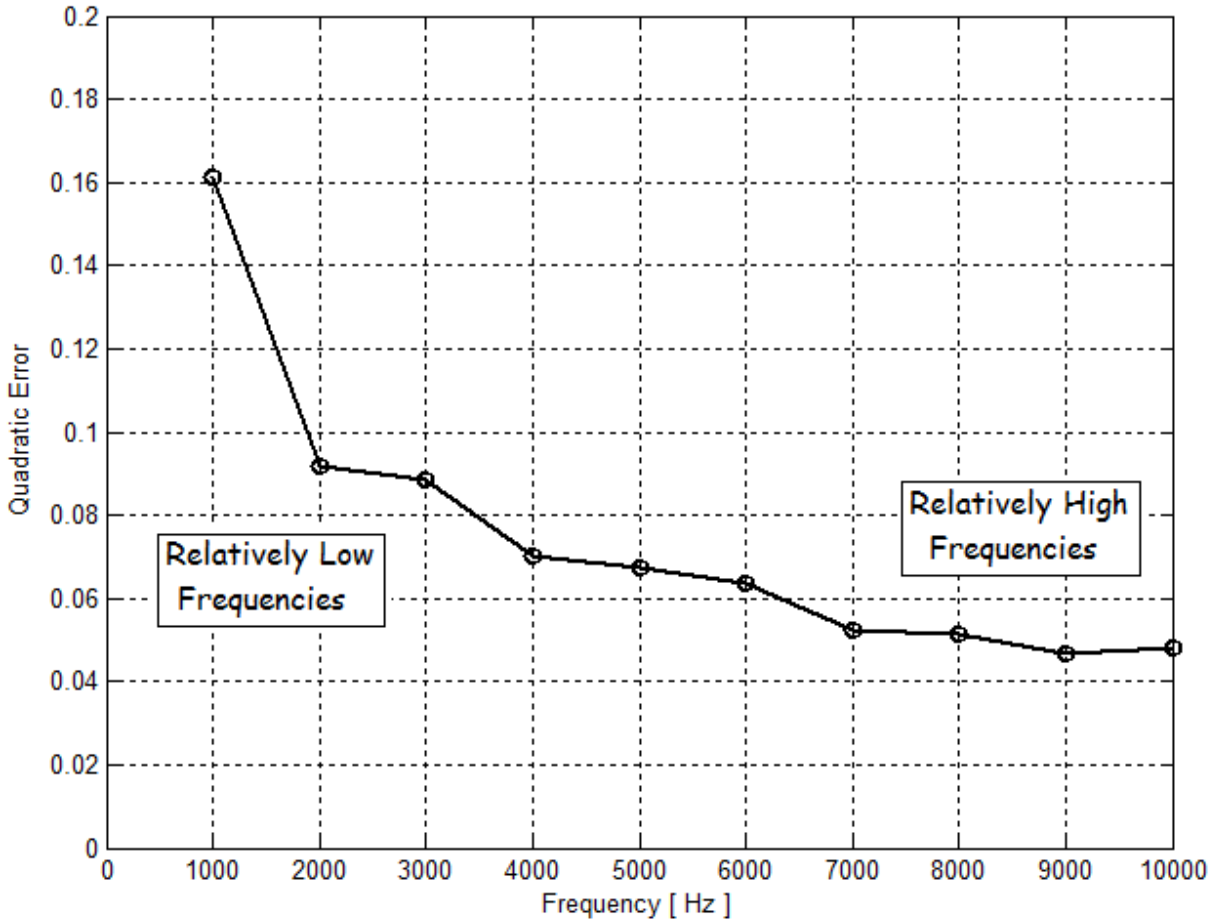


Figure 35. Experimental Quadratic error of a square cylindrical cavity.

The error was significantly reduced when the significant frequencies were covered. It occurs along the relatively low frequencies from 50 Hz to 4 kHz. A very low reduction of the error is computed in the range of frequency of 4 kHz – 7 kHz. Above 7 kHz the error seems to be constant. However, graphically it improves the resolution of the sharp discontinuity in the cylindrical cavity.

## 6.5 Comparison between simulation and experimentation for a square cavity

The simulation model was performed under ideal conditions where there is no limit in the frequency generated and where losses of the acoustic waves do not exist. On the other hand, the experimental situation is not only limited by the audible bandwidth, but also it requires compensation of losses along the source tube, improving the signal-to-noise ratio at high frequencies, and compensating the DC offset component at low frequencies.

A comparison of the impulse response in the frequency domain, between the result obtained in the simulation and the experimental situation, is displayed in Figure 36.

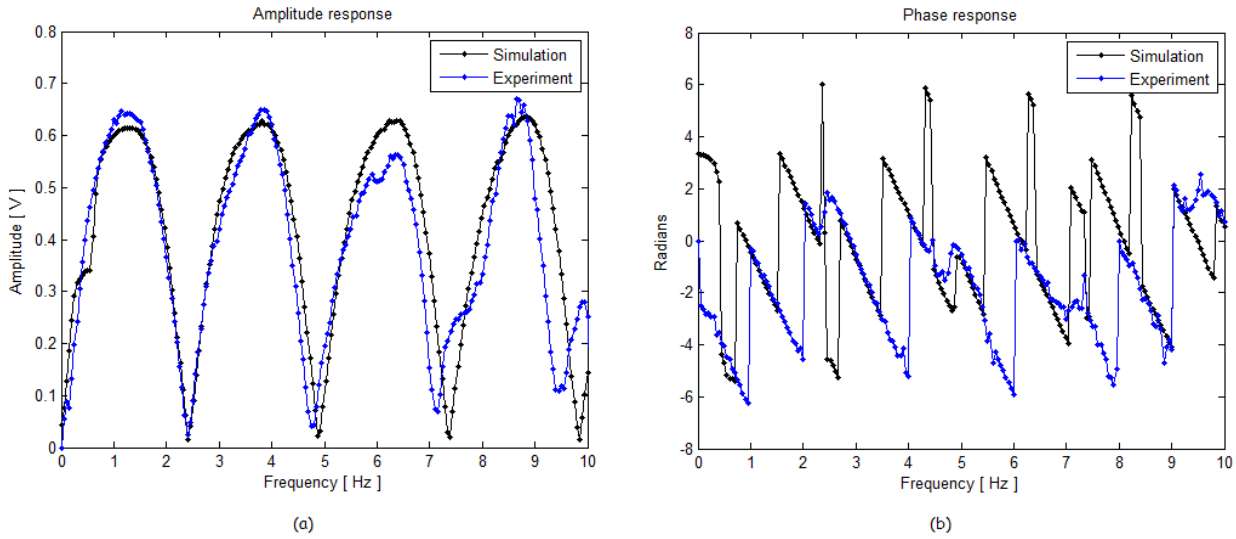


Figure 36. Comparison of frequency impulse responses for a square cylindrical cavity.

Despite of a difference in the results obtained experimentally, it is possible to say that the relatively low frequencies are well estimated in amplitude.

Likewise, a comparison of both impulse responses in time domain, as shown in Figure 37, is characterized by a small difference in amplitude.

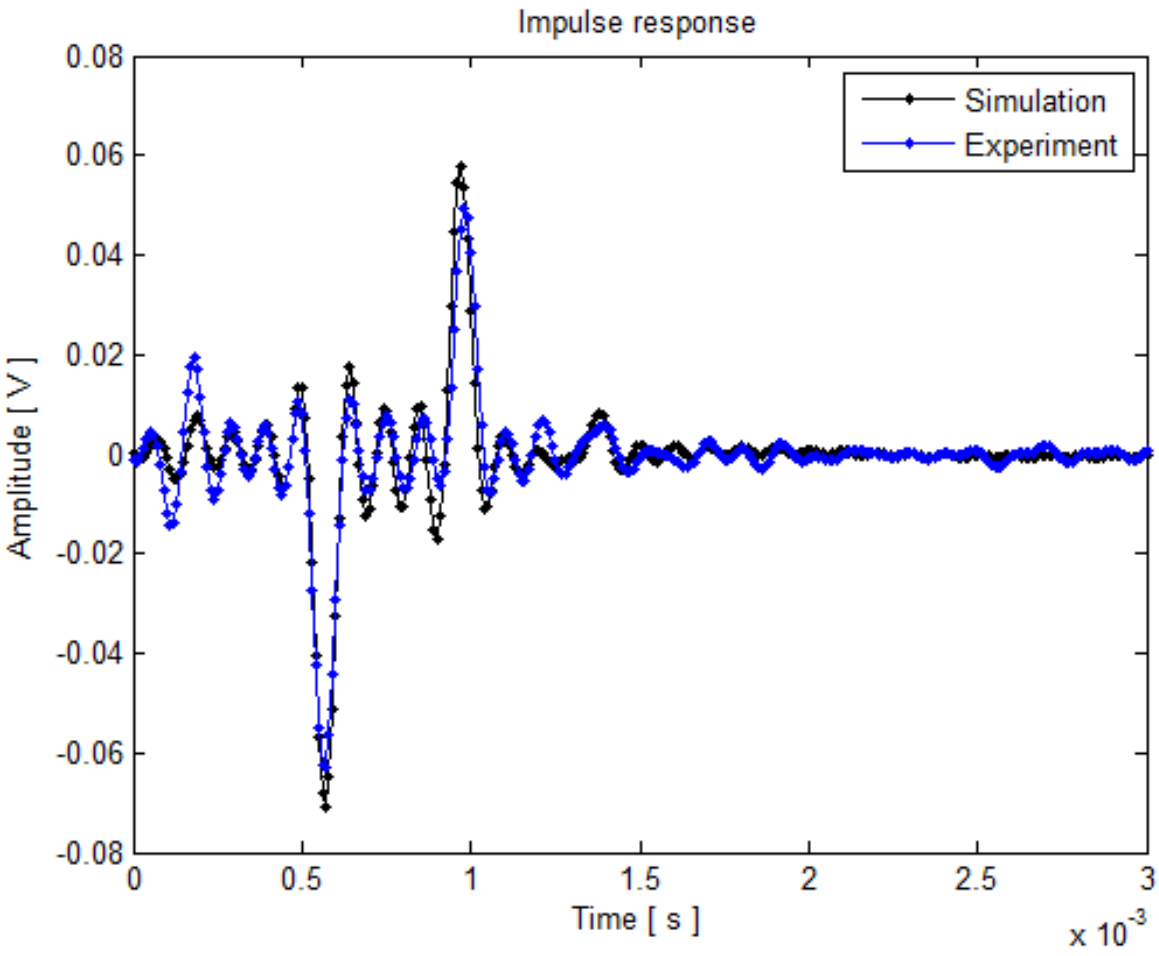


Figure 37. Comparison between amplitude responses for a square cylindrical cavity.

This difference in amplitude is shown in the reconstruction of the bore profile, as shown the Figure 38, where both bore profiles, simulated and experimental, are compared to the proposed test cavity.

The results obtained in this simple cylindrical cavity shows that the solution of the inverse problem has been well defined in this dissertation.

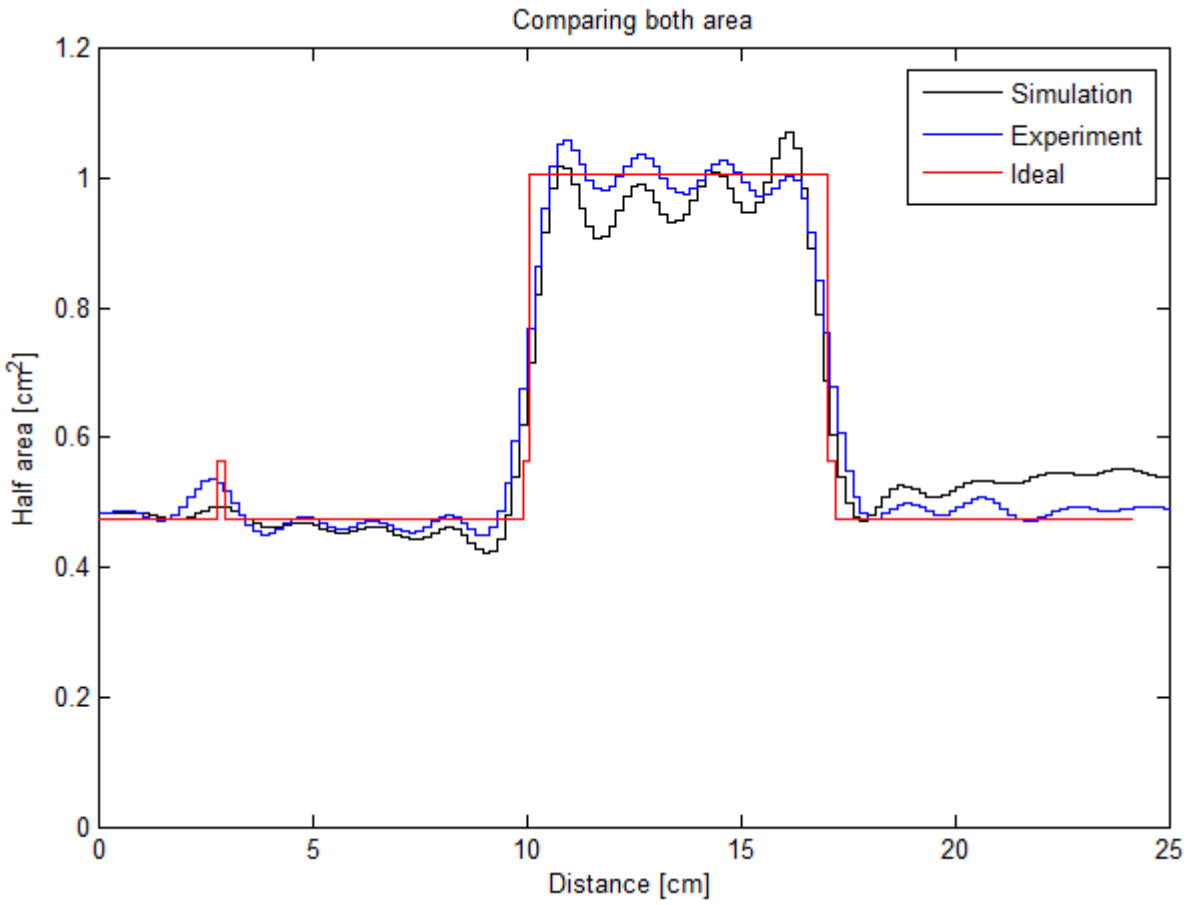


Figure 38. Comparison among bore profiles for a square cylindrical cavity.

## 6.6 Concluding remarks

This chapter covers the solution of the inverse problem using Gaussian-modulated sinusoidal waves and the Ware-Aki algorithm. The results obtained by simulation model and experimental situation were used to estimate the bore profile of a simple cylindrical cavity with satisfactory accuracy. It is necessary to evaluate the technique by using a longer cylindrical cavity to evaluate the effect of losses in the reconstruction.

# Chapter 7

# Part II: Results

## 7.1 Introduction

Several applications are found in acoustic reflectometry. However, one of the most important consists of evaluating the patency of either a human upper airway or an endotracheal tube in hospitals.

The last chapter of this dissertation is focused on applying the simulation model to evaluate the acoustic parameters needed to estimate the bore profile of a vitro model of a human upper airway. In other words, this chapter qualifies and quantifies the solution of the inverse problem such that the parameters in acoustic reflectometry are defined to apply the technique in a model in vitro of a human upper airway.

A sampling frequency of 100 kHz is used to estimate the frequency impulse response of a cylindrical cavity. A relatively small constant frequency step size of 50 Hz is used to sweep a frequency interval from 50 Hz to 10 kHz.

The bore profile of the proposed test cavity, representing a human upper airway, is displayed in red. The results obtained by simulation model were displayed in black, and the experimental results are displayed in blue.

## 7.2 Bore profile of a human upper airway

The measurement of a human upper airway is a practical implementation of acoustic reflectometry. The estimation of its bore profile makes possible to identify some pathologies. For example, it is used to evaluate some diseases like sleep apnea, the anesthetic management of patients and nasal/airway surgery. Figure 39 describes the physiology of a human upper airway [33]. Acoustic reflectometry has been used to evaluate the bore profile from the vocal tract until the end of the trachea which is named carina.

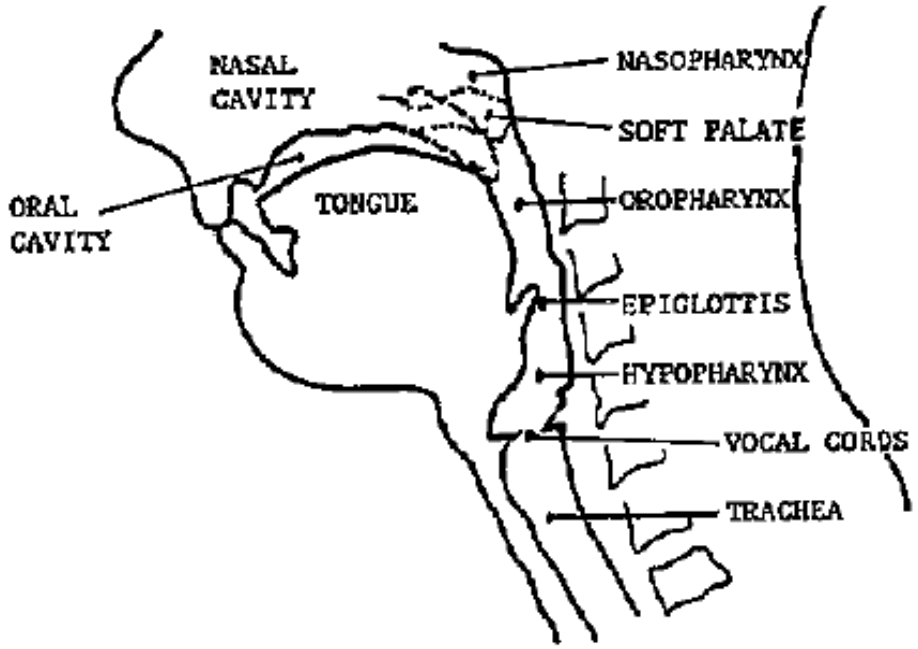


Figure 39. The human respiratory system (from [33])

Anthony et al. [34] used acoustic reflections to estimate glottic areas. The results were validated by computerized tomography. Figure 40 shows the results obtained from such research. An acoustic pulse was used to estimate the bore profile in 11 subjects with a history of glottic pathology, mean age 56 and range 29 to 72 years old.

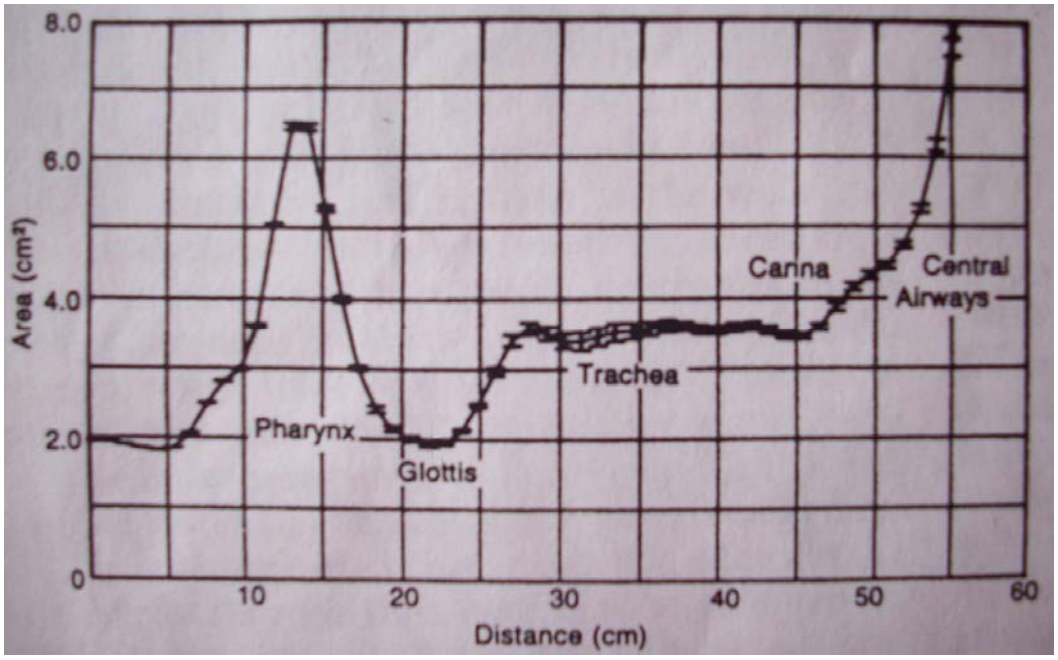


Figure 40. Bore profile of a human upper airway (from [34])

The area obtained seems to have a regular shape for all patients, except for the region of the trachea. On the other hand, it is noted that the central airway is described by an increment in the magnitude of area. It is due to the branching way after the point named Carina, which is connected to the lungs.

## 7.3 Proposed test cavity of a human upper airway

The solution of the inverse problem was evaluated through the simulation model using a cylindrical cavity with a bore profile of an upper airway. Hence, the dimensions of the bore profile were carefully measured from Figure 40 to replicate the measurements of a proposed test cylindrical cavity for a human upper airway.

Figure 41 shows the proposed test cavity composed by 342 cylindrical segments with an axial length given by (6.1). This bore profile was used in the simulation model to analyze the frequency content in the solution of the inverse problem.

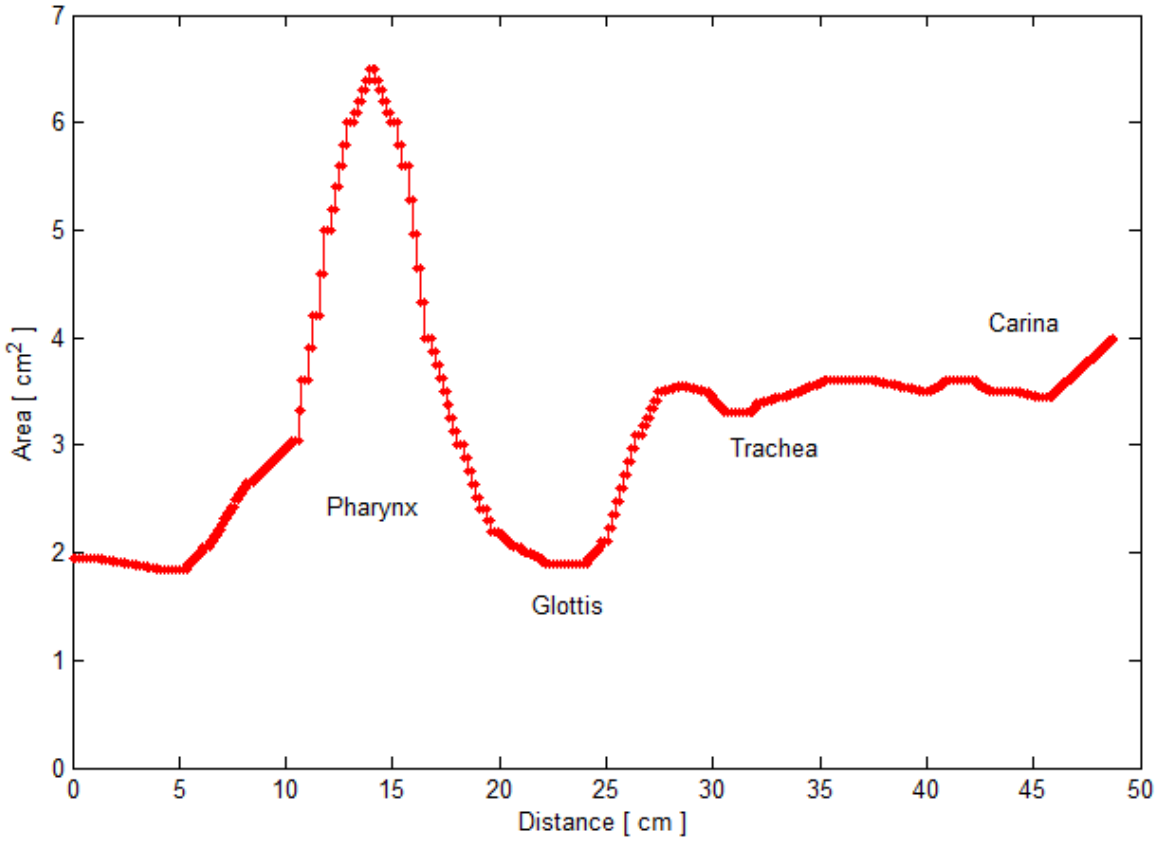


Figure 41. Proposed test cylindrical cavity of a human upper airway.

## 7.4 Predominant frequencies of a human upper airway

The simulation model was used to identify the predominant frequencies of a human upper airway. Because the cavity to study is composed by a long number of cylindrical segments, the maximum frequency step size that may be used is 300 Hz. The bandwidth was increased at a rate

of 1 kHz to cover the interval from 50 Hz to 10 kHz. The quadratic error was computed by using a constant increment of the frequency step size of 10 Hz for each interval, as shown in Figure 42.

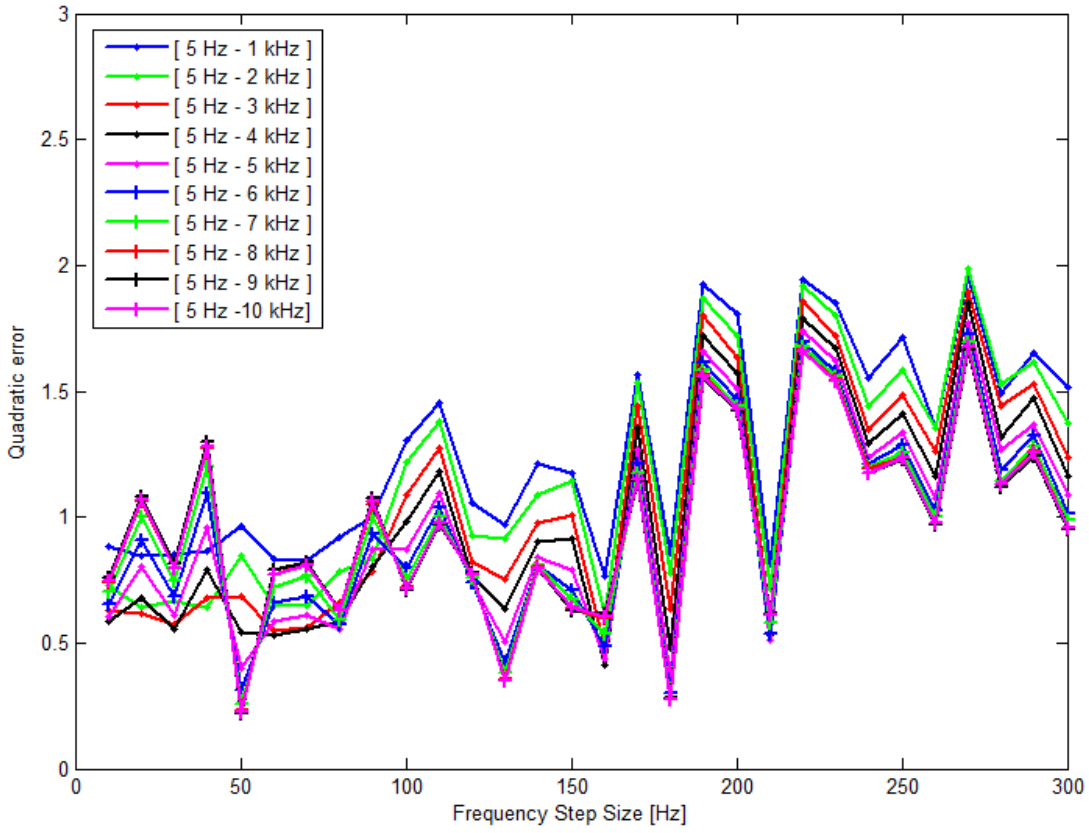


Figure 42. Quadratic error as function of frequency step size for an upper airway.

The results show that the lowest quadratic error was computed at a frequency step size of 50 Hz, and the error increased for some intervals of frequency below this frequency step size. The predominant frequencies are located within the frequency interval from 50 Hz to 50 kHz.

## 7.5 Estimated test cavity of a human upper airway by simulation

A decomposition of the bandwidth in frequency subintervals of 1 kHz is used to display the bore profile. The results obtained by simulation in the solution of the inverse problem are displayed in black in Figure 43 and the proposed test cavity in red.

The simulated bore profile was coupled to the dimensions of the source tube. In other words, the ends of the cylindrical cavity for study were joined to a uniform cross sectional area where the acoustic waves are supposed to propagate. In this way, the simulation model is used to analyze the result of coupling the cavity at its ends. Figure 43 displays the results of the impulse response and the bore profile in the same way as it was initially described in Figure 18.

The decomposition of the spectrum shows that the first three frequency intervals, which cover the range of 50 Hz to 3 kHz, provide a long variation of the bore profile. It means that such frequencies contribute with a main shape of the cavity.

The frequency intervals from 3 kHz to 5 kHz are denoted by a very small variation in the bore profile, and the rest of frequencies are characterized by having a constant bore profile. In fact, the last three frequency intervals, which cover the frequency interval from 8 kHz to 10 kHz, do not significantly contribute with the bore profile.

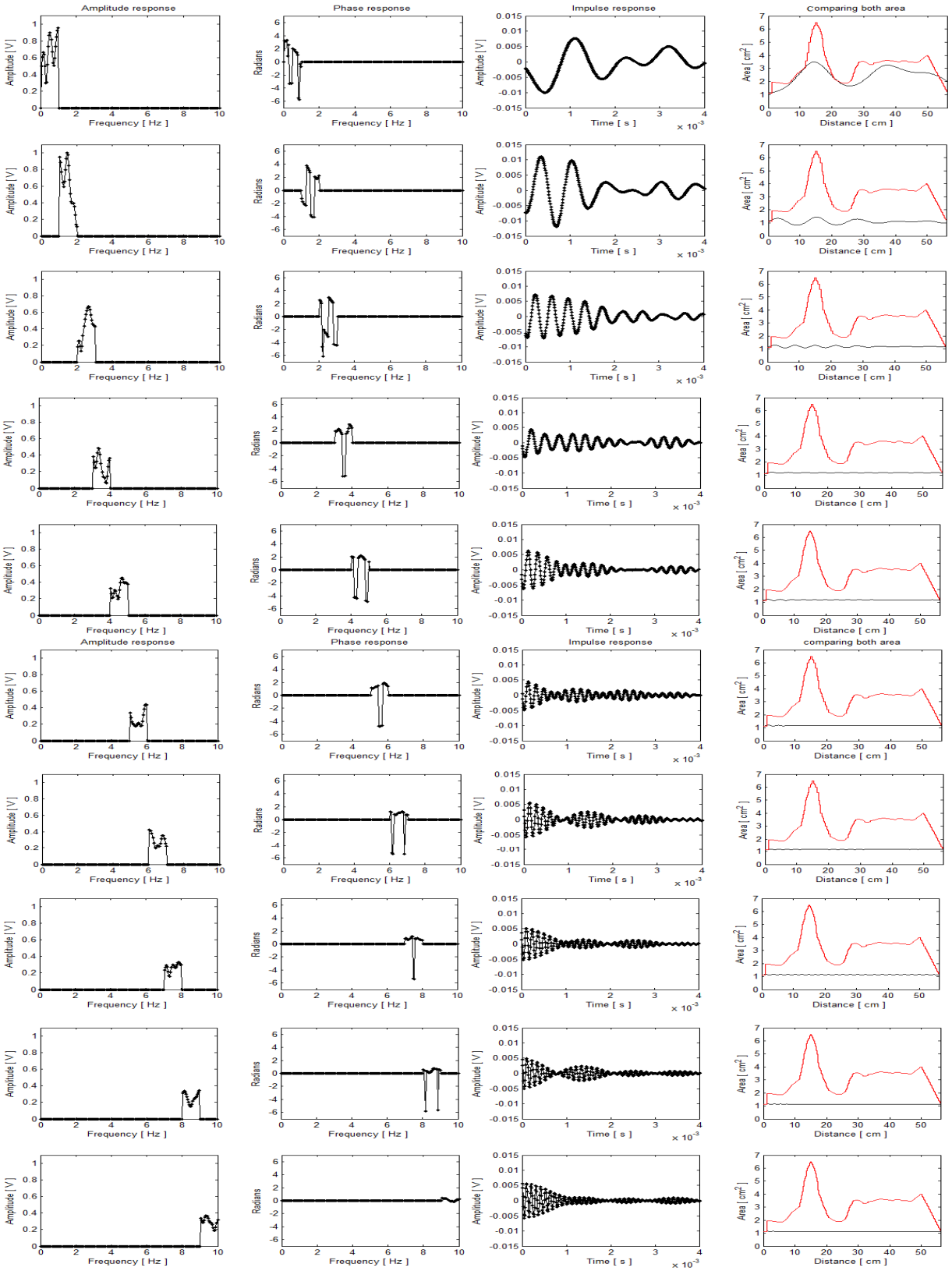


Figure 43. Decomposition of the impulse response of a proposed upper airway

## 7.6 Superposition of impulse response in the simulation of an upper airway

Figure 44 shows the superposition of the impulse response with an increment of 1 kHz along the bandwidth. The first two columns show the frequency impulse response, the third column displays the integrated impulse response and the fourth column displays the cavity estimated (black) and the proposed test cavity (red).

Despite of a little difference between both bore profiles along the segments which represent the regions of pharynx and glottis. The qualitative analysis shows that the general bore profile is well approximated by the frequency components from 50 Hz to 7 kHz. Above 7 kHz, the results show that there is not a significant improvement.

Figure 45 displays the error computed as function of an increment in the bandwidth. It quantifies what it was described in Figures 43 and 44. The error is mainly reduced when the bandwidth of 7 kHz is covered. It denotes that significant frequencies are located within this frequency range.

The simulation model suggests that it is possible to use Gaussian modulated acoustic waves to estimate the bore profile of a human upper airway using the Ware-Aki algorithm. The analysis shows that the bore profile in the proposed test cavity is not a complex cylindrical cavity. In other words, it is not necessary to cover a large bandwidth to estimate an appropriate axial resolution.

The advantage of covering a frequency from 50 to 7 kHz lies in the fact that the artifacts of relatively high frequencies may be avoided when the right conditions in the relatively low frequencies are well performed.

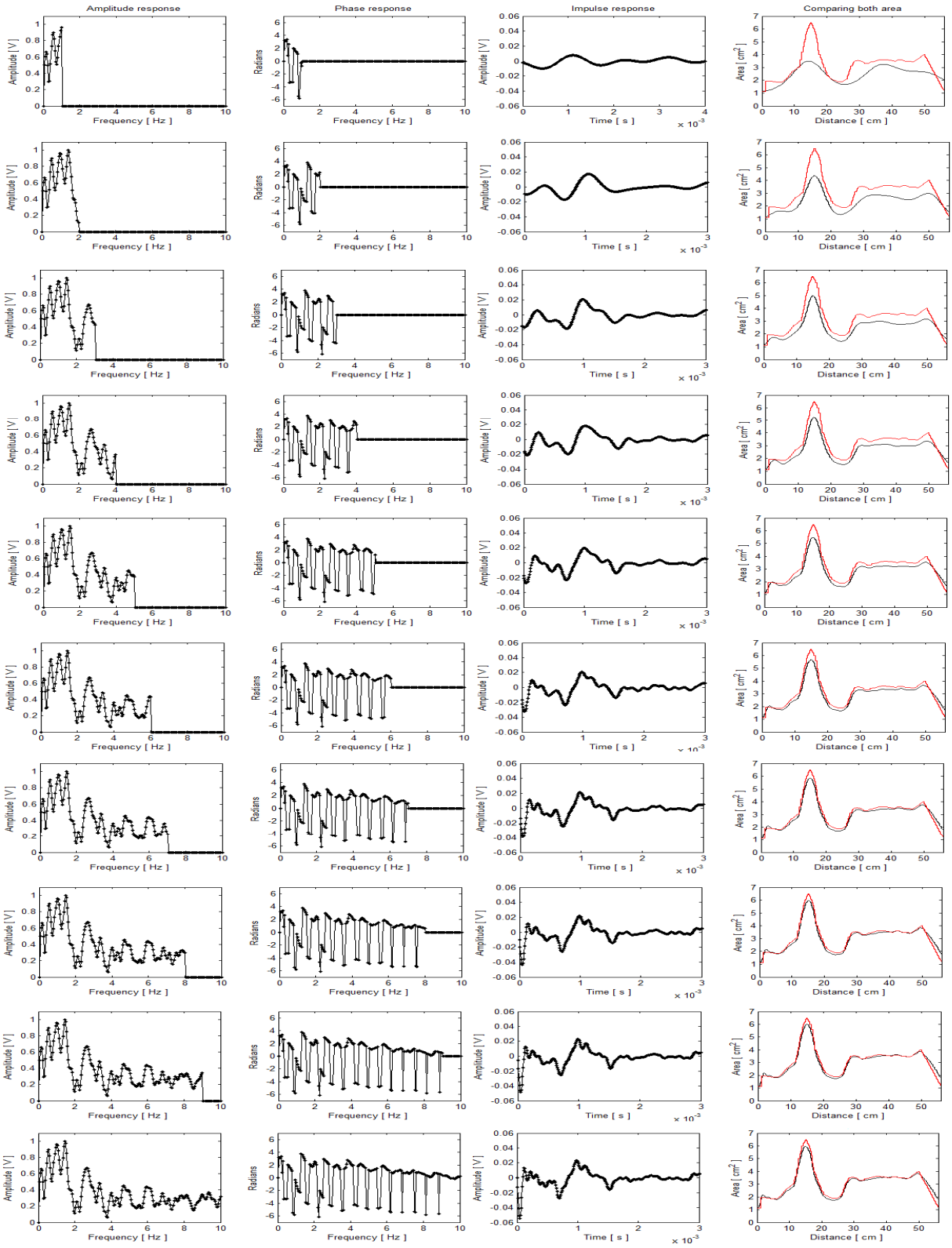


Figure 44. Superposition of the impulse responses proposed test cavity for an upper airway.

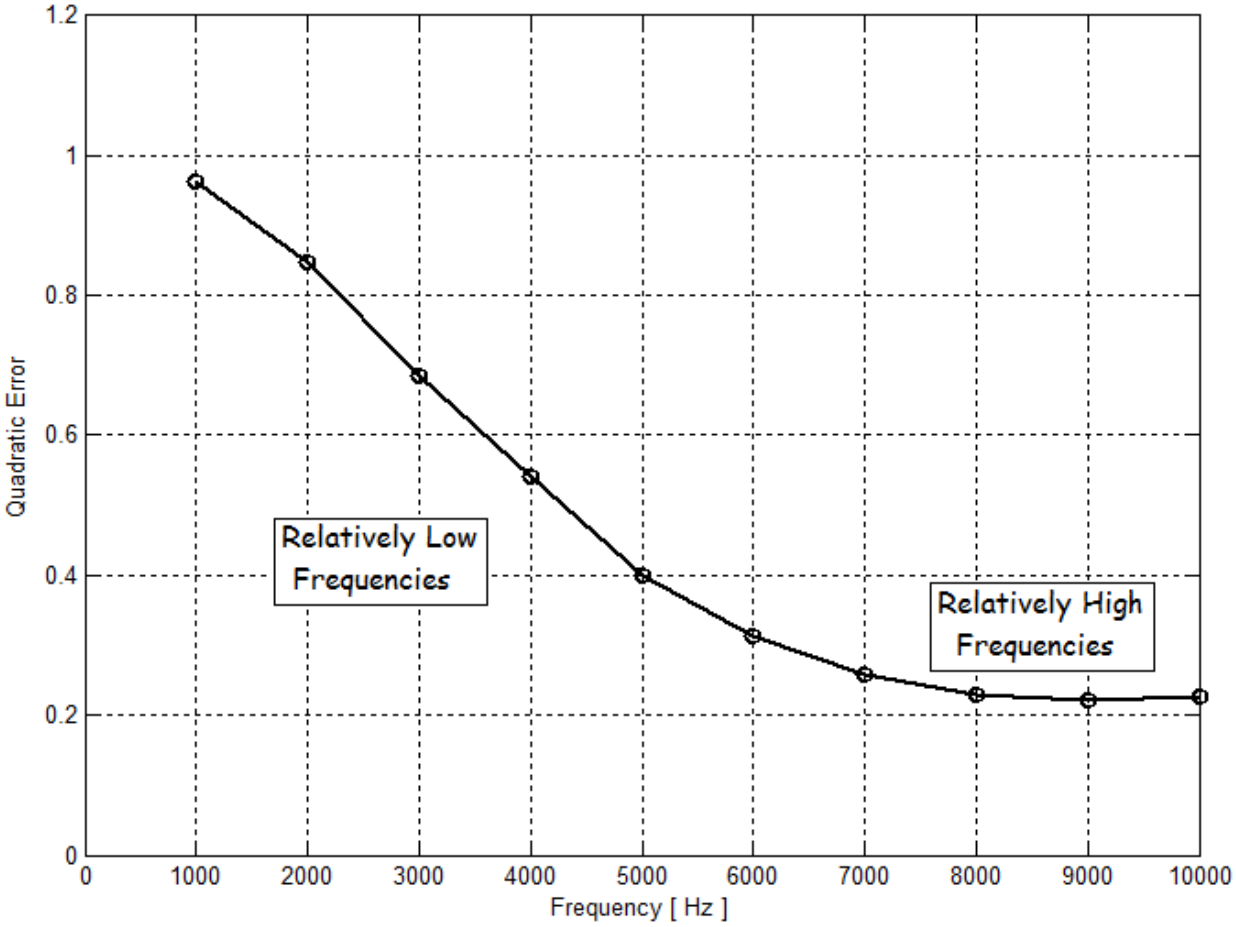


Figure 45. Quadratic error of a proposed test cavity for an upper airway.

The results show that it is possible to estimate the bore profile of a human upper airway, but it is necessary to evaluate the experimental results using solid cylindrical cavity with this profile.

## 7.7 Experimental results in a vitro model of a human upper airway

A solid cylindrical cavity with the same bore profile used in the above simulation was designed and built using stereolithography technique in the W.M. KECK CENTER at the University of Texas at El Paso to evaluate the solution of the inverse problem. Figure 46 (a) shows a 3D image of such bore profile and Figure 46 (b) shows the real cavity made of polymer.

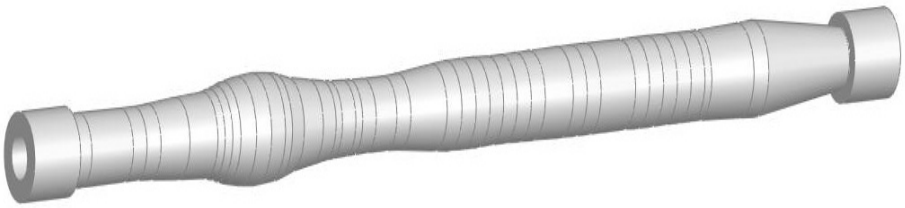

(a)

(b)

Figure 46. A vitro model of the human upper airway.

Figure 47 shows the solid cylindrical cavity coupled to the source tube to estimate its bore profile by using acoustic reflectometry technique. The measurements were performed using the same parameters by the simulation model.

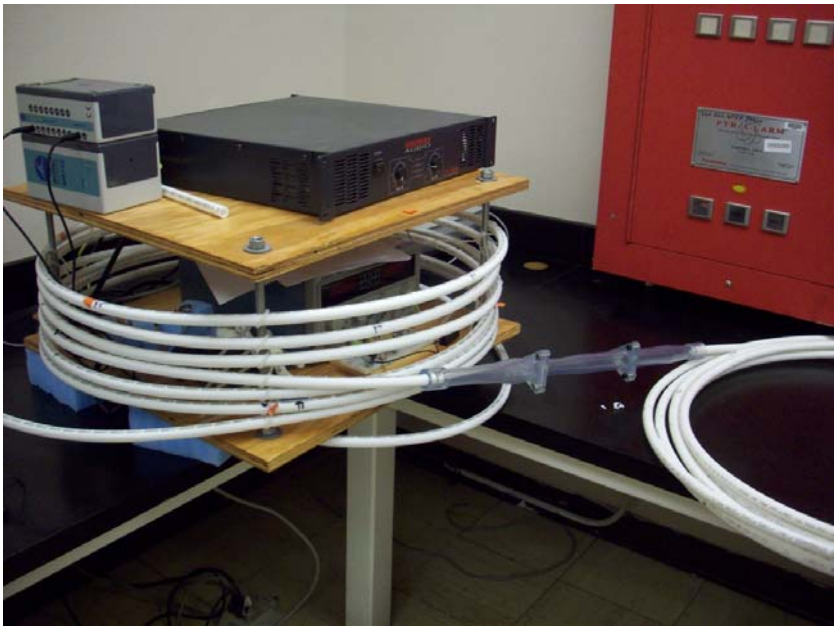

Figure 47. The acoustic reflectometer coupled to the vitro model of the human upper airway.

Figure 48 shows the decomposition of the frequency impulse response and the bore profile experimentally computed (blue) for each frequency subinterval which in turn is compared to the proposed test cavity (red).

The bore profile computed shows an important variation in the first four frequency intervals, which cover an interval from 50 Hz to 4 kHz. The rest of the bore profiles computed is represented by a constant bore profile. In fact, the experimental results suggest that the last three intervals from 7 kHz to 10 kHz do not contribute to improve the bore profile.

A comparison between the results obtained by simulation, (Figure 43), and experimentation, (Figure 48), shows good agreement for each frequency interval analyzed.

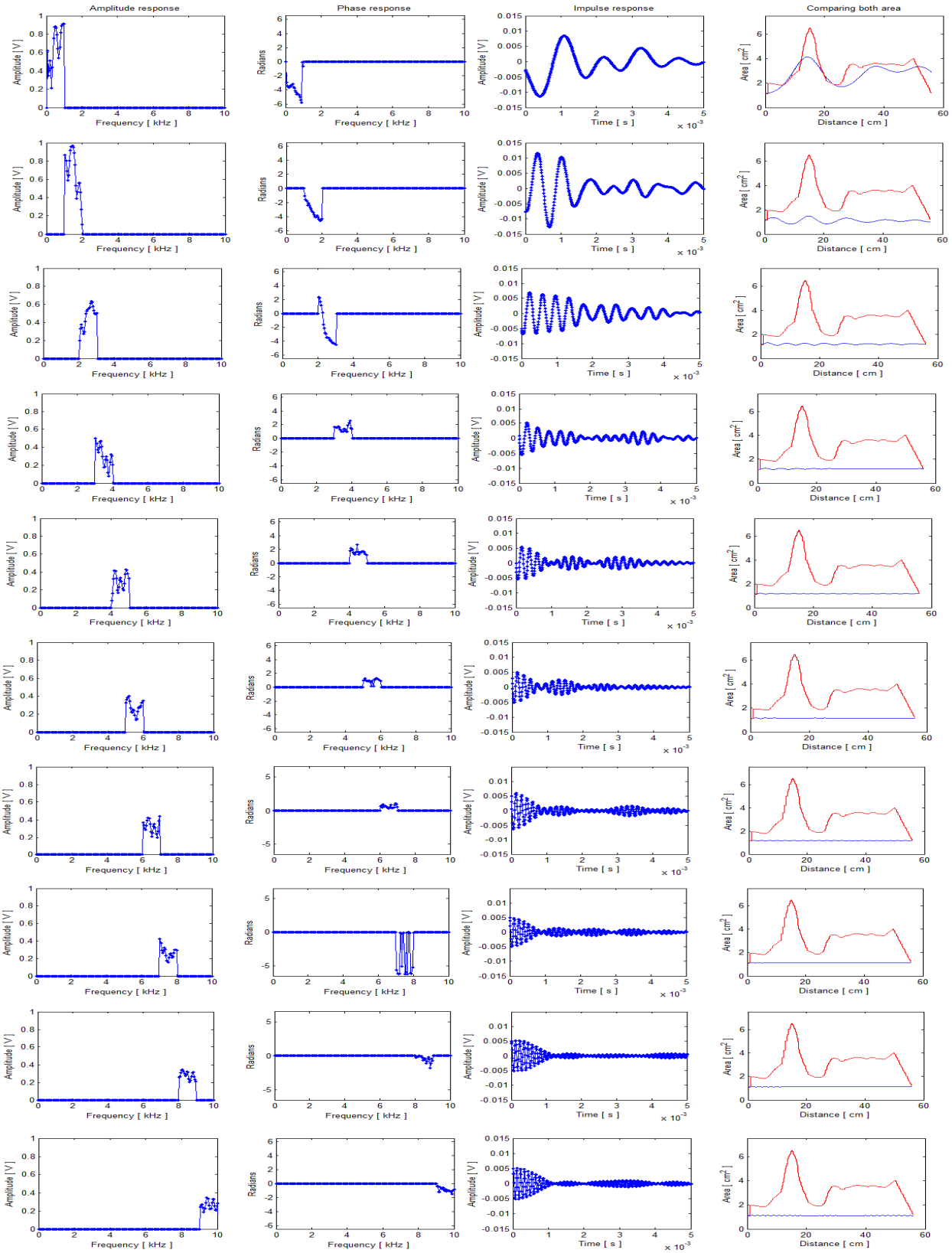


Figure 48. Decomposition of the impulse response of a vitro cavity for a human upper airway.

## 7.8 Superposition of impulse response in a vitro model the of upper airway

Figure 49 shows the superposition of the frequency impulse response and a comparison between the bore profile computed (blue) and the proposed test cavity (red).

The qualitative analysis shows that a good axial resolution is computed for a frequency interval from 50 Hz to 5 kHz. Above this frequency range, there is a small difference mainly along the region corresponding to the pharynx.

A quantitative analysis in the quadratic error is displayed in Figure 50 and it shows that the significant frequencies in the experiment cover an interval from 50 Hz to 5 kHz. This frequency interval is closed to the interval found in the simulation. It is also noted that the quadratic error is almost constant above 5 kHz.

This quantitative result suggests that general shape of the bore profile is estimated with an appropriate axial resolution, when the significant frequencies are covered, but the relatively high frequencies are not contributing to refine the result.

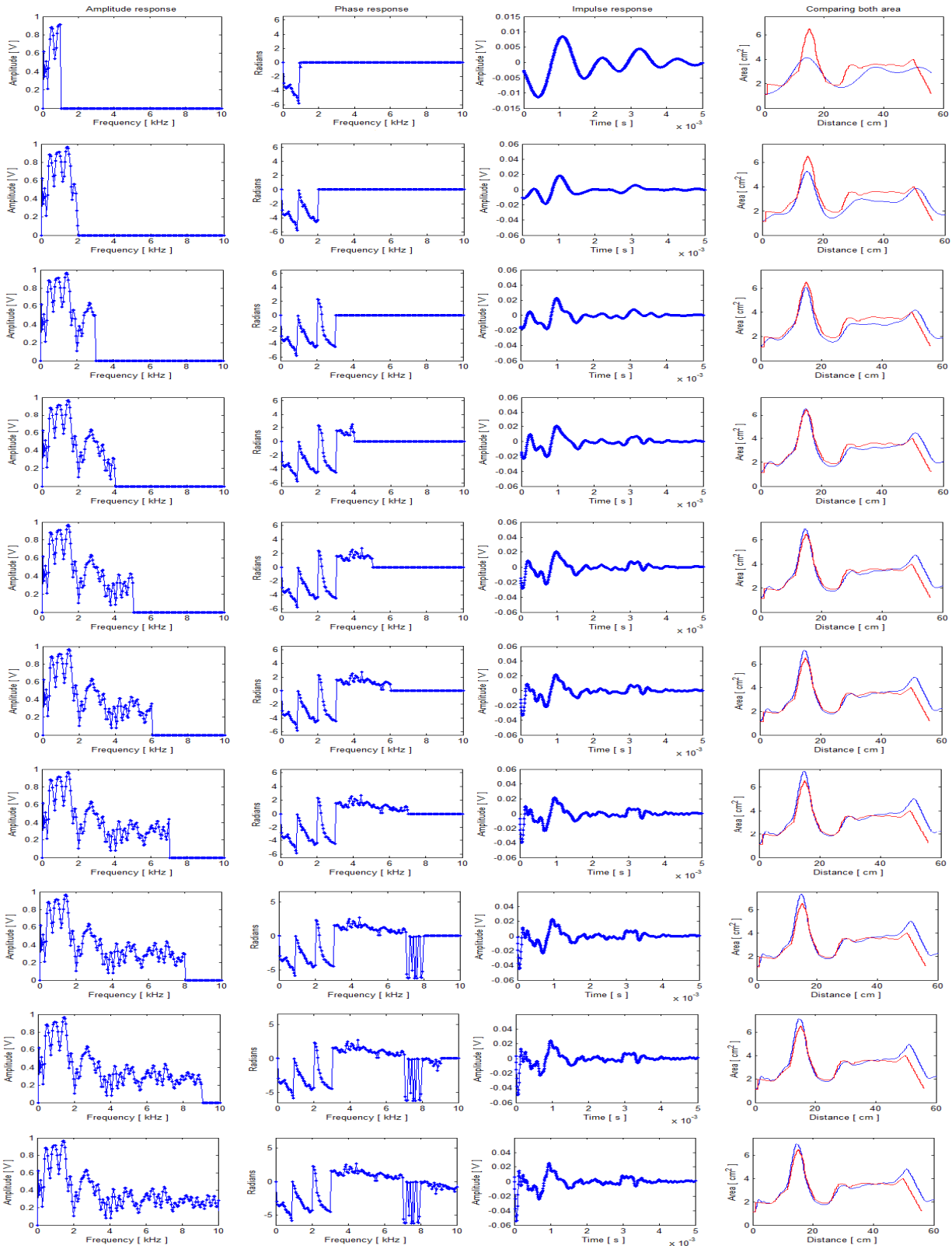


Figure 49. Superposition of the impulse response for a model vitro.

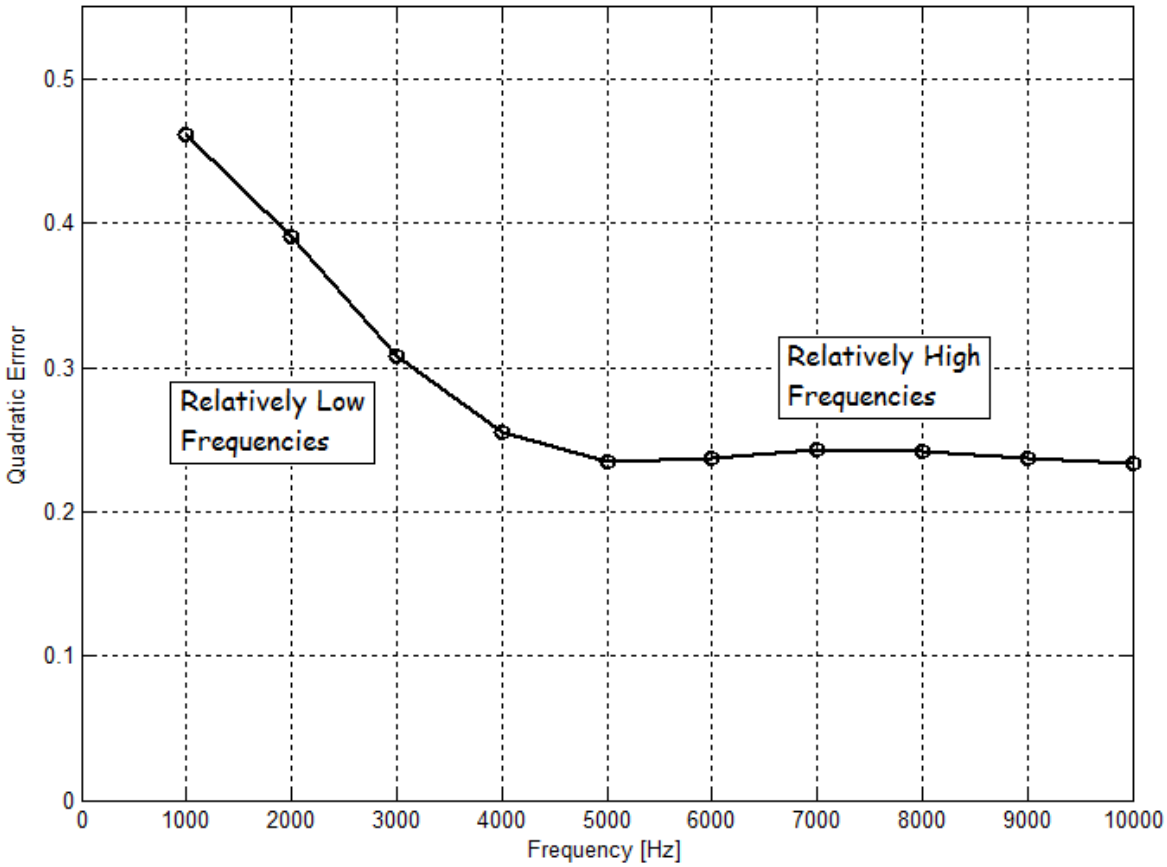


Figure 50. Quadratic error computed of a model in vitro using a frequency step size of 50 Hz.

## 7.9 Comparison between simulation and experimentation of a vitro model

A comparison of impulse response obtained by simulation and experimental acoustic reflectometer is shown in Figure 51.

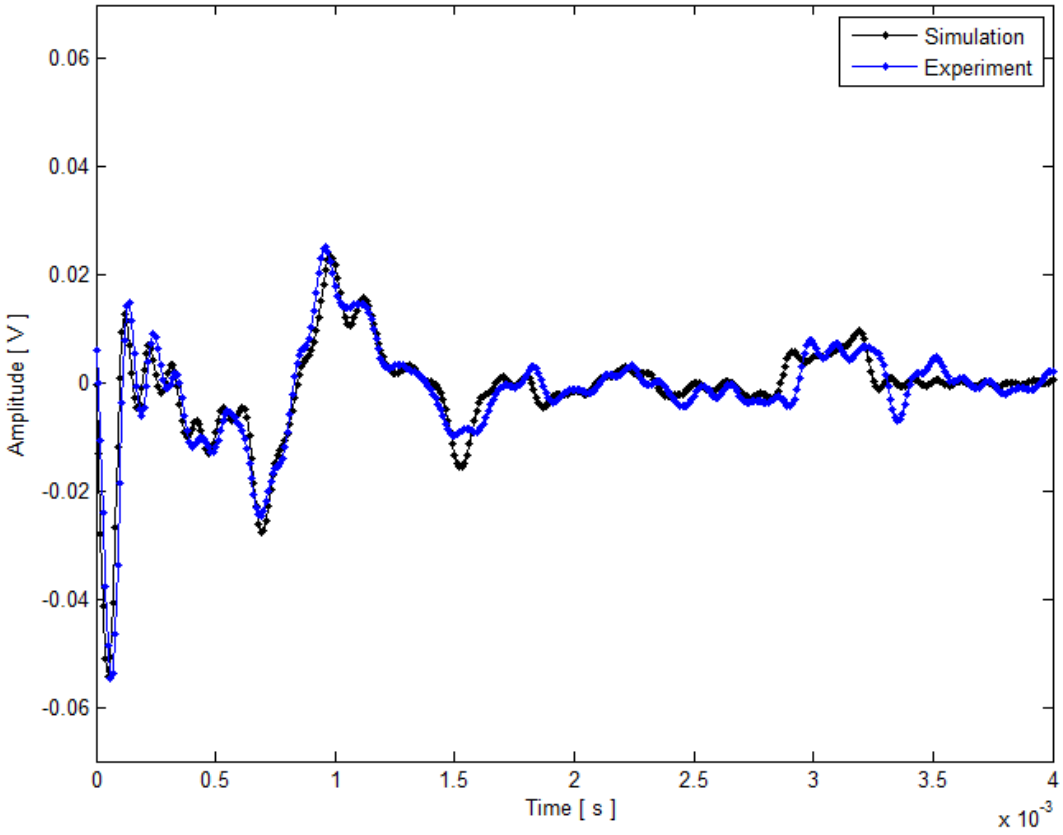


Figure 51. Comparison of impulse responses of a vitro model for an upper airway

Figure 52 displays a qualitative result using Gaussian-modulated acoustic waves and the Ware-Aki algorithm. The bore profiles obtained by simulation (black) and experimental acoustic reflectometer (blue) are compared to the proposed test cavity (red).

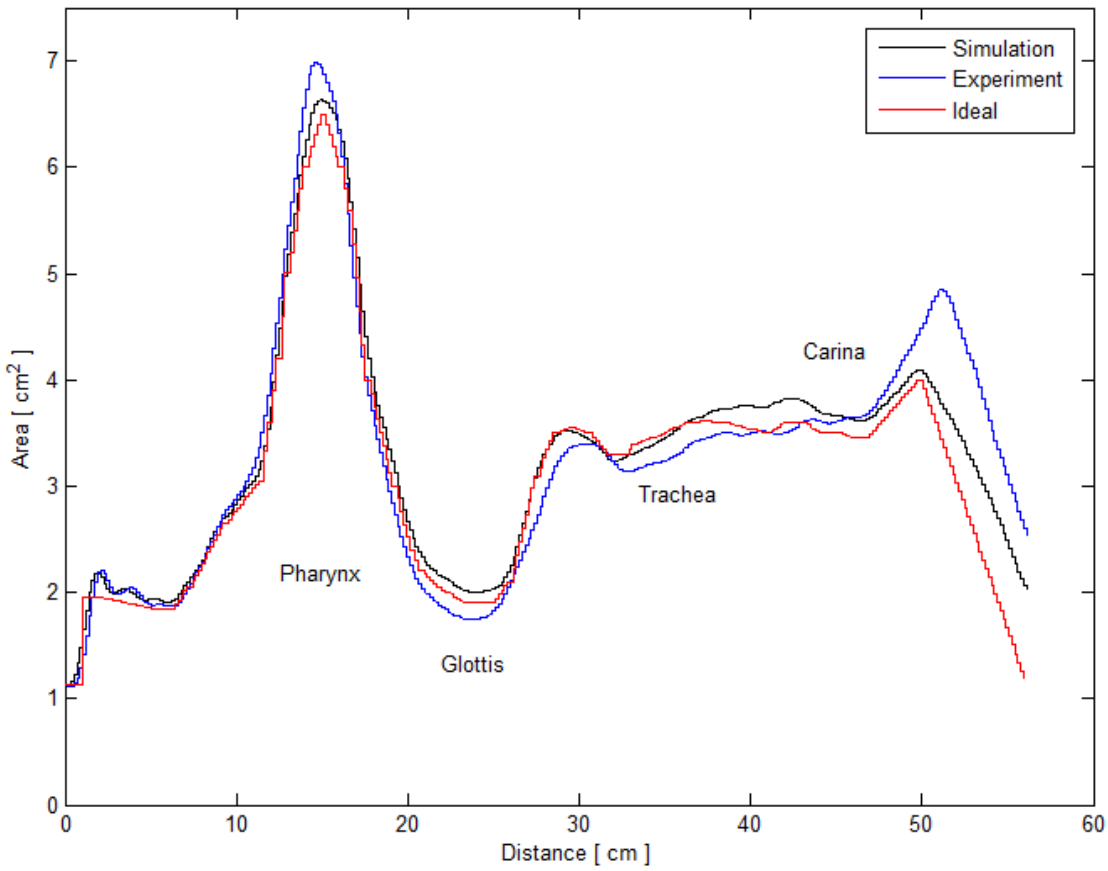


Figure 52. Comparison among bore profiles for an upper airway.

## 7.10 Discussion

The mathematical procedures for solving both forward and backward problems were implemented in a simulation model assuming ideal conditions. The results were validated using a simple cylindrical cavity, and they were determined with an appropriate resolution along its bore profile.

The solution of the inverse problem in this dissertation did not require of acoustic pulses to estimate the impulse response at low frequencies, and the frequency analysis made possible to decomposed the bandwidth to find the predominant frequencies which provide the general shape of a cylindrical cavity.

One of the scenarios found to estimate the bore profile by using the simulation model shows that under ideal conditions, the axial resolution may be improved at a low computational cost using a large frequency step size, and adding a very small DC offset component along its impulse response. However, the solution of the inverse problem is very sensitive to acquisition noise and such situation is not possible to be experimentally performed.

The experimental results depend on both the right calibration of the acoustic reflectometer to compensate the losses along the source tube, and the improvement of the signal-to-noise ratio at high frequencies.

Despite of the compensation between the middle and the end distal of source tube may be used to compensate the forward and backward acoustic waves, a better result was obtained when the compensation between the loudspeaker and the end distal of the source tube.

Although Ware-Aki algorithm does not consider the losses within a cylindrical cavity, the solution of the inverse problem can estimate the axial resolution for a short cylindrical cavity with good accuracy.

# Chapter 8

# Conclusions and Future Enhancements

## 8.1 Conclusions

In regard to the solution of the inverse problem, the conclusions are specified below according to the aims defined at the beginning of this dissertation.

1) Gaussian modulated sinusoidal waves and the Ware-Aki algorithm can be used to estimate a cylindrical cavity with an appropriate axial resolution. In this work, the inverse problem was tested through the performance of a simulation model and experimentally validated using an acoustic reflectometer.

2) The solution of the inverse problem was used to evaluate the acoustic parameters of several cylindrical cavities. A high sampling frequency of 100 kHz was used to represent their bore profile with an appropriate resolution as function of distance. The analysis made possible to sweep and decompose the audible frequency to evaluate the frequency content in the bore profile for each interval swept.

3) An inexpensive acoustic reflectometer characterized by a long source tube reduced the computational cost to identify the acoustic waves. Furthermore, the length of the source tube was also used to identify the frequency impulse response by generating a short-time acoustic wave. In this way, the mathematical procedure to obtain the impulse response made possible to calculate and compensate the DC offset component at very low frequencies without the requirement of using an actual DC tube.

4) A tradeoff between the axial resolution and the number of frequencies used was evident in the solution of the inverse problem. However, it was possible to propose the use of either logarithmic or linear frequency step sizes when the solution of the inverse problem does not require of sweeping a large bandwidth. On the other hand, a constant frequency step size of 50 Hz provided a good resolution in the frequency impulse response to reduce the computational cost. Hence, 200 acoustic waves were required to sweep the frequency bandwidth, by using only one loudspeaker and one microphone.

5) The use of matched filter not only filtered undesired components of frequency, but also improved the signal-to-noise ratio at high frequencies. The procedure was relatively simple. Thereby, it was not necessary to filter the impulse response using neither complex digital filters nor with robust cutoff frequencies.

6) The calibration of the system was required to compensate the attenuation of acoustic waves along the source tube. The procedure was required for both amplitude and phase responses.

## 8.2 Future enhancements

The simulation model and the acoustic reflectometer serve as research tools to evaluate the solution of the inverse problem using several types of acoustic waves, and covering certain ranges of frequency.

The future work includes not only improving the quality of the instrumentation used, but also designing and building an automated system such that the acoustic waves may be collected in a

short time. It would make possible the application of the technique to estimate the results in real time, and perform a calibration every time that the technique is used.

Because there exists a tradeoff in the axial resolution and in the number of frequencies used along a bandwidth, the system would be designed to use a diversity of several frequency step sizes and covering specific ranges of frequency. The acoustic reflectometer would be clinically validated using normal patients and defining a protocol to perform the test in safety conditions.

It also would be necessary to establish a relationship with some medical center to determine the type of pathologies that the physicians are interested in evaluating along the upper airway. It would be possible to use this technique on patients and validate the results through endoscopies or computerized tomography.

The simulation model may be used to evaluate the effect of using a linear couple at the distal end of the source tube. In this way, high discontinuities are avoided and less content of frequency would be required.

# References

[1] M. R. Schroeder, “Determination of the geometry of the human vocal tract by acoustic Measurements”. J. Acoust. Soc. Am., Vol. 41, no. 4, pp. 1002-1010, 1967.

[2] J. A. Ware and K. Aki, “Continuous and discrete inverse scattering problems in a stratified elastic medium. I: Planes at normal incidence”. J. Acoust. Soc. Am., Vol. 45, no.4, pp. 911-921, 1969.

[3] M. M. Sondhi and B. Gopinath, “Determination of vocal tract shape from impulse response at the lips”. J. Acoust. Soc. Am., Vol. 49, no. 6, pp. 1867-1873, 1971.

[4] M. M. Sondhi and J. R. Resnick, “The inverse problem for the vocal tract: numerical methods, acoustical experiments, and speech synthesis”. J. Acoust. Soc. Am., Vol. 73, no.3, pp. 985-1002, 1983.

[5] A. C. Jackson, J. P. Butler, E. J. Millet, F. G. Hoppin Jr, and S. V. Dawson, “Airway geometry by analysis of acoustic pulse response measurements”. J. Appl. Physiol., Vol. 43, no. 3, pp. 523-536, 1977.

[6] A. C. Jackson and D. E. Olson, “Comparison of direct and acoustical area measurements in physical models of human central airways”. J. Appl. Physiol., Vol. 48, no. 5, pp. 896-902, 1980.

[7] J. J. Fredberg, M. E. Wohl, G. M. Glass, and H. L. Dorkin, “Airway area by acoustic reflections measured at the mouth”. J. Appl. Physiol., Vol. 48, no. 5, pp. 749-758, 1980.

[8] L. J. Brooks, R. G. Castile, G. M. Glass, N. T. Griscom, M. E. Wohl, and J. J. Fredberg, “Reproducibility and accuracy of airway area by acoustic reflection”. J. Appl. Physiol., Vol. 57, no. 3, pp. 777-787, 1984.

[9] V. Hoffstein, R. G. Castile, C. R. O’Donnell, G. M. Glass, D. J. Strieder, M. E. Wohl, and J. J. Fredberg, “In vivo estimation of tracheal distensibility and hysteresis in normal adults”. J. Appl. Physiol., Vol. 63, no.6, pp. 2482-2489, 1987.

[10] A. H. Benade and J. H. Smith, “Brass wind instrument impulse response measurements”. J. Acoust. Soc. Am., Vol. 70, S22, 1981.

[11] A. P. Watson and J. M. Bowsher, “Recent progress in time domain work on brass instruments”. Proceedings of the Institute of Acoustics, Vol. 9, no.3, pp. 103-109, 1987.

[12] A. P. Watson and J. M. Bowsher, “Impulse measurements on brass musical instruments. Acustica”. Acustica, Vol. 66, no. 3, pp. 170-174, 1988.

[13] I. Marshall, M. Rogers, and G. Drummond, “Acoustic reflectometry for airway measurement. Principles, limitations and previous work”. Clin. Phys. Physiol. Meas., Vol. 12, no. 2, pp. 131-141, 1991.

[14] I. Marshall, “Acoustic reflectometry with an arbitrarily short source tube”. J. Acoust. Soc. Am., Vol. 91, no. 6, pp. 3558-3564, 1992.

[15] B. Louis, G. M. Glass, B. Kresen, and J. J. Fredberg, “Airway area by acoustic reflection: The two microphone method”. J. Biomech. Eng., Vol. 115, no.3, pp. 278-285, 1993.

[16] B. Louis, G. Glass, and J. J. Fredberg, “Pulmonary airway area by the two microphone acoustic reflection: method”. J. Appl. Physiol., Vol. 76, no. 5, pp. 2234-2240, 1994.

[17] N. Amir, G. Rosenhouse, and U. Shimony, “A discrete model for tubular acoustic systems with varying cross section - The direct and inverse problems. Parts 1 and 2: Theory and experiment”. Acustica, Vol. 81, no. 5, pp. 450-474, 1995.

[18] N. Amir, U. Shimony, and G. Rosenhouse, “Losses in tubular acoustic systems - Theory and experiment in the sampled time and frequency domains”. Acustica, Vol. 82, no. 1, pp. 1-8, 1996.

[19] D. B. Sharp, “Acoustic pulse reflectometry for the measurement of musical wind instruments”. Ph.D. Dissertation, Department of Physics and Astronomy, University of Edinburgh, UK, 1996.

[20] J. P. Mansfield, D. C. Shannon, and G. R. Wodicka, “Acoustic method to qualitatively assess the position and patecy ofinfant endotracheal tubes”. Pediatric Pulmonology, Vol. 26, no.5, pp. 354-361, 1998.

[21] J. Huang, M. Itai, T. Hoshiba, T. Fukunaga, K. Yamanouchi, H. Toga, K. Takahashi, and N. Ohya, “A new nasal acoustics reflection technique to estimate pharyngeal cross-sectional area during sleep”. J. Appl. Physiol., Vol. 88, pp. 1457-1466, 2000.

[22] B. J. Forbes, D. B. Sharp, J. A. Kemp and, L. Aijun, “ Singular sytem methods in acoustic pulse reflectometry”, Acustica, Vol. 89, no.5, pp. 743-753, 2003.

[23] B. J. Forbes, R. E. Pike, D. B. Sharp, and T. Aktosun, “Inverse potential scattering in duct acoustics”. J. Acoust. Soc. Am., Vol. 119, no. 1, pp. 65-73, 2006.

[24] W. Kausel, “Bore reconstruction of tubular ducts from its acoustic input impedance curve”. Presented at the IEEE Instrumentation and Measurement Technology Conference, Vail, Colorado, May 20-22, 2003.

[25] M. J. Babb, R. L. Hilsinger Jr., H. W. Korol, and R. D. Wilcox, “Modern acoustic reflectometry: Accuracy in diagnostic otitis media with effusion”. Ear, Nose and Throat Journal, Vol. 83, no. 1, pp. 622-644, 2004.

[26] L. Aijun, D. B. Sharp, and B. J. Forbes, “Increasing the axial resolution of bore profile measurements made using acoustic pulse reflectometry”. Meas. Sci. Technol., Vol. 16, no. 10, pp. 2011-2019, 2005.

[27] L. Aijun and D. B. Sharp, “The problem of offset in measurements made using acoustic pulse reflectometry”. Acta Acustica United with Acustica. Vol. 91, no. 4, pp. 789-796, 2005.

[28] G. Gligor, R. T. David, E. Shlomo, and G. Gary. “Pediatric airway and esophageal profiles with acoustic reflectometry”. International Anesthesia Research Society. Vol. 103, no. 5, pp. 1126-1130, 2006.

[29] T. D. Raphael, “Acoustic reflectometry imaging of the airway”. Seminars in Anesthesia, Perioperative Medicine and Pain, Vol. 26, no. 4, pp. 210-217, 2007.

[30] N. J. Kinar and J. W. Pomeroy, “Automated determination of snow water Equivalent by acoustic reflectometry”. IEEE Transactions on Geoscience and Remote Sensing, Vol. 47, no. 9, pp. 3161-3167, 2009.

[31] L. E. Kinsler, A. B. Frey, A. B. Coppens, and J. V. Sanders, “Fundamentals of Acoustics”. John Wiley and Sons Inc., 2000, ch. 6.

[32] The Sleep Therapy Clinic Pty Ltd. Available: http://www.sleeptherapyclinic.com/acoustic-reflectometry.html

[33] I. Marshall, N. J. Maran, S. Martin, M. A. Jan, J. E. Rimminton, J. J. K. Best, G. B. Drummond, and N. J. Douglas, “Acoustic reflectometry for airway measurement in man: implementation and validation”. Physiol. Meas., Vol. 14, no. 2, pp. 157-169, 1993.

[34] A. D. D’urzo, I. Rubinstein, V. G. Lawson, K. P. Vassal, A. S. Rebuck, A. S. Slutsky, and V. Hoffstein, “Comparison of glottis areas measured by acoustic reflections vs. computerized tomography”. J. Appl. Physiol., Vol. 64, no. 1, pp. 367-370, 1988.

# List of Conferences

E. Ceron, J. H. Pierluissi, and T. Sarkodie-Gyan, “Interpolation of the impulse response of a cylindrical cavity using steady state acoustic reflectometry”. Biomedical Engineering Society Annual Conference, Los Angeles, Cal., September 25-28, 2007.

E. Ceron, J. H. Pierluissi, and T. Sarkodie-Gyan, “Increasing the frequency response of acoustic reflectometry”. SACNAS Conference, Kansas City, Mo., October 12-14, 2007.

E. Ceron, J. H. Pierluissi, and T. Sarkodie-Gyan, “Starting points in acoustic reflectometry to estimate the shape of a human trachea”, Twenty Fourth Southern Biomedical Engineering Conference, El Paso, Tx, April 18-20, 2008.

E. Ceron and J. H. Pierluissi, “Identifying predominant frequencies in steady state acoustic reflectometry”, Biomedical Engineering Society Annual Conference, St. Louis, Mo., October 2-5, 2008.

E. Ceron, J. H. Pierluissi, and Ricardo F. von Borries, “Gaussian-modulation sinusoidal wave in acoustic reflectometry”, Biomedical Engineering Conference Annual Conference, Pittsburgh, Pen. October 7-9, 2009.

# Curriculum Vita

Ernesto Ceron was born in Mexico City, Mexico, in 1972. He is the first one to get a bachelor degree in his family. Ernesto obtained the degree of Physicist Engineering in the area of Instrumentation and Equipment, at the Universidad Autonoma Metropolitana, Azcapotzalco, Mexico City in 1997. He obtained the degree of Master of Science in the area of Biomedical Engineering, at the Universidad Autonoma Metropolitana, Iztapalapa, Mexico city in 2003. He worked as Research Assistant at the National Cardiology Institute Ignacio Chaves, in 2000, in the Department of Bioprothesis. He has been an Associate Professor at the Universidad Autonoma Metropolitana, campus Azcapotzalco in the Department of Electronics since 2001. He joined the research group of Sensors and Processing Signals in 2002. He has taught courses of Electronics, Electric Circuits, Instrumentation and Equipment, Digital Signal Processing, and Microelectronics. In 2006, Ernesto Ceron started the Doctorate of Computer Engineering in the Department of Electrical and Computer Engineering at the University of Texas at El Paso. He won an award in engineering from the SACNAS chapter at the University of Texas at El Paso in 2007. He worked as Teaching Assistant at University of Texas at El Paso, 2008 and 2009, teaching Computational Methods, Electromagnetic Fields, and Electronic Devices. He has been participating in the Biomedical Engineering Society with poster presentations on acoustic reflectometry since 2007.

Permanent address: Colector La Quebrada, No. 8, Casa 32

Col. Valle Esmeralda

Cuautitlan Izcalli, Edo. Mex., C.P. 54769

ervc@correo.azc.uam.mx